Cartography M.Sc.

Master thesis

Mapping the Relief of Mount Ushba (Georgia) as a Contribution to an Alpine Club Map

Anouska Jaspersen

Technical University of Munich

TECHNISCHE UNIVERSITÄT WIEN Vienna University of Technology

TECHNISCHE UNIVERSITÄT DRESDEN

UNIVERSITY OF TWENTE. ITC

2021

Mapping the Relief of Mount Ushba (Georgia) as a Contribution to an Alpine Club Map

submitted for the academic degree of Master of Science (M.Sc.)
conducted at the Department of Aerospace and Geodesy
Technical University of Munich

Author: Anouska Jaspersen
Study course: Cartography M.Sc.
Supervisor: Dr.rer.nat. Nikolas Prechtel (TUD)
Reviewer: Dr.rer.nat. Georg Gartner (TUW)

Chair of the Thesis
Assessment Board: Prof. Dipl. Phys. Dr.-Ing. habil. Dirk Burghardt (TUD)

Date of submission: 05.11.2021

Statement of Authorship

Herewith I declare that I am the sole author of the submitted Master's thesis entitled:

"Mapping the Relief of Mount Ushba (Georgia) as a Contribution to an Alpine Club Map"

I have fully referenced the ideas and work of others, whether published or unpublished. Literal or analogous citations are clearly marked as such.

BARNEVELD, 05.11.2021 Anouska Jaspersen

Task description

Topic:
Mapping the Relief of Mount Ushba (Georgia) as a Contribution to an Alpine Club Map

Keywords:
Photogrammetric DEM, PlanetScope images, rock drawing, contour lines, scree depiction, Caucasus, Alpine Club Map.

Objective:
A detailed high-quality cartographic depiction of the alpine and nival zone of Mount Ushba, Georgia, mostly composed of rock, debris, and ice, shall be produced from a customized, photogrammetrically generated DEM and other sources (images and maps). It shall become an exemplary central section of an Alpine Club map currently in preparation.

Description:
Greater Caucasus, a high mountain range of Alpidic origin, divides Europe from Asia. Prominent peaks are located in its central parts, Mount Elbrus (5,642 m) and the dual-peaked Ushba (4,710 m). The Caucasus is facing growing interest for both summer and winter tourism, what forms a motivation to produce and publish Alpine Club map sheets. Caucasus is presently not covered at all. Reliability and a superior quality of the graphic depiction of the relief information is a central argument in the use of Alpine Club maps. The present task combines a technical task (DEM derivation from stereo imagery) and, at the same time, a design task (large-scale relief depiction). It is, on the other hand, limited to a rather small study area of around 40 km^2.

Mapping of the Ushba for a target scale of 1:33,000 may include various steps:

(1) Using archived high-resolution PlanetScope imagery for a DEM generation. Target planimetric resolution might be around 10m by 10m, but a final decision will depend on the results of image correlation. This part of the master thesis relates to a second actual topic proposal “Creation of a high-resolution Digital Elevation Model …”, but has, in contrast, to the other topic, only a small spatial focus with presumably less consistency problems by use of a small number of stereo pairs. Obviously, a cooperation of two students is sensible if both topics are chosen by students of the present intake.

(2) Evaluation of the results of DEM generation by comparing the output DEM to a) existing map sheets, b) SRTM-30 DEM data that are both stored and available. In such a

comparison surfaces have to be avoided that are subject of major elevation changes (as, for instance, glacier surfaces).

(3) Experiments with contours of a sensible equidistance (vertical interval), e.g. 20 m, in respect to the resulting line density, effects of careful smoothing, etc., and design of a quality depiction of steep rock cliffs (rock drawing).

(4) Production of a rock (including scree) and ice map layer as a reference for the whole map design.
The thesis will profit from a) the existence of PlanetScope image data on a TUD server (curtesy of an image grant by Planet Coop.) and b) the recently completed master thesis of Maximilian Schröder (2020) who has produced reliable rock and ice masks for the area under consideration from Sentinel-2 data.

The thesis shall include an assessment of usability and reliability of the mentioned sources.

References

Pieczonka, T. und T. Bolch (2015). Region-wide glacier mass budgets and area changes for the Central Tien Shan between ~1975 and 1999 using Hexagon KH-9 imagery. Global and Planetary Change, 128, p. 1-13.

Ghuffar, S. (2018): DEM Generation from Multi Satellite PlanetScope Imagery. Remote Sens. 2018, 10, 1462; doi:10.3390/rs10091462

Geisthövel, R. (2017): Automatic Swiss style rock depiction. Zürich: ETH Zurich.

Pieczonka, T. (2017): Untersuchung und Visualisierung von Gletschervolumenänderungen im Tarim-Einzugsgebiet, Zentralasien, unter Verwendung multi-temporaler digitaler Geländemodelle. Diss. TU Dresden. https://tud.qucosa.de/landing-page/?tx_dlf[id]=https%3A%2F%2Ftud.qucosa.de%2Fapi%2Fqucosa%253A30942%2Fmets

Domain
TU Dresden

Supervisors: Dr. Nikolas Prechtel (TUD), Prof. Dirk Burghardt (TUD)

Abstract

Characterized by its double summit, Mount Ushba (Georgia) is one of the most prominent peaks of the Caucasus Mountains. Tourism has been growing in the Mestia region over the past couple of years, with many hikers visiting the region. This led the Alpine Club to create a map sheet focusing on the hiking possibilities of the Caucasus region around Mount Ushba and Mestia, with a target scale of 1:33,000. This project is carried out together with the Technical University of Dresden. This master thesis focuses on mapping the relief of Mount Ushba (Georgia) as a Contribution to this Alpine Club Map. Using high-resolution PlanetScope Imagery a digital elevation model of the area is generated and evaluated. The Dove-1 satellites image the entire world's landmass every day, and are therefore a valuable source for studying dynamic phenomena. The results are evaluated by comparing statistics of the elevation differences between a 30-meter resolution SRTM DEM, map sheets of the region and field measurements taken during a mapping campaign in the summer of 2021 and the PlanetScope DEM. The RMSE of the elevation differences between the generated PlanetScope DEM and the STRTM is 46.9m and 14m over stable terrain. For the elevation difference with the map sheets the RMSE is 36.8m and the RMSE is 14.3m for the field measurements. These deviations are rather large due to the mountainous terrain, but the PlanetScope DEM performs better in most accuracy assessments than the commonly used SRTM DEM. The results show that it is possible to generate a DEM of sufficient quality with the PlanetScope imagery. Based on this DEM a relief depiction is created. After carefully smoothing the DEM, contour lines can be drawn. The shaded relief is produced with Blender and the rock depiction is made in the Swiss style using the software by Roman Geisthövel.

Preface

Before you lies the thesis 'Mapping the Relief of Mount Ushba (Georgia) as a Contribution to an Alpine Club Map'. This thesis is written as part of the master program Cartography, an Erasmus Mundus Program at the Technical Universities of Munich, Vienna, Dresden and Twente. I worked on collecting the data, analyzing and writing from April until November 2021.

Throughout the writing of this thesis I have received a great deal of support and assistance. I would first like to thank my supervisor Dr. Nikolas Prechtel for his help, support and feedback during this process. I also want to thank all the participants of the mapping campaign in Georgia, for their help with collecting the field measurements needed for this study. Last, I would also like to thank Mathias Gröbe for his help with the processing of the GPS measurements.

I hope you enjoy reading this thesis.

Anouska Jaspersen

Barneveld (The Netherlands), November 5th, 2021

Contents

Figures

Tables

Equations

Abbreviations

DEM	Digital Elevation Model
DSM	Digital Surface Model
DTM	Digital Terrain Model
EGM	Earth Gravitational Mode
GCP	Ground Control Point
GIS	Geographical Information System
GNSS	Global Navigation Satellite System
GPS	Global Positioning System
IGN	Institut Géographique National
InSAR	Interferometric SAR
IQR	Interquartile Range
LIC	Line Integral Convolution
ME	Mean Error
NGA	National Geospatial-Intelligence Agency
NMAD	Normalized Median Absolute Deviation
PPP	Precise Point Positioning
PS	PlanetScope
RINEX	Receiver Independent Exchange Format
RMSE	Root-Mean-Square Error
RPC	Rational Polynomial Coefficient
SAR	Synthetic Aperture Radar
SGM	Semi-Global Matching
SIFT	Scale-Invariant Feature Transform
SRTM	Shuttle Radar Topography Mission
WGS	World Geodetic System

1 Introduction

Characterized by its double summit, Mount Ushba (Georgia) is one of the most prominent peaks of the Caucasus Mountains. In 2019 Georgia received a record number of over 5 million tourists and the country plans on letting this increase to 11 million by 2025 (Georgian National Tourism Administration, n.d.). Its growing popularity also brings more tourists and specifically hikers to the Ushba region. The Alpine Club maps currently do not cover the Caucasus Mountains and they therefore decided to produce a map of the Ushba and Mestia region.

This master thesis is a contribution to the project that the Alpine Club is carrying out together with the Technical University of Dresden. The outcome of the project will be a map sheet focusing on the hiking possibilities of the Caucasus region around Mount Ushba and Mestia, with a target scale of 1:33,000. The exact extent of the map can be found in chapter 4.2. Previously there have been three master theses written for this project. These focused on mapping the vegetation (Hallet, 2020), the rock and ice layers (Schröder, 2020) and a guideline for data acquisition from OpenStreetMap for the region (Masino, 2020). In this study the focus lies on mapping the relief of Mount Ushba and its surroundings.

For high quality maps with accurate relief information and depiction that hikers can rely on a Digital Elevation Model (DEM) of the region is needed. For this study high resolution PlanetScope Imagery is available. This imagery can be a valuable data source for DEM generation, since Planet captures the entire world's landmass every day. This makes the PlanetScope Imagery very suitable for studying and analyzing dynamic phenomena, like glacier surges. The in total 136 Dove satellites that were launched in 2017 image the world in 4 spectral bands (blue, green, red and near-infrared) (Planet, n.d.) at a resolution of approximately 3.7 meters (Planet, 2021). The combination of the daily revisit time and high resolution offers a high potential, as other available imagery often has a lower revisit time or resolution. Also, on demand acquisition of imagery to study temporal changes is very costly (Ghuffar, 2018).

The quality and accuracy of a DEM depends on the image size, camera constant, flying height and base to height ratio. Especially the base to height ratio will be of influence for this study. The view angle of the satellites varies within a few degrees from the nadir and together with the small scene footprint of the imagery this leads to a small base to height ratio of the overlapping images (Ghuffar, 2018). This study will therefore research the feasibility of generating a high quality DEM with the PlanetScope Imagery and evaluate the results with field measurement collected in Georgia in the summer of 2021 and a reference DEM and map sheets.

There is plenty of literature available on DEM generation, the different methods and their pros and cons (Rothermel & Haala, 2012; Hirschmuller, 2008). There are also some studies that researched the use of MicMac, the intended free open-source software for this study, or other open source photogrammetric software for DEM generation (Friedt, 2014; Dukuzemariya, 2017; Beyer et al., 2018). There is however not a lot of literature available on the use of PlanetScope imagery for DEM generation and the use of MicMac in combination with PlanetScope imagery seems to not have been researched at all.

Ghuffar (2018) looks at the potential of PlanetScope (PS) Imagery for the generation of multi temporal DEMs. It takes into account the small baseline to height ratio of the PS imagery, something that is also relevant for this study, as this influences the quality of the DEM. The study compares the resulting DEM with existing DEMs and also accounts for the elevation differences over glaciers, due to time difference. The paper concludes that it is possible to create good quality DEMs with the PS Imagery. The research by Ghuffar deviates from this study in the methodology (a volumetric stereo reconstruction technique) used to generate the DEM.

There are multiple studies that look at the use of MicMac, although not all of them focus specifically on DEM generation (e.g. J.M. Friedt, 2014). Rupnik et al. (2017) and Rupnik et al. (2018) describe and explore the options that MicMac has to offer, while Letortu et al. (2021) and Niederheiser et al. (2016) compare different photogrammetric software and their results. The first states that the best results were achieved using MicMac and the latter explains that MicMac is very challenging but also offers the most possibilities to influence the processing workflow.

Since many people and map makers rely on DEMs, a good evaluation and quality assessment is important. Gómez et al. (2012) have assessed the accuracy of the ASTER and SRTM DEMs by looking at the geolocation, elevation, and morphological accuracy. Höhle and Höhle (2009) also look at the requirements for the reference data and use robust statistical methods for the accuracy assessment, like the median, normalized median absolute deviation (NMAD), and sample quantiles.

There are different methods to depict the relief on a map. Hill shades, hachuring, form lines and contours (Collier et al., 2003) are all used to convey the landscape to the map user. Brunner and Welsch (2002) have specifically studied the high-mountain cartography of the Alpine Club. They look at how, among other things, the depiction methods changed over the years or which ones have been in use since the beginning. They state that high-mountain cartography is not only a science but also an art. The modern Alpine Club maps use the design method by Leonhard Brandstätter which has a “full depiction of the topography by contour lines up to a steepness of 75° in maps to a scale of 1:25,000. For steeper inclinations, hachures are used together with index

contours. By drawing the positive and negative edges, a clear representation of the rocky area is achieved and the course of the contour lines was made evident."

1.1 Research Objective

The main research objective of this study is to develop a detailed high-quality cartographic depiction of the alpine and nival zone of Mount Ushba, Georgia. This will be done as a contribution to a map sheet for the Alpine Club Map. The map sheet will cover a larger region but for this study only the alpine and nival zone of Mount Ushba will be included. The methodology and relief depiction can serve as an exemplary section for similar mountain regions. This study will therefore not only serve hikers and other users of the Ushba region, but also other cartographers creating digital elevation models from PlanetScope imagery and/or making maps of high-mountain regions.

To create this exemplary map section the following two sub-objectives and their respective research questions are defined:

1. **The generation and evaluation of a Digital Elevation Model of the Mount Ushba region, Georgia, with the use of high-resolution PlanetScope Imagery.**
   - 1.1. How is it possible to photogrammetrically generate a DEM with PlanetScope Imagery and which spatial resolution and height accuracy can be reached?
   - 1.2. How does the quality and accuracy of the generated DEM compare with existing elevation models and map sheets?
2. **The creation of a large-scale relief depiction based on the cartographic depiction of the Alpine Club.**
   - 2.1. Which relief depiction methods are currently used by the Alpine club?
   - 2.2. How can the relief of Mount Ushba and the ice and rock surfaces be visualized?

1.2 Reader's Guide

Chapter 2 offers an overview of the literature available on photogrammetric DEM generation, with a focus on the use of PlanetScope imagery. Besides this, literature on existing relief depiction techniques in general and those used by the Alpine Clubs is discussed. In chapter 3 the data needed and used is this study is described. Chapter 4 presents the methodology used for the DEM generation and the creation of a relief depiction. The results are discussed in chapter 5. The limitations of the study and recommendations for further research are identified in chapter 6. Finally, in chapter 7, the research questions will be answered.

2 Theoretical Framework

This chapter provides an overview of the existing literature on the topic of DEM generation and relief depiction. First, the literature available on digital elevation models, the terminology, and the DEM generation, specifically focusing on DEM generation with the use of PlanetScope imagery will be discussed. Next, the literature on relief depiction, divided into the topics contour lines, shaded relief and rock depiction, is analyzed. Also a specific look is taken into the literature available on the relief depiction in Alpine Club Maps.

2.1 DEM generation

A digital elevation model (DEM) is a quantitative representation of the earth's surface. It provides information on the elevation of each location in the terrain. From this DEM one can also derive other information like slope, aspect, drainage networks, etc. Digital elevation models are therefore important data sources when it comes to the assessment and analysis of a terrain and its relief (Jacobsen, 2003). The data comes as an image (raster) and contains an elevation value for each pixel referenced to a vertical datum.

While DEM is a commonly used term, it is not a very specified term. The terms digital terrain model (DTM) and digital surface model (DSM) are more precise. A digital surface model represents the earth's surface including all its objects, like trees and man-made objects. A digital terrain model represents the bare ground of the earth's surface, without any vegetation or buildings. This difference is also visualized in Figure 1. DEM is often used as a generic term for both DTMs and DSMs, but sometimes also given the same definition as a DTM (L3Harris, n.d.). In this study the generic term DEM will be used.

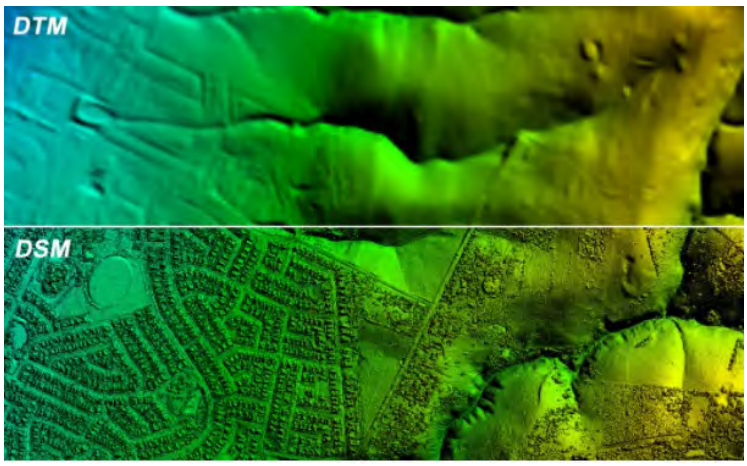

Figure 1 The difference in a digital terrain model (DTM) and a digital surface model (DSM) (Singh, 2013)

When generating a digital elevation model of an area, first the points on top of the visible surfaces will be detected. The first model will thus be a digital surface model. Only after filtering out all the points that do not lie on the earth's surface, a DTM is generated. Because this study focusses on the alpine and nival zone of Mount Ushba, where there are no man-made objects and very little vegetation, this step is not necessary.

Digital elevation models can be generated using satellite imagery, radar or lidar. When using optical images, cloud free imagery and sufficient light conditions are needed. Radar is not hindered by clouds, although heavy rainfall does affect the measurements. Also the geometric situation in mountainous areas is difficult with radar (Jacobsen, 2003).

To generate a DEM with optical images, two or more images showing the same area from different directions are needed. This stereo-photogrammetry technique is shown in Figure 2. To determine the location and elevation of the ground point the projection center has to be known as well as the exact view direction.

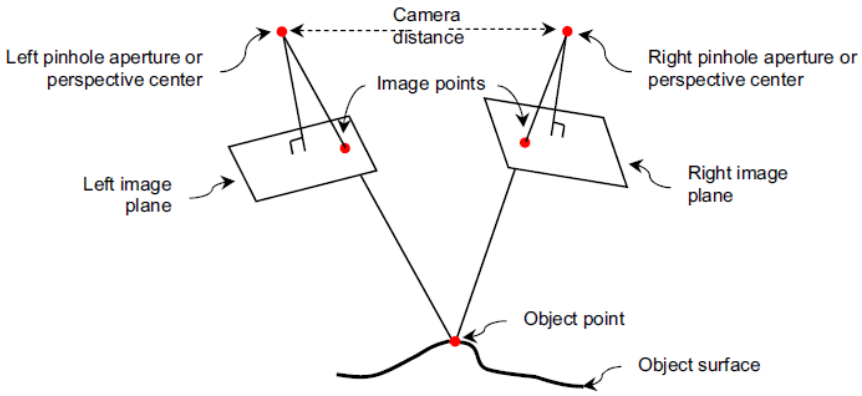

Figure 2 Stereo-photogrammetry (Thevara & Ch, 2018)

Stereo matching thus finds points in one image of the stereo pair that corresponds with a point in the second image. There are different algorithms to correlate points in the stereo-pairs. One of the commonly used methods that gives good results is semi-global matching (SGM), which combines the concepts of global and local stereo methods for fast, accurate, pixel-wise matching (Dall'Asta & Roncella, 2014). This method was developed by Heiko Hirschmüller (2008) in 2005. The SGM method uses two competing cost functions. The first step is a simple area based matching, where an image patch of is converted into a binary vector. Pixels with a grey value larger than the value of the center pixel are set to 1, the others to 0. The Hamming distance can then be computed for the different values in both vectors, resulting in a cost function. This is a very fast method that is not sensitive to radiometric difference and robust to outliers (i.e. occlusions and discontinuities). The second step is pixelwise matching. Here the Hamming distance over all pixels is calculated, with penalties for pixels with disparities.

Because of the pixelwise matching the method is also able to handle object discontinuities, which would be smoothened out when only using a global stereo method.

The quality of the generated DEM can be assessed by looking at the accuracy. This is most commonly done by looking at the standard deviation, defined on a probability level of 68%. The accuracy of the height value that is retrieved using the two images, depends on the accuracy of the x-parallax Spx (px = difference of image coordinates x' – x") and the height to base relation of the imaging configuration (Jacobsen, 2003).

The base to height (B/H) ratios differ for each satellite and influence the accuracy of the DEM. Hasewega et al. (2000) researched how exactly this ratio of stereo images influences the DEM accuracy. Traditionally a ratio between 0.35 and 0.75 was needed for manual photo interpretation, but these numbers differ for automatic stereo matching. By using image pairs with B/H ratios ranging from 0.1 to 1.35, they created digital elevation models and compared the outcome elevations with ground control points that were measured with a GPS survey. The height offset was clearly bigger with a B/H ratio below 0.5. The height accuracy also decreased with B/H ratios higher than 1.0. They therefore conclude that base to height ratios between 0.5 to 0.9 are the best values for automatic DEM creation form stereo pairs.

2.1.1 DEM generation with PlanetScope Imagery

The PlanetScope imagery used in this study has a small scene footprint and a small off-nadir angle, resulting in a B/H ratio that is often below 0.1 (ratios of the imagery used in this study can be found in chapter 3.1). This is clearly not the most ideal ratio for DEM generation. The weak stereo geometry due to the small B/H ratio can partially be compensated by better image matching due to the smaller baseline and bigger overlap of the images. The small baseline also leads the less occlusion, something that is particularly of interest in mountainous terrain like Mount Ushba and its surroundings. Ghuffar (2018) shows that also with the small base to height ratio it is possible to generate a DEM with a sufficient quality. The DEM he generated with the PlanetScope imagery was compared with a reference LiDAR and ALOS DEM. The normalized median of absolute deviation (NMAD) is calculated, which is a robust estimator of the standard deviation. The NMAD of the elevation differences between the LiDAR and the PlanetScope DEM is 4.1 meter, and 3.9 meters for the ALOS DEM over stable terrain. When considering the entire area the NMAD of the elevation differences between the ALOS and PS DEM is a lot larger however, at 20.69 meters. A visual comparison of the three digital elevation models with the use of a hill shade, does show that PlanetScope DEM contains more noise than the other DEMs (Figure 3). Both the ALOS DEM and the PlanetScope DEM are created from stereo/multi view images. This technique comes with low texture areas and occluded pixels, leading to higher elevation errors. In shadow areas, common in imagery of mountainous terrain, the texture is not discernible,

resulting in a poor image matching performance. This results in a bias towards higher elevations in shadowed regions of the terrain (Ghuffar, 2018).

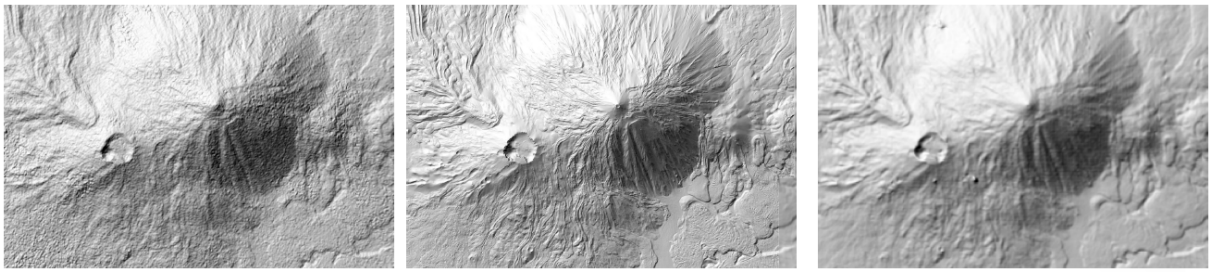

Figure 3 Hill shade of PlanetScope DEM (left), LiDAR DEM (center) and ALOS DEM (right) (source)

2.2 Relief Depiction

> "*As relief influences disposition of all the other objects displayed on maps, terrain representation plays one of the key roles in the map creation process.*" (Farmakis-Serebryakova & Hurni, 2020, p.1)

This representation of the terrain, the topographic information, can be depicted in multiple ways. The common methods for relief depiction are hachuring, hill shading, form lines and contours. "As technology has advanced, mapmakers have been confronted by a dichotomy of requirements: maps, on the one hand, can be made to portray the surface so that the viewer can develop a clear understanding of the nature of the land surface. On the other hand, maps can be made to provide specialists with a means of measuring and analyzing the surface" (Robinson, 1982, in Collier et al., 2003, p.25).

2.2.1 Contour Lines

The first relief depiction technique discussed are the contour lines, or also known as isolines. These lines connect points on the surface with an equal value. Contour lines are often used to depict lines of constant elevation but are also used for the visualization of for example air pressure or population density (Eynard & Jenny, 2016). The first map with contour lines is attributed to Milet de Mureau in 1749. But already around 1696 did Pierre Ancelin make use of a line that shows equal depths on his map *Mondt van de Maes* (Figure 4). Due to the lack of height information the use of contour lines on a larger scale took a bit longer. The heights shown on the maps had to be derived with the use of triangulation or barometric heighting, a time consuming process. It was not until the national surveys in the 19th century that the contouring was generally adopted. It was also common to combine the contour lines with hachures and/or a shaded relief. It was believed that this results in a better relief visualization (Collier et al., 2003).

Figure 4 Mondt van de Maes (Wouda, 2014)

In the beginning the production of contour lines was a time consuming and costly technique. The higher the density and accuracy of the contours, the higher the costs. Most maps did therefore not have a very high accuracy and the maps could not really be used for scientific research. For this, more accurate measurements still had to be taken in the field. The opinions on the required accuracy of the contour lines were very varied. Collier (1972) has also shown that the contouring made in the late 19th and early 20th century could have significant errors, when comparing them to photogrammetric contours. The planimetric errors could be up to 750 meters, and errors in the elevation values, especially on steep slopes, could be up to 30 meters. The photogrammetric contours nowadays have much better accuracies, with errors of plus or minus half the contour interval.

In different parts of the world different approaches to contouring have been developed. Most maps at a 1:25,000 scale use a 5-meter equidistance for the contour lines, and a 10-meter interval for maps at 1:50,000. Countries with a more mountainous terrain use larger intervals, with 20 meters for 1:50,000 scale maps. Another aspect that is approached differently are the contour labels. These can be placed up-slope, putting them upside down on north facing slopes. This is the most common approach, but it is also possible to place the labels on a west to east direction, which would prevent inverted values. Both have their advantages. The first approach makes it easier to determine the aspect of the slope the values are depicted on. The second approach

makes it easier to navigate with the map, since north can stay north on the map while still being able to read all the labels. In the United Kingdom it is also common practice to place the labels in flights up the slope, placing them in ladders. This way one can easily see which direction the numbers are going, making it easier to also determine the aspect of the slope (Collier et al., 2003).

Collier (2003, p.25) also states “contouring is generally regarded as the least effective method of creating the illusion of three dimensions in the mind of the map user”. These contour lines do however offer the advantage of the option to extract the height location for a certain location more accurately (Imhof, 2007). The use of color for layer tinting could be a solution to the lack of a 3D illusion. Eynard and Jenny (2016) have researched the impact of illuminated and shadowed contour lines on the terrain representation and the user’s ability to read the topography correctly. With the illuminated contour method the goal is to create the feeling of a third dimension. This is done by varying the line width and color based on the illumination coming from a specific angle. This is similar to the technique to create a shaded relief. The shadowed contour line method does not use multiple colors, only the width of the lines varies. The lines are the thickest on the shadow side and thinnest on the illuminated side (Figure 5).

Figure 5 Different styles of contour lines (Eynard & Jenny, 2016)

Eynard and Jenny (2016) tested how well the height differences were interpreted with the different methods. Map readers could interpret the relative height differences between points better with the illuminated contour lines technique compared to the conventional contour lines and a shaded relief. The study participants were also able to determine the highest location on the map with the same speed and accuracy with illuminated contour lines as with labeled conventional contour lines. Due to a lack of GIS software packages that offer illuminated and shadowed contour lines, they are not widely used to date. Eynard and Jenny (2016) suggest that these alternative contour line techniques could me used more often for an improved terrain visualization and also created a software package to do so.

2.2.2 Shaded Relief

Another way to depict the relief of the terrain is with relief shading. The shaded relief creates a 3D effect which allows the map user to read the topography of the terrain in a more intuitive way. This terrain representation was originally done by hand. Nowadays there are digital elevation models available for every corner of the earth's surface and is analytical relief shading the more common technique. Analytical relief shading is the computer-based process of generating a shaded relief from a digital elevation model (DEM) (Jenny & Räber, 2015). Even though this technique is a lot faster and makes the process repeatable, it often does not perform as well as manually created hill shading. It is not capable of displaying all features in the landscape as clearly for the user, for them to be able to distinguish correctly between all different landforms (Farmakis-Serebryakova & Hurni, 2020).

Eduard Imhof (1965) explains how hill shading can be integrated into the topographic map effectively to give the map user a three dimensional impression of the relief. This will provide a better perspective view on the earth's surface and understanding of the terrain. However, not everyone agrees with the use of shaded reliefs. Leonhard Brandstätter (1983) writes in his book that hill shading "distorts the view from the essential topographic information and has only the effect of misleading the user" (Kriz, 1999). Some parts of the terrain will be emphasized more and others will be pushed back into the background. According to Brandstätter this could convey false topographic information.

For the hill shading the metric framework of the topography gets transformed into a continuous surface. The most common method in analytical relief shading takes an artificial light source under a certain angle. The tonal variations of the shading depend on the angle of each slope faced to the light source (Collier et al., 2003).

There are three main hill shading methods based on the angle of illumination. The first method contains a vertical light source. The light comes directly from above, which produces darker tones on the steep areas and lighter tones for the flat areas in the terrain. The second method uses an oblique light source. In this case the light rays will reach the terrain from an angle, commonly from the north-west direction. With this method the flat areas will receive a medium tone since they are at an angle from the light source. The slopes however that are facing towards the light source will be in the lightest tone, and vice versa, the slopes facing away from the light source will get a darker tone, the shadow side of the hills and mountains. The tone of the hill shade is thus dependent on the slope, aspect, and steepness of the area (Collier et al., 2003). The third method is a combination of the two different light source angles. The flat areas remain un-shaded, but the slopes with different orientations keep different levels of shading.

The interaction between the light source and the objects also influences the shaded relief. There are two types of illumination models, local and global models. When using a local model, only the direct effect of the light source on the objects is taken into account. A global model on the other hand also incorporates the interaction between the different objects, including the reflection, transmittance, or refraction (Jenny & Räber, 2015b).

Some aspects are hard to mimic with the use of an automatic hill shading technique. Trained cartographers are able to distinguish quickly between important characteristics that will represent the topography well. They also have knowledge about the terrain and its different landforms, something that is not considered with analytical hill shading. When creating the shaded relief by hand, it is also possible to slightly deviate the direction of the light source for some areas of the terrain that have their ridges or valleys in the same direction (Collier et al., 2003). This way also these areas will receive some more variation in the tone of the hill shade and are easier to interpret by the map user. This will increase the recognition of landforms on the map by the map user (Hurni, 2008).

The tone of the hill shade can also be adapted to convey specific parts of the terrain effectively to the map user. Big changes in slope angle, for example on a ridge, should also clearly show a sharp change in the tone of the hill shade. Also, the more or less horizontal areas that are in between the light and dark tones, have a medium, less present tone so the symbols and other layers in the map will be brought out better. The shading can also be done in different colors, for example based on the landcover. A green tone of shading for forest are a blue tone for glaciers for example (Collier et al., 2003).

To create a proper shaded relief that represents the terrain and the landforms well, the cartographer has to be able to read the terrain. Because there are many different types of terrain and the drawing is also artistically influenced by the cartographer, it is difficult to establish a convention when it comes to hill shading (Farmakis-Serebryakova & Hurni, 2020).

An influential cartographer that helped invent the Swiss style shaded relief is Fridolin Becker (1854-1922). Becker followed five main principles to create his shaded reliefs (Schertenleib, 1997, in Räber et al., 2009):

1. The map's highest elevations are depicted by the brightest tones on the illuminated sides and the darkest tones on the shadow sides.
2. The strength of the shading diminishes towards the valleys.
3. Instead of white, a medium tone is used for valley floors that visually connect the two adjacent mountain slopes.

4. The highest mountain peaks must be depicted with the strongest color contrast. Colors should be attenuated for lower areas to simulate the effect that aerial perspective has on colors. Color contrast must be reduced for the lowest terrain features (i.e., valley floors).
5. Cast shadows should not be used.

These principles are clearly seen at work in one of the first map examples made by Becker. Figure 6 shows a section of the Cantus Glarus map, produced in the Swiss style. The highest elevations show the brightest tones that switch to a dark shadow side, resulting in sharp ridges. Also, the medium tone in the valleys is visible, with a light green tone. The higher elevations have more vivid colors compared to the valleys, contributing to the feeling of an aerial perspective.

Figure 6 Section of the Cantus Glarus map (Räber et al., 2009)

Over the years these principles are still used and adapted by cartographers. Many hiking and tourist maps are based on his ideas. Even though some of his principles have been changed, developed further, or experimented with, Becker's main principle remains the same and is still valid today: "a brief look at the map should be enough to grasp the shape of the terrain" (Räber et al., 2009).

2.2.3 Rock Depiction

Most rocky areas of mountains are difficult to reach due to their ruggedness and high elevation. This together with its complexity, rock areas have been difficult to map accurately. Only when the rock hachuring was invented in the nineteenth century, with the shading hachures applies to the rocky areas, did the rock depiction reach a higher accuracy (Imhof, 2007).

With the introduction of photogrammetry, contour lines could also be generated for high rocky mountainous areas, at the same accuracy as the rest of the terrain. According to Imhof (2007) “contours, in steep rocky areas, often lead to an indecipherable, illegible and confusing chaos of lines”. This can be solved by increasing the contour interval for those areas, combining the contours with skeletal lines or by adding color and shading. Imhof however also states that combining different techniques of portrayal seldom provide satisfying solutions to the graphic problem. One has to find the best possible solution for each situation, for the specific problem and purpose of the visualization. “Generally speaking, there are no ideal solutions to the problem of steep rocks” (Imhof, 2007, p.236).

Rock can be represented in multiple ways and different styles. The depiction can be achieved by contour lines, contour tones, ridge lines, hachures, hairlines and orthophotos. Dahinden (2002) created a classification of all the different rock representations (Figure 7). However, the paper does not draw a conclusion on the most effective method.

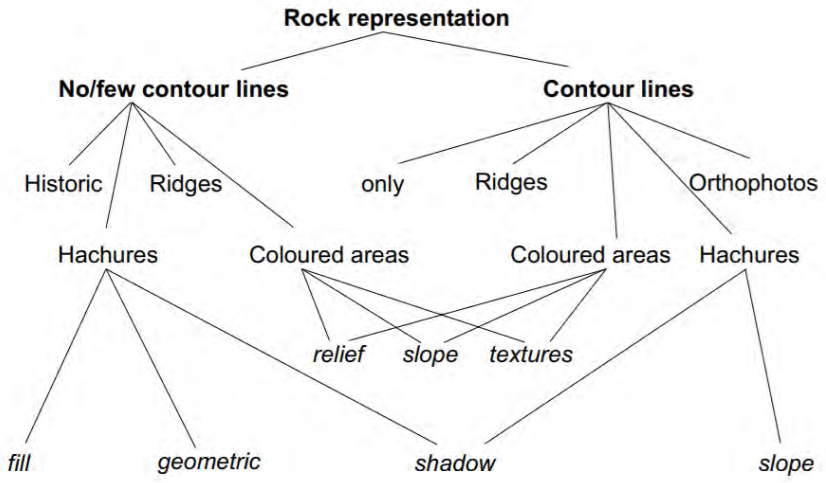

Figure 7 Classification of rock representations (Dahinden, 2002)

Dahinden (2002) does provide multiple reasons on why it could sometimes be preferable to create a rock depiction without contour lines:

1. Height information is sometimes not accurate enough for high rocky areas to draw contour lines.
2. Sometimes a more accurate map is not required (this could save costs)
3. The distance between the contour lines in steep areas is so small, that the map becomes illegible.
4. Map users are not trained well enough to properly read the contour lines.

As mentioned before, a very well known and common method of rock depiction is hachuring. These hand drawn rock hachures are produced by specialists, a time consuming and expensive method, known as one of the most difficult cartographic endeavors (Dahinden, 2002). “The [Swiss] hachures method uses contour lines and skeletal outlines of geomorphological features to provide a general framework that is eventually filled in with hachures” (Jenny et al, 2014, p.360). The hachure length depends on the length of the slope, the thickness is established by the steepness of the slope and the density can be used to determine the degree of slope. To convey the relief even better to the user, shadow hachures are applied. A light source, normally from the north-west, illuminates the hachures, resulting in darker lines on the shadow side and lighter ones on the illuminated side, giving a 3D-impression (Collier et al., 2003).

At the ETH Zurich a lot of research has been done into the interactive and automatic generation of a rock depiction. Hurni et al. (2001) created software that simulates the cliff hachure technique applied in the Swiss National Maps, using fill hachures. The first method automatically drew the ridge lines and the upper and lower edge lines, using random functions to simulate a natural appearance (Hurni et al., 2001). The upper and lower edges still had to be digitized by hand however, which required someone with a good knowledge of the relief interpretation. For the second method the software was developed further and automatically created cliff hachure fillings similar to those in the Swiss maps. The edge and ridge lines are no longer needed. “Continuous cliff faces with equal slope and aspect are covered with regularly placed hachures, either horizontally or vertically” (Hurni et al., 2001, p.62). These areas of equal slope still have to be digitized by hand, and the desired type of hachures (single or filled) and the direction have to be indicated (parameters that can be set can be found in Figure 8). This led to good results, but it is still an interactive technique that requires sound knowledge of the terrain and relief interpretation by the cartographer.

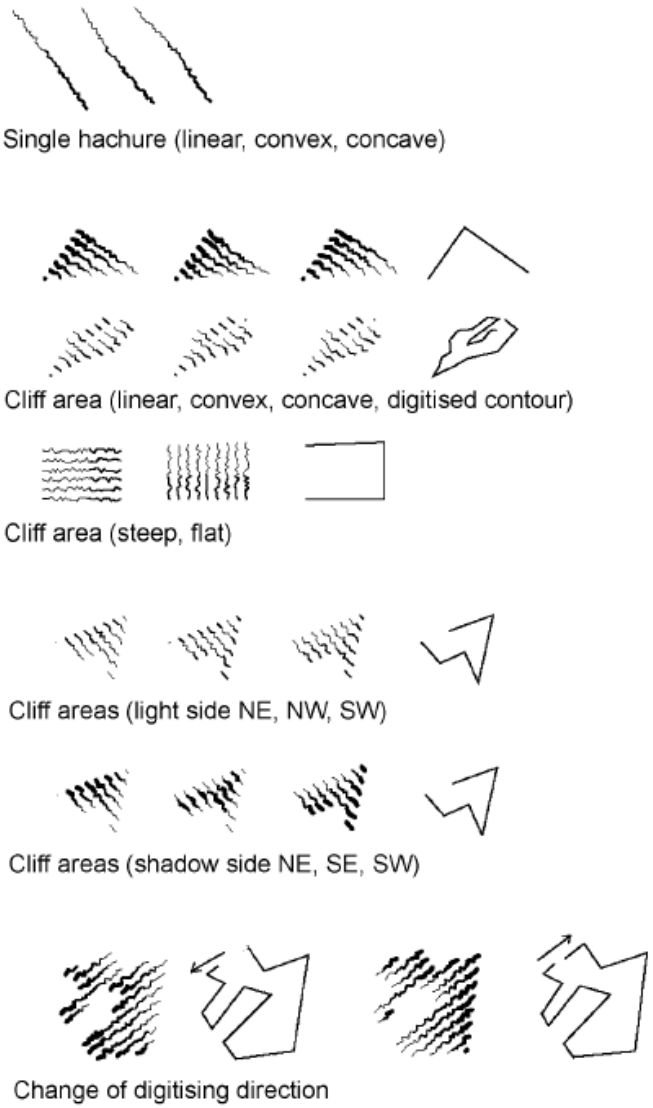

Figure 8 Parameters for interactive rock depiction (Hurni et al., 2001)

At the Institute of Cartography of ETH Zurich a joint study was carried out to evaluate the potential of digital techniques for automating rock drawing (Jenny et al., 2011). Roman Geisthövel developed a method for which no expert knowledge on the terrain and hachuring techniques is needed (Geisthövel, 2017). The program automatically generates a rock depiction based on a digital elevation model, a rock mask and parameters set by the user. More information on how this program exactly works can be found in chapter 4.8.

2.3 Relief Depiction in Alpine Club Maps

Two of the main organizations responsible for creating mountain maps in Europe are the German and Austrian Alpine Club. They have been producing maps for over 150 years and have created a tradition when it comes to high-mountain cartography. The Alpine Clubs have been making maps for the Eastern Alps but are more recently also focusing on regions outside the Alps. So have map sheets been produced for Nepal and now for the Caucasian mountains in Georgia. Most of the map sheets of the Eastern Alps come at a scale of 1:25,000. The contour lines are at an equidistance of 20 to 25 meters. The maps of the extra-Alpine ranges have been produced for about 90 years now as well and have varying scales, ranging between 1:25,000 and 1:100,000 (Brunner & Welsch, 2002).

The first maps that were created had different scales, different visualizations and were created with topographic surveys. These maps are not in use anymore, but the maps that were created at the beginning of the last century still are. This period where a lot of maps were made, almost all at a scale of 1:25,000, is often called the “classic era of Alpine Club cartography”. The maps in use now are mostly updated versions of the maps produced back then. The updating is necessary due to updates in the Alpine landscape, for example new settlements, new infrastructure, or the retreat of glaciers. These revisions happen in intervals of around 8 years (Brunner & Welsch, 2002).

The Alpine Club has a different approach for the rock depiction than the Swiss topographic maps. Where the Swiss maps mainly try to give a three dimensional impression of the area with the use of a schematic, geometric and perspective rock depiction, the Alpine Club uses a more realistic approach. With the Swiss manner the “major ridges are depicted but they are subordinate in order to achieve a holistic impression” (Kriz, 1999, p.2). The Alpine Club Cartography combines a schematic realistic rock depiction with a perspective view of the rocks. All the contour lines are still present in the rock areas, unless the slope is too steep, and there is no difference in illumination of the rock depiction.

Figure 9 Difference in rock depiction of Swiss topographic maps and Austrian topographic maps (Kriz, 1999)

The Alpine Club has been mapping for over 150 years and developed different styles and methods for rock depiction over the years. Arnberger (1970) groups these into four approaches that are also shown in Figure 10:

1. The **genetic** approach does not use contour lines in the rock areas. This improves the legibility but the map does not have a very high geometric accuracy due to the missing isolines.
2. The **signature** (delicate hachuring line) approach does include contour lines in the depiction. These maps have a reasonable geometric accuracy and the rock depiction is created with very delicate hachuring lines.
3. The **geometric integrated** approach is the most recent style and uses the contour lines as the main representation for the rock depiction. “Furthermore, rock depiction is supported by using schematic, geometric hachuring and in most cases originally not combined with hill shading in order not to distort the genuine topographic information” (Kriz, 1999, p.3).
4. The **Combined Federal Mapping Agency** approach is a reproduction of special areas by the Federal Mapping Agency.

Figure 10 The different approaches of rock depiction of the Alpine Club Cartography (Kriz, 1999)

3 Data

To conduct a study, data about the research area is needed. To generate a digital elevation model and create a relief depiction one needs satellite imagery for the topography and information on the landcover for the relief depiction.

3.1 PlanetScope imagery

For the generation of a digital elevation model satellite imagery is needed. For this study high resolution PlanetScope imagery is available for the Ushba region through the University of Dresden. This imagery can be a valuable data source for DEM generation, since Planet captures the entire world's landmass every day. This makes the PlanetScope Imagery very suitable for studying and analyzing dynamic phenomena, like glacier surges. The combination of the daily revisit time and high resolution offers a high potential, as other available imagery often has a lower revisit time or resolution. Also, on demand acquisition of imagery to study temporal changes is very costly (Ghuffar, 2018).

Planet operates the PlanetScope Earth-imaging constellation which consists of multiple launches of groups of individual satellites. Planet launched 136 so-called Dove satellites in 2017. These satellites are all CubeSat 3U form factor satellites. CubeSats are miniature satellites that come with the small dimensions of 10 cm by 10 cm by 10 cm and weigh as little as 1.33 kilograms. In total 1600 CubeSats have been launched as of August this year. The Dove-1 satellites image the world in 4 spectral bands (blue, green, red and near-infrared) (Planet, n.d.) at a resolution of approximately 3.7 meters (Planet, 2021). The satellites carry a PS2 telescope paired with a 2D frame detector. The detector is 6600 pixels wide and 4400 high (see Figure 11) and has a Bayer pattern filter. This filter separates the wavelengths of light into red, green, and blue. On top of the Bayer filter is an additional 2-stripe filter. This filter only lets through RGB light to the top section, and only NIR wavelengths to the bottom section.

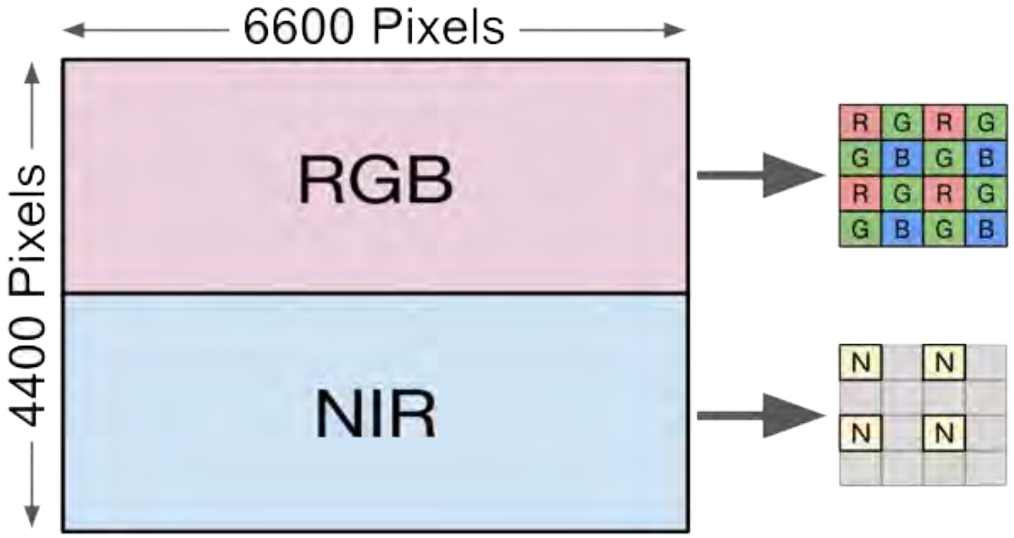

Figure 11 PS2 telescope (Planet, n.d.)

Because of these filters, each scene made by one of the satellites consist of a top half in RGB and a bottom half in NIR (see Figure 12). To create a 4-band image, with both RGB and NIR for every section, the adjacent imagery is used. By combining the RGB half with the NIR half of the overlapping adjacent scene, a 4-band image is created.

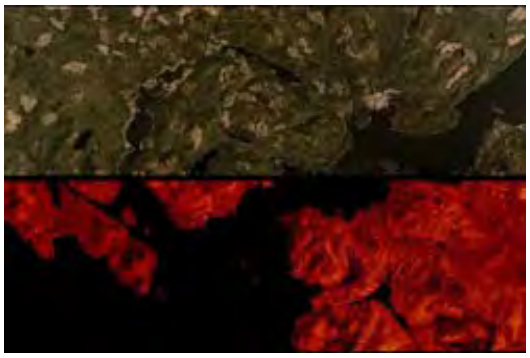

Figure 12 RGB and NIR half in each frame (Planet, n.d.)

The imagery comes as a TIF file and is accompanied with two data masks, an unusable and usable data mask (UDM and UDM2) and a rational polynomial coefficients (RPC) file. The RPC file contains the transformation between the pixels in the imagery and their ground location, the geographic coordinates. The ground sampling distance (nadir) is on average 3.7 meters at a reference altitude of 475 km. This means that the pixel size is between 3.7 meters and 4.1 meters, dependent on the altitude. Geometric corrections are applied using altitude telemetry and ephemeris data and refined using ground control points. The positional accuracy of the imagery is stated to be less than 10-meter RMSE (Planet, 2021).

The scene footprint is approximately 24 km by 8 km. A new image is captured every second, so there is a small overlap between the adjacent images. Planet tries to capture all these images in a nadir pointing mode, but there is a light variation from the strict nadir angle. This so there is better daily coverage of the Earth. This does however result in off-nadir angles up to ±5 degrees. The combination of the relatively small footprint and the small off-nadir angle of most scenes, results in a baseline to height (B/H) ratio that is not optimal for DEM generation. The overlapping PlanetScope images often have a B/H ratio of less then 1:10. For this study 11 images were selected that cover Mount Ushba and its surroundings. All 11 scenes were taken in August 2019 and are listed below. The B/H ratios for the 11 selected images can be found in Table 1 Base to height ratios of the 11 selected images

1. 20190809_061956_1054_1B_AnalyticMS.tif
2. 20190815_062014_1048_1B_AnalyticMS.tif
3. 20190815_062015_1048_1B_AnalyticMS.tif
4. 20190815_073155_0e0f_1B_AnalyticMS.tif
5. 20190815_073156_0e0f_1B_AnalyticMS.tif
6. 20190816_061701_0f49_1B_AnalyticMS.tif
7. 20190816_061702_0f49_1B_AnalyticMS.tif
8. 20190823_061631_104b_1B_AnalyticMS.tif
9. 20190823_061632_104b_1B_AnalyticMS.tif
10. 20190823_074023_1032_1B_AnalyticMS.tif
11. 20190823_074024_1032_1B_AnalyticMS.tif

IMAGE	1	2	3	4	5	6	7	8	9	10	11
1	0.000	0.072	0.072	0.095	0.092	0.069	0.069	0.046	0.045	0.115	0.114
2		0.000	0.017	0.117	0.109	0.140	0.141	0.116	0.116	0.120	0.114
3			0.000	0.113	0.108	0.141	0.140	0.118	0.115	0.114	0.110
4				0.000	0.016	0.114	0.110	0.101	0.094	0.031	0.036
5					0.000	0.114	0.112	0.099	0.094	0.035	0.032
6						0.000	0.017	0.026	0.027	0.143	0.145
7							0.000	0.034	0.026	0.139	0.143
8								0.000	0.017	0.128	0.128
9									0.000	0.121	0.124
10										0.000	0.017
11											0.000

Table 1 Base to height ratios of the 11 selected images

As described in chapter 2.1 a small B/H ratio leads to lower accuracy in 3D reconstruction. For the 11 selected images the ratio is mostly around or below 1/10. This

is not optimal for generating high quality DEMs, since there will be a weak stereo geometry. The shorter baselines however do lead to better image matching.

3.2 Existing digital elevation models

To assess the accuracy of the generated PlanetScope DEM, the results are evaluated with the use of a digital elevation model. These models can be generated in different ways, with satellite imagery, radar or lidar. The DEM that is used for the comparison in this study is made with the SRTM elevation data. The Shuttle Radar Topography Mission (USGS, n.d.-a) is an international research effort to create digital elevation models of the Earth's surface. The radars used in the SRTM mission were present on two Endeavor missions in 1994. During the 11-day mission the Endeavour orbited the Earth 16 times each day. This resulted in radar data that covers over 80% of the Earth's land surface, between 60° north and 56° south latitude (USGS, n.d.-a). The C-band radar has a wavelength of 5.6 cm. The technology is based on the principle of interferometric SAR (Ghuffar, 2018). By using two or more synthetic aperture radar (SAR) images, the height can be derived. This is done by looking at the differences in the phase of the waves that are returning to te satellite (Bürgmann et al., 2000). Since 2014, version 3 of the STRTM data is available worldwide at a 1-arcsecond (±30 meter) resolution instead of the previous 3-arcsecond (±90 meter) resolution. The data can be downloaded for free through the United States Geological Survey (USGS) via the EarthExplorer (https://earthexplorer.usgs.gov/).

The SRTM comes in the horizontal datum WGS84 and uses the EGM96 geoid as vertical datum. The resolution and horizontal and vertical datums for the different elevation data sources can be found in Table 2.

	RESOLUTION	HORIZONTAL DATUM	VERTICAL DATUM
SRTM DEM	30 meters	WGS84 / UTM 38N	Geoid | EGM96
PLANETSCOPE DEM	3.6 meters	WGS84 / UTM 38N	Ellipsoid | WGS84
MAP SHEETS		WGS84 / UTM 38N	WGS84 / EGM96
FIELD MEASUREMENTS		WGS84 / UTM 38N	Ellipsoid | WGS84

Table 2 Horizontal and vertical datums for the different elevation data sources

The accuracy of the SRTM data has been evaluated in various studies and meet the accuracies set by the Shuttle Radar Topography Mission. The horizontal accuracy is 20 meters and vertical accuracy 16 meters. Sun et al. (2003) state that the absolute accuracy of the SRTM height in open areas exceeds these accuracies set by the Shuttle Radar Topography Mission. The vegetation does however have a positive bias on the height, as the SRTM C-band interferometric SAR measures a height within the tree canopy. They also noticed a slight increase in the elevation errors with an increasing terrain slope. Gorokhovich and Voustianiouk (2006) on the other hand discovered that the DEM accuracy on slopes steeper than 10° significantly decreases. The SRTM data also underestimates the slopes facing north-west and overestimates the elevation on slopes facing south-east. According to Ludwig and Schneider (2006) the mean error can be up to 30 meters for a slope of 50°.

The original C-band product is also missing data in significant areas. This could be “due to geometric artifacts, specular reflection of water, phase unwrapping artifacts, and voids due to complex dielectric constants because of the nature of radar remote sensing and the interferometric process applied to create the DEM” (Reuter et al., 2007). These voids occur mostly over water bodies or in steep mountainous areas (Gomez et al., 2012). The National Geospatial-Intelligence Agency (NGA) filles these voids using interpolation algorithms together with other sources of elevation data (USGS, n.d.-b).

3.3 Map sheets

Through the University of Dresden multiple sets of topographic map sheets are available. For this study the map “Elbrus and the upper Baksan valley” published by EWP in 2007 is used. This map has a 1:50,000 scale and covers the upper part of the research area. Besides this map also 4 other sheets (13-a-4, 13-b-3, 13-c-2, and 13-d-1) from the trekking maps by Geoland are used for the comparison. These maps come at a scale of 1:25,000 and were printed in 2020. All map sheets have been georeferenced in GIS to be able to use them as a reference source for the PlanetScope DEM. Which vertical datum has been used in the Geoland map for the elevation values is unfortunately not completely clear. Based on the values displayed at the peaks/points, this would correspond with an ellipsoidal height. The contour lines, however, do not match with the elevations given at the points (see Figure 13), and correspond better with the 23 to 24 meter lower elevation values using the global geoid.

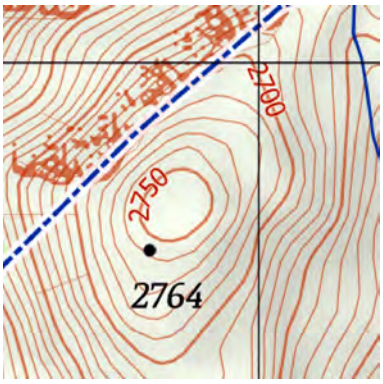

Figure 13 Elevation difference contour lines and points

3.4 Rock and glacier layers

The last data source used for the project, are rock and ice layers. These data sets are the outcome of the master thesis by Maximilian Schröder (2020) on the creation and depiction of rock and ice areas in the Ushba region (Georgia) with the use of multitemporal satellite imagery. Most of the data used for the classification comes from the freely available Sentinel-3 and Landsat 8 missions. By looking at the NDSI and NDVI, the rock and ice areas are detected in the imagery from 2018 and 2019. Figure 14 shows the resulting rock and ice layers, which nicely cover the test area for this study.

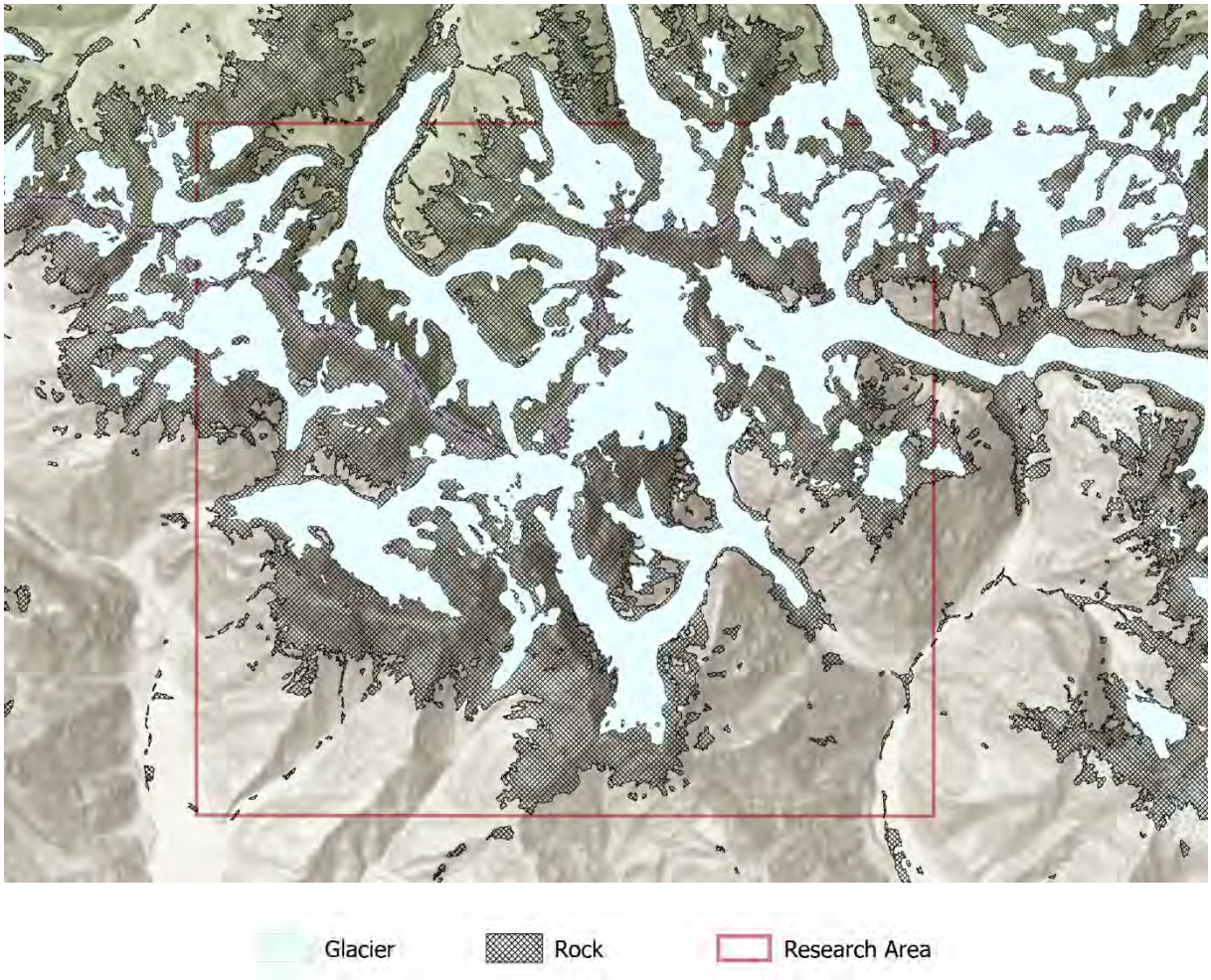

Figure 14 Rock and ice layers by Schröder and the extent of the research area

4 Methodology

This chapter provides the software and methodology used to create the digital elevation model and relief depiction. Also a short description of the area of research is given.

4.1 Software

The processing of the data is done with multiple different programs, different steps require different software. The generation of the digital elevation model is done with Agisoft Metashape. Agisoft provides photogrammetric processing of digital imagery and generates 3D spatial data. For this research Agisoft Metashape Professional (2021), version 1.6.5 was used. The program can perform the orientation of the imagery as well as the dense stereo matching, using a multi-image approach. Unfortunately Agisoft Metashape does not provide any statistical results on the image matching and DEM generation. The entire process is highly automated and very intuitive. However, as described by Dall'Asta and Roncella (2014), the program is almost like a black-box. There is very little information availbale on the algorithms that are used in the software for the different steps and even the parameters that can be set, do not give a clear explanation on what the setting exactly means for the processing step. Based on information available on the user forum, it appears that the depth map calculation is performed pair-wise, where all the overlapping image pairs are used. These are then merged to create the final 3D model.

For the analysis of the DEM and the creation of part of the relief visualization, ArcGIS Pro was used. This GIS application offers many tools for the data processing and analysis. For this, tools from the following toolboxes are used:

- Spatial Analyst tools
- Data Management tools
- Analysis tools
- Conversion tools
- 3D Analyst tools
- Cartography tools
- Image Analyst tools

A tool to fill gaps in the raster data set with a spline interpolation is not available in ArcGIS Pro, only interpolation with inverse distance weighting (IDW) is possible. This option is however offered through a plugin in QGIS. QGIS is a free open-source GIS application. Here the r.fillnulls algorithm provided by GRASS (GRASS Development Team, n.d.) could be used for the spline interpolation.

WAPPP is used to extract the elevation values from the field observations made with the Garmin GPSMAP 66sr. This software, developed by Pr. Lambert Wanninger (2020), processes the GNSS observation in Precise Point Positioning (PPP).

For the relief depiction several programs were used for the different aspects of the visualization. The contour lines could be generated with the use of ArcGIS Pro, but for the creation of a shaded relief Blender was brought in. Blender (2020) is a free and open-source 3D creation suite. With the program it is possible to create a realistic 3D model of the terrain based on the height map. The rock depiction is created with the program PIOTR (2019). This software has been developed by Roman Geisthövel (2017) and accompanies his PHD thesis on Automatic Swiss style rock depiction and can be downloaded for free from the website Motlimot (http://motlimot.net/software.html). The program automatically generates a rock depiction based on the Swiss style. The last software that is used is Adobe Photoshop. In this program for imaging and graphic design the different visualization layers are put together.

4.2 Area of research

Commissioned by the German Alpine Club (Deutsche Alpen Verein), the Technical University of Dresden is creating a map of the area around Mount Ushba. Characterized by its double summit, Mount Ushba in Georgia is one of the most prominent peaks of the Caucasus Mountains. The intended extent of the area to be mapped can be seen in Figure 15, at a scale of 1:33,000.

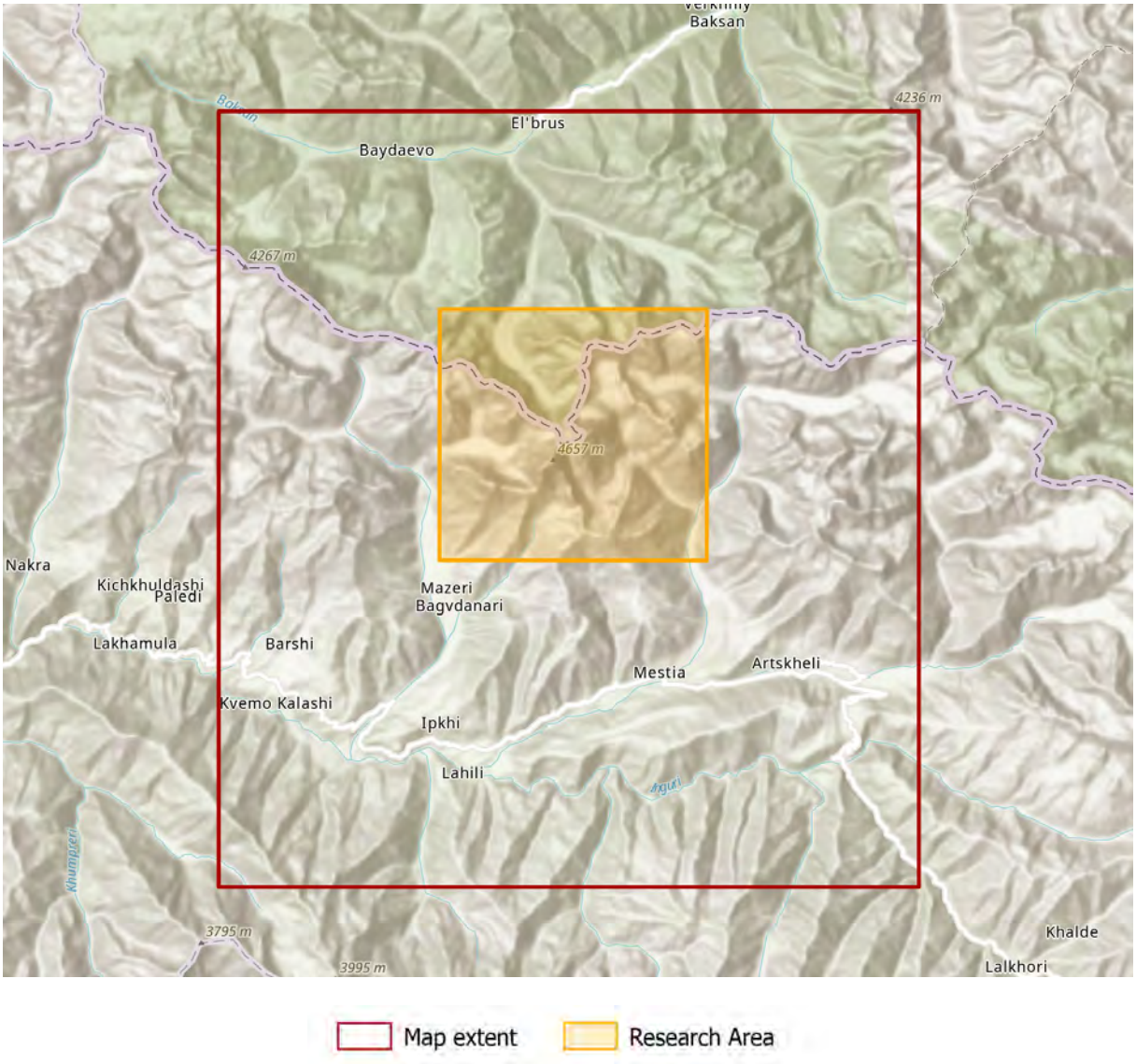

Figure 15 Intended extent of area to be mapped and research area

For this research only a smaller section of that area will be used to test the imagery, DEM quality and processing steps. The size of this section is dependent on the outcome of the DEM generation. For this step 11 satellite images are used, that overlap and contain or lie close to Mount Ushba and cover the alpine and nival zones. Figure 16 shows the overlap of the 11 selected images, the black dots represent the location of the camera.

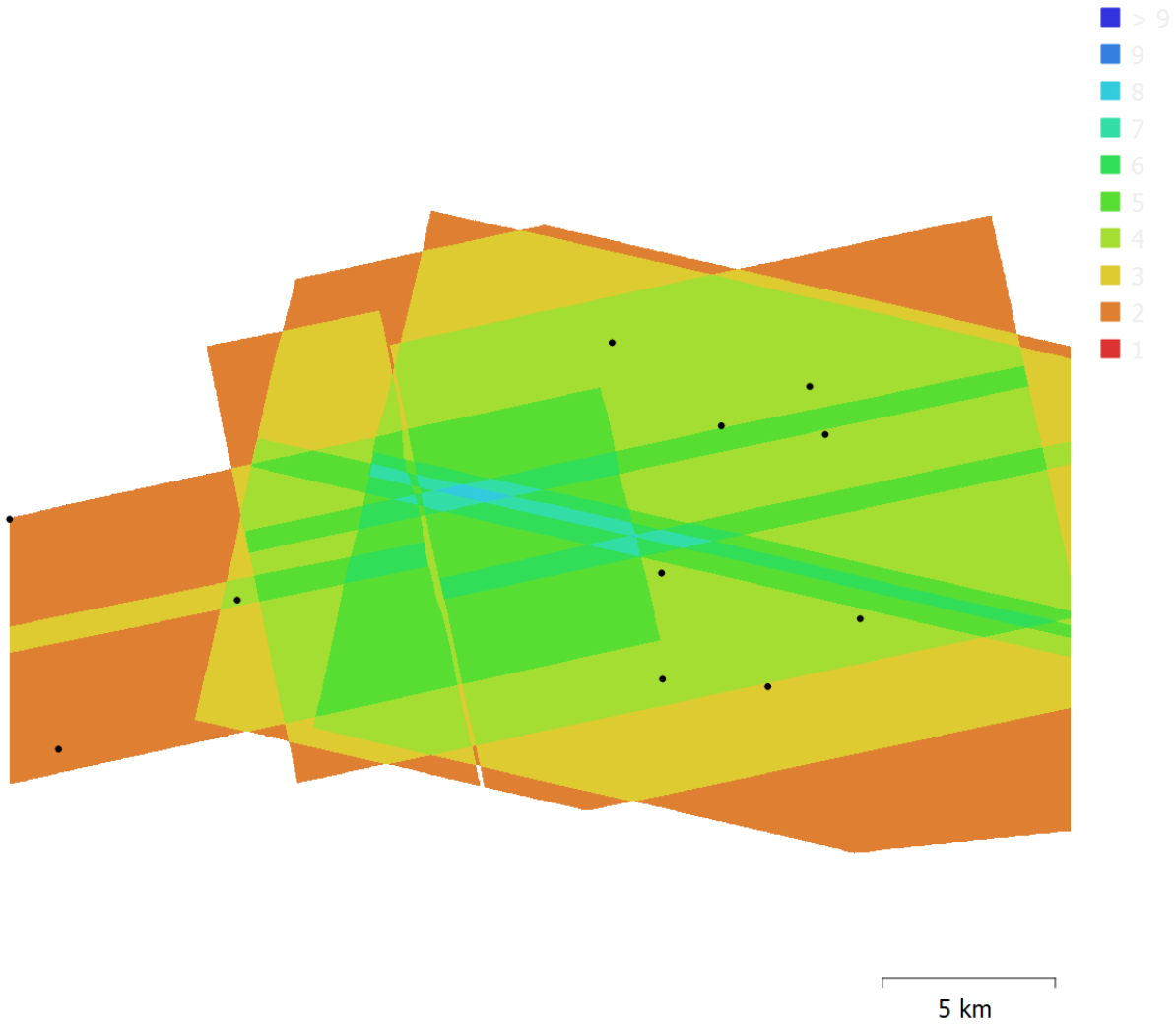

Figure 16 Overlap and location of 11 satellite images

Some areas are only covered in 1 image, others even in 8. For the image matching to take place a point should be at least visible in 2 images. The final extent of the area for which a digital elevation model can be created will therefore be smaller than the extent of the 11 images together.

4.3 DEM generation

In chapter 2.1 a description of the stereophotogrammetry is given. Based on this process a digital elevation model will be generated. This was first attempted with the open-source tool MicMac, and later performed with the commercial software Agisoft Metashape. This process is described in this subchapter.

4.3.1 MicMac

The first attempt at generating a digital elevation model with the PlanetScope imagery was done with MicMac. MicMac is an open-source tool created by the Institut National de l'information Géographique et Forestière in Paris (IGN). With the tool you can carry out all the typical steps involved in generating a digital elevation model. It processes the imagery at multiple resolution levels. The program computes tie points for all image pairs for each of these resolution levels and performs a bundle block adjustment (Dall'Asta & Roncella, 2014). After this the depth maps and 3D models can be produced from the oriented images. This is done with the semi-global matching approach where the surface gets reconstructed by applying the minimization of an energy function (Pierrot-Deseilligny & Paparoditis, 2006).

To start MicMac from the command prompt the command mm3d is used. After mm3d follows the name of the tool and after that the arguments. MicMac is run in the folder with the files.

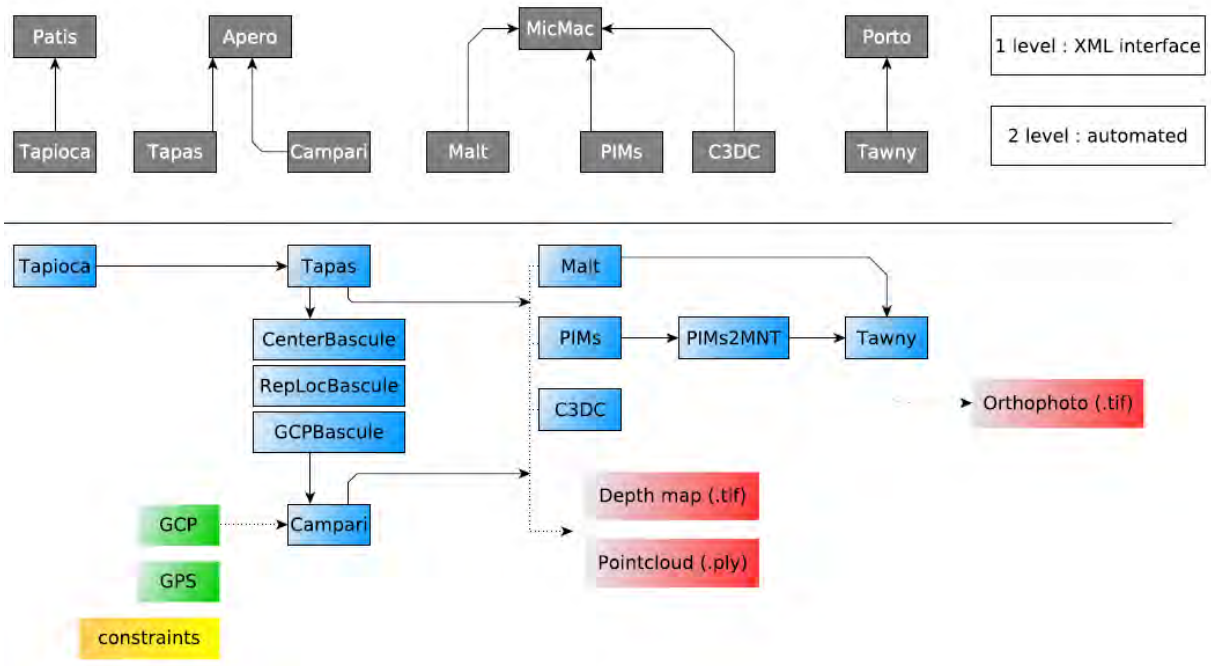

Figure 17 Simplified overview of the core MicMac modules (top) and the processing workflow (below) (Rupnik, 2017)

The first step to create a DEM is to compute the tie points between all images. This is done with the Tapioca tool and the following syntax:

```
mm3d Tapioca All "(.*)AnalyticMS.tif" -1
```

All specifies the way that the tie points are computed. This can for example be done in multiple steps with different scales (*MulScale)* or for all images at a given resolution (*All).* The second argument contains the name of the input files. The last argument is the resolution used to look for tie points in all image pairs. -1 means that it makes use of the full resolution of the image.

After looking for the tie points in the images, the input files with the rational polynomial coefficients have to be converted into a MicMac readable format. The tool used for this is Convert2GenBundle. In windows this command has to be run for every input file. The syntax for the first input file looks as follows:

```
mm3d Convert2GenBundle 20190809_061956_1054_1B_AnalyticMS.tif
20190809_061956_1054_1B_AnalyticMS_RPC.TXT RPC ChSys=WGS84toUTM.xml
Degre=5
```

The first two arguments are the filename of the input image and the corresponding RPC file. The third argument contains the output folder. ChSys defines the metric coordinate system that is to be used in the project (decided by user, see WGS84toUTM.xml below), as MicMac does not work with geodetic coordinates.

```
<?xml version="1.0"?>
<SystemeCoord>
      <BSC>
            <TypeCoord>eTC_Proj4</TypeCoord>
            <AuxStr>+proj=utm +zone=38 +north +ellps=WGS84 +datum=WGS84
      +units=m +no_defs</AuxStr>
      </BSC>
</SystemeCoord>
```

After extracting the tie points and converting the RPC into a MicMac readable format an RPC bundle adjustment is performed with the Campari tool. This tool refines the orientation parameters and takes the imagery and converted RPC information as input.

```
mm3d Campari "(.*)AnalyticMS.tif" RPC RPC-adj DegFree=5 DRMax=5
```

After the bundle adjustment the dense image matching can be carried out, with the Malt tool.

```
mm3d Malt Ortho "(.*)AnalyticMS.tif" RPC-adj DirMEC=MEC DefCor=0
AffineLast=1 Regul=0.005 HrOr=0 LrOr=0 ZoomF=1
```

The first argument, Ortho, specifies the kind of matching that is required. The second argument is the imagery, the third contains the bundle adjusted RPC information and the fourth the output folder. DefCor is the default correlation in uncorrelated pixels, which is

set to 0 instead of the default 0.2. The regularization factor is set to 0.005, computing a high and low resolution ortho are both set to false, and the final zoom is changed to 1.

The malt tool generates depth maps by iteration on sub-sampling models. For the generation of the DEM, the highest resolution output from the iterations is used, Z_Num8_DeZoom1_STD-MALT.tif. After setting the output filename, the DEM can be generated.

```
mm3d to8Bits MEC/Z_Num8_DeZoom1_STD-MALT.tif Out=Ushba_dem.tif
```

The output of this workflow is shown in Figure 18 and unfortunately makes no sense at all. After some contact with one of the developers of the program MicMac and tweaking many of the settings, it seems like generating a DEM with PlanetScope Imagery in MicMac does not lead to any useful results. There is not much literature available on the topic, nor have many people tried to generate a DEM with the combination of this software and imagery. More people on forums also mention that they are running into problem, and no answers to solve this problem were suggested anywhere.

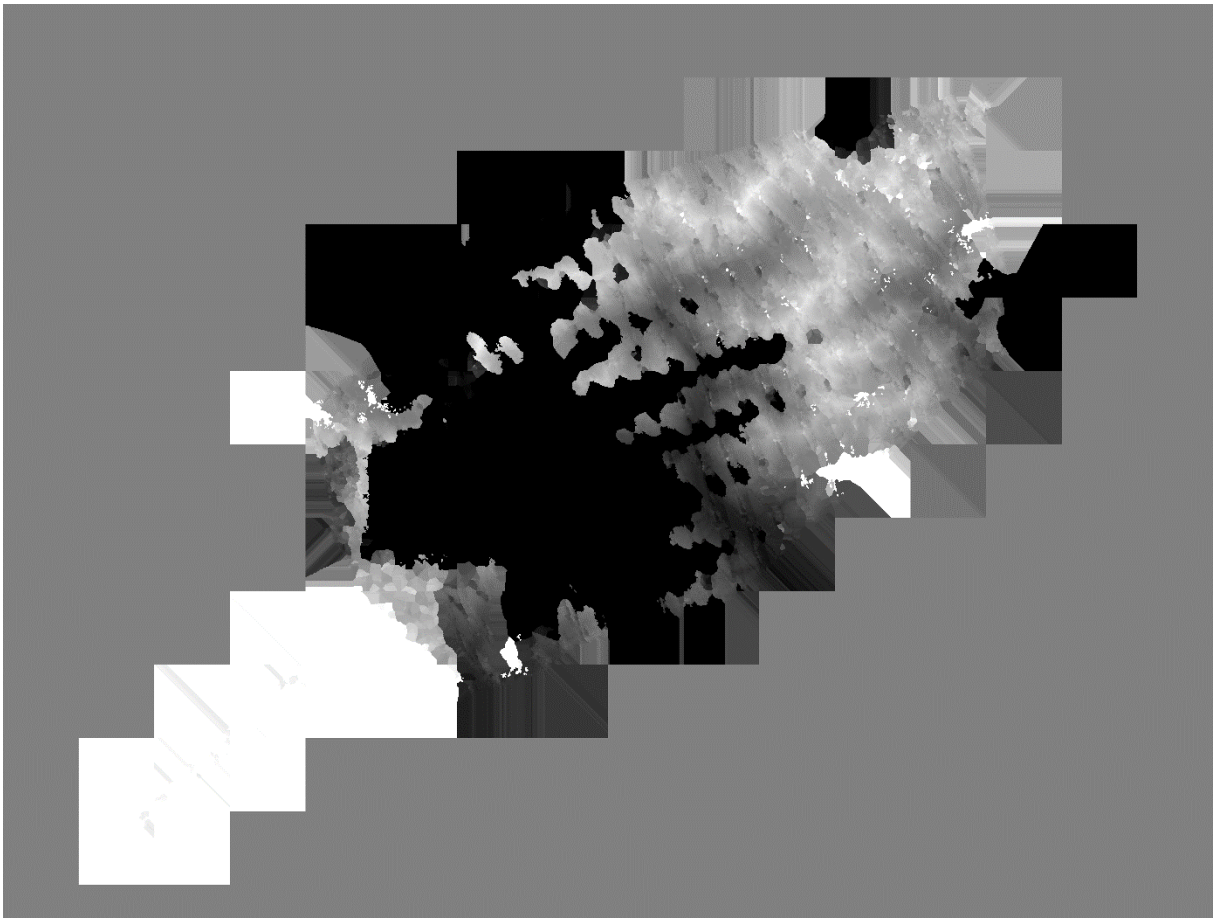

Figure 18 Output DEM generated with MicMac

4.3.2 Agisoft

Because no satisfying results were achieved using MicMac, another program was used in an attempt to create a better DEM, Agisoft Metashape Professional. Agisoft provides photogrammetric processing of digital imagery and generates 3D spatial data. To create the DEM, there are four main steps to be taken.

The first step is the camera alignment. To align the cameras, the imagery first has to be loaded. The 11 selected images are added to the workspace. Before aligning the imagery one can add ground control points (GCP) or RPC information. In the advanced Metashape Preferences, the box is checked to load satellite RPCC data from auxiliary TXT files. These are stored in the same folder as the images and have the same filename as their corresponding image. After completing these settings, the cameras can be aligned. The program will search for common points in the photographs and match these, as can be seen in Figure 19. According to Semyonov (2011) on the user forum of Agisoft the program “detects points in the source photos which are stable under viewpoint and lighting variations and generates a descriptor for each point based on its local neighborhood. These descriptors are used later to detect correspondences across the photos. This is similar to the well known SIFT (scale-invariant feature transform) approach, but uses different algorithms for a little bit higher alignment quality.” It will also find the location of the cameras. To make sure the RPC data is taken into account, the *reference preselection* is set to *Source*, when starting the alignment. The accuracy of the alignment is set to *highest,* and the *key* and *tie point limit* are set to 0, which means there is no limit. The output is a sparse point cloud with 330,880 tie points and the camara positions.

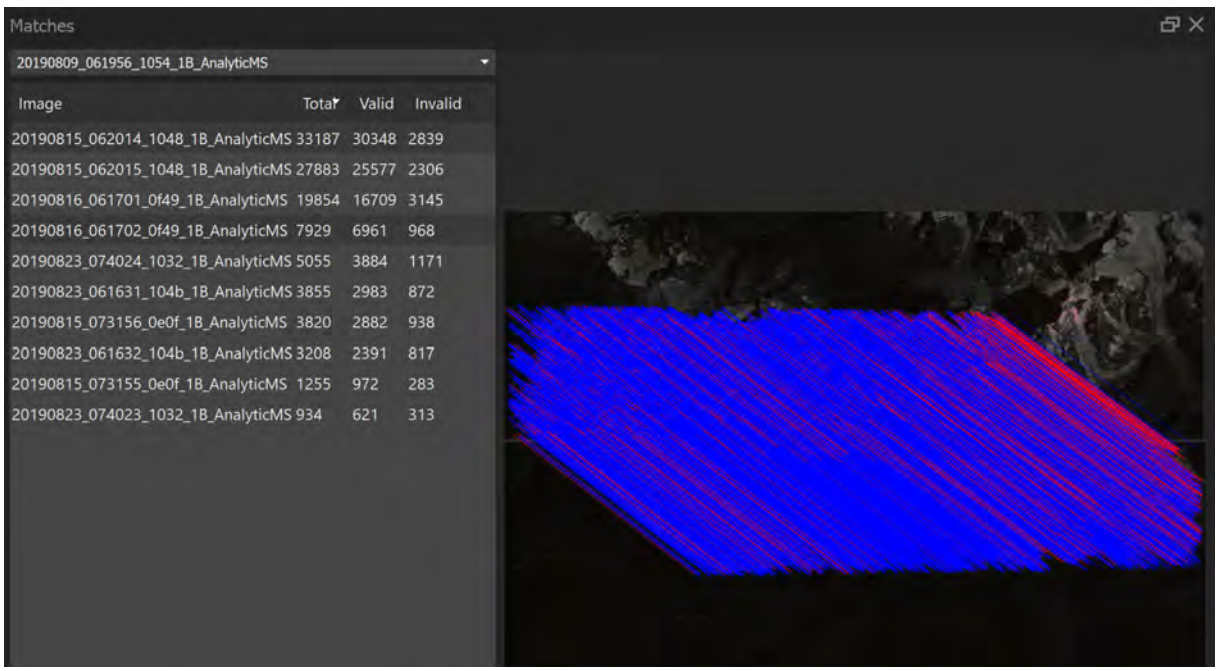

Figure 19 Matches found in the images in Agisoft

As is visible in Figure 19 not all tie points are valid (blue lines are valid, magenta lines are invalid). The certainty of the matching also differs for tie points. To only consider the matches with the better accuracy and certainty, a *gradual selection* is applied to the sparse point cloud. To clean the point cloud, the *Projection accuracy* is set to 10 and the *Reprojection error* to approximately 90% of the maximum number. These settings are based on suggestions by Agisoft users (*Recommended Gradual Filter Settings*, 2017) and tested for the best result, at which thresholds does noise get removed but not the detail or a peak. This creates a selection of approximately 6000 points. These points (see pink points in Figure 20) are deleted from the sparse cloud. The cameras are subsequently optimized (check the boxes cx and cy), so that they will not consider the deleted points for the image matching.

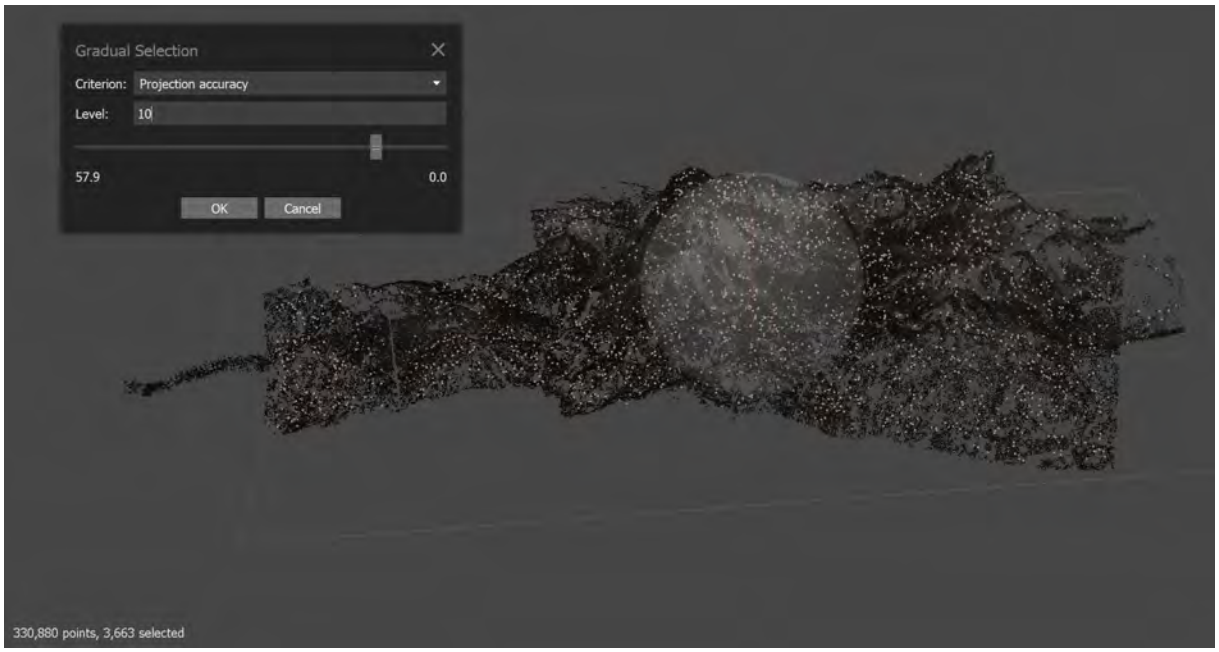

Figure 20 Cleaning of the sparse point cloud in Agisoft

The next step is to generate a dense point cloud. Agisoft Metashape builds this point cloud based on the camera positions and the imagery itself. For the dense cloud generation, the program calculates a depth map for every image. The quality is set to *Ultra High*, so that the photos will be processed at the original resolution. Some issues with the images, like noise or unfocused images, can cause outliers among the points. To filter these out, Agisoft has 3 depth filtering modes. *Mild* filtering is used when there are important small details in terrain that is being constructed. To not loose this detail, one can apply a mild filtering algorithm, so that the important features are not defined as outliers and deleted from the point cloud. When there is a lot of unnecessary detail and noise in the area, then a more aggressive filtering algorithm can be applied. The *Aggressive* depth filtering mode filters out most of the outliers. This setting is

recommended for aerial data processing. There is also a mode that lies in between the discussed *Mild* and *Aggressive* approach, the *Moderate* depth filtering mode.

Based on the dense point cloud created in the previous step, the last step is to generate a digital elevation model. The DEM is rasterized from the dense point cloud, with each raster cell containing the height value for that location. When starting the *Build DEM* tool, several parameters have to be filled. The projection is set to WGS84 / UTM zone 38N, with ellipsoidal heights. Georgia lies in UTM zones 37N and 38N. Because most of the country and the research area lies in 38N, this is the projection chosen for this research and the final map. The maps that are used as reference for this study have their elevation data displayed in ellipsoidal heights. To be able to make a comparison between the PlanetScope DEM and the elevation information in the reference map, they both have to use the same vertical coordinate system. The next parameter, *Source data*, is set to *Dense Cloud*, this gives the most accurate results. The *Interpolation* is enabled, so that the program will calculate a height by interpolation for each area that is visible in at least one of the images. This way voids in the data will be filled by interpolating the surrounding values with inverse distance weighting (IDW). Because all steps were run at the highest quality, the output resolution is the same as the original resolution, approximately 3.6 meters. The resulting digital elevation model is shown below.

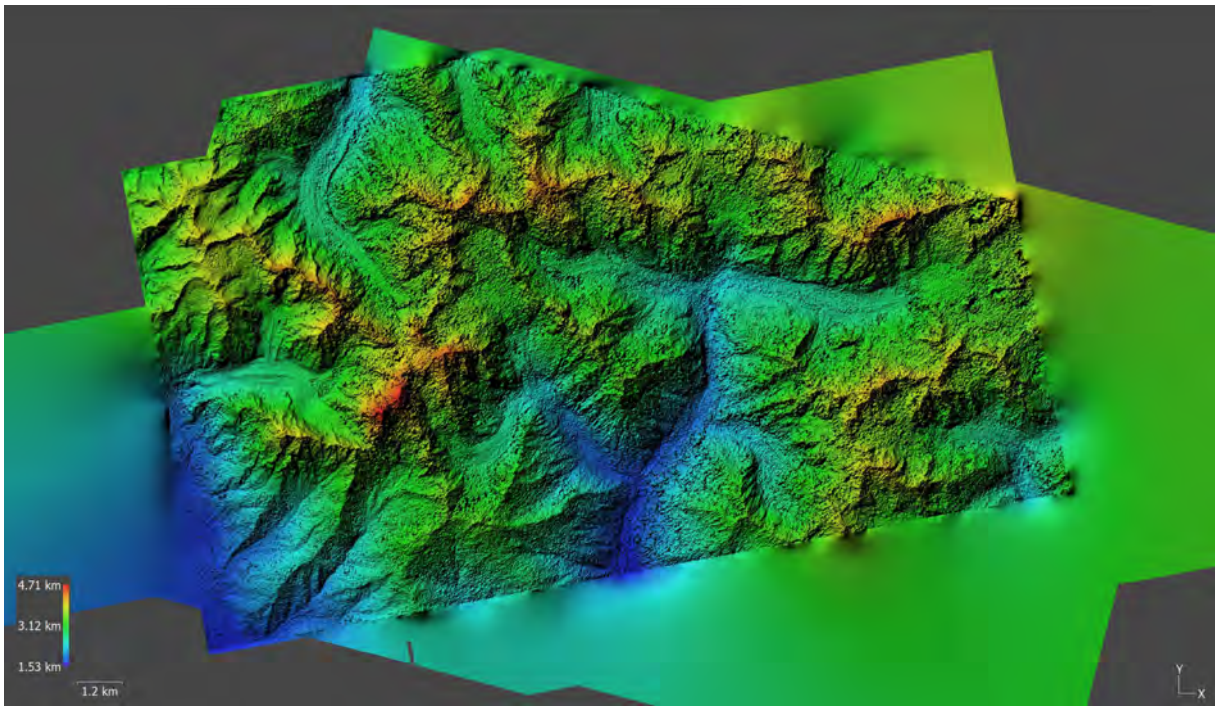

Figure 21 Digital Elevation Model generated with Agisoft

4.4 DEM evaluation

The digital elevation model that was built with the use of Agisoft Metashape has to be evaluated. Several aspects can affect the accuracy of the DEM, like errors during the data collection or in the imagery. Errors in the DEM can also be caused by the terrain. Because of shadows or secluded areas in the imagery due to the mountainous terrain, elevation measurements can have a lower accuracy. To evaluate the accuracy of the generated PlanetScope DEM, the data is compared with several other elevation data sources: the Shuttle Radar Topography Mission (SRTM) DEM, existing maps of the area and elevation measurements taken in the field. This evaluation is done in ArcGIS Pro.

4.4.1 Existing digital elevation models

To evaluate the generated DEM overall, for every point in the terrain, to see if the elevation and shape is the same, it is compared to an existing DEM. The SRTM DEM is open source and can be downloaded for free. As discussed in chapter 3.2 it has a 30-meter resolution and uses the Earth Gravitational Model from 1996 (EGM96), which uses a geoid height. To be able to compare the elevation data of the PlanetScope DEM and the SRTM DEM, they both have to be in the same vertical coordinate system. The SRTM DEM is therefore changed from EGM96 to the World Geodetic System of 1984 (WGS84) ellipsoid.

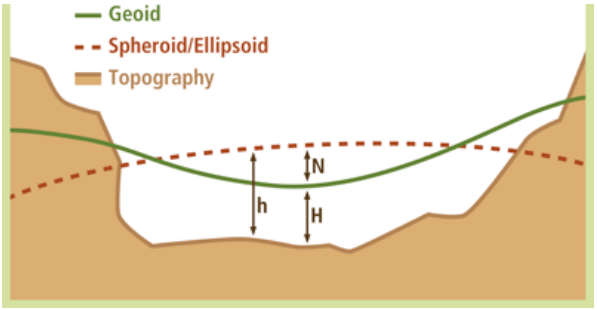

Figure 22 Geoid and Ellipsoidal model (Esri, n.d.-b)

To change the elevation data to the new vertical coordinate system, the following equation is applied:

$$h = H + N$$

To convert the EGM96 height value to the ellipsoidal value, N has to be added to the geoid height. The N values are stored in a raster set that comes with the ArcGIS Pro software, WGS84.img. By applying the equation, a new raster is created with the height above the ellipsoid.

To simply detect the differences between the two DEMs, the raster datasets are subtracted from each other with the *Raster Calculator*. This was done for the entire area, but also for a small section with more stable terrain (see Figure 23). Also, a profile line was created for both DEMs, to compare the shape of the DEM, the topology of the study area.

An analysis of the differences between the two DEMs can further be done by calculating the mean of the error values (ME) and the root mean square error (RMSE). The mean error (**Equation 1**) can give us information on the general deviation of the model. Are the measurements consistently underestimated or overestimated? Or are these more or less balanced, which would result in a ME closer to 0. The RMSE (**Equation 2**) is the standard deviation of the residuals, the square root of the average of squared errors. It measures how spread out the residuals are and is therefore an indicator for the accuracy of the data.

$$ME = \frac{1}{n}\sum_{i=1}^{n}(PSDEM - SRTM)^2$$

Equation 1 Mean error

$$RMSE = \sqrt{\frac{1}{n}\sum_{i=1}^{n}(PSDEM - SRTM)^2}$$

Equation 2 Root Mean Square Error

4.4.2 Existing maps of the area

To be able to evaluate the generated PlanetScope DEM and compare it with map sheets, the elevation information in the map sheets has to be digitized. This is done in two ways, with a profile line and elevation points.

A profile line of approximately 14 kilometers that crosses through the entire area and covers stable, mountainous, and glacial areas is drawn on the map in GIS (see Figure 23). For every contour line the profile line crosses a point is created with the elevation value according to the map. When all points have been digitized manually, they are connected with the tool *Points to Line*. To also get the elevation values from the DEM along the line feature, the profile line needs to adapt the raster cell values as z-values. This is done with the *Interpolate Shape* tool. The PlanetScope DEM is used as input surface, where the values will be extracted from. The input feature is the profile line in which the z-values

will be interpolated. The values from this line can subsequently be compared to the elevation derived from the contour lines in the map sheets.

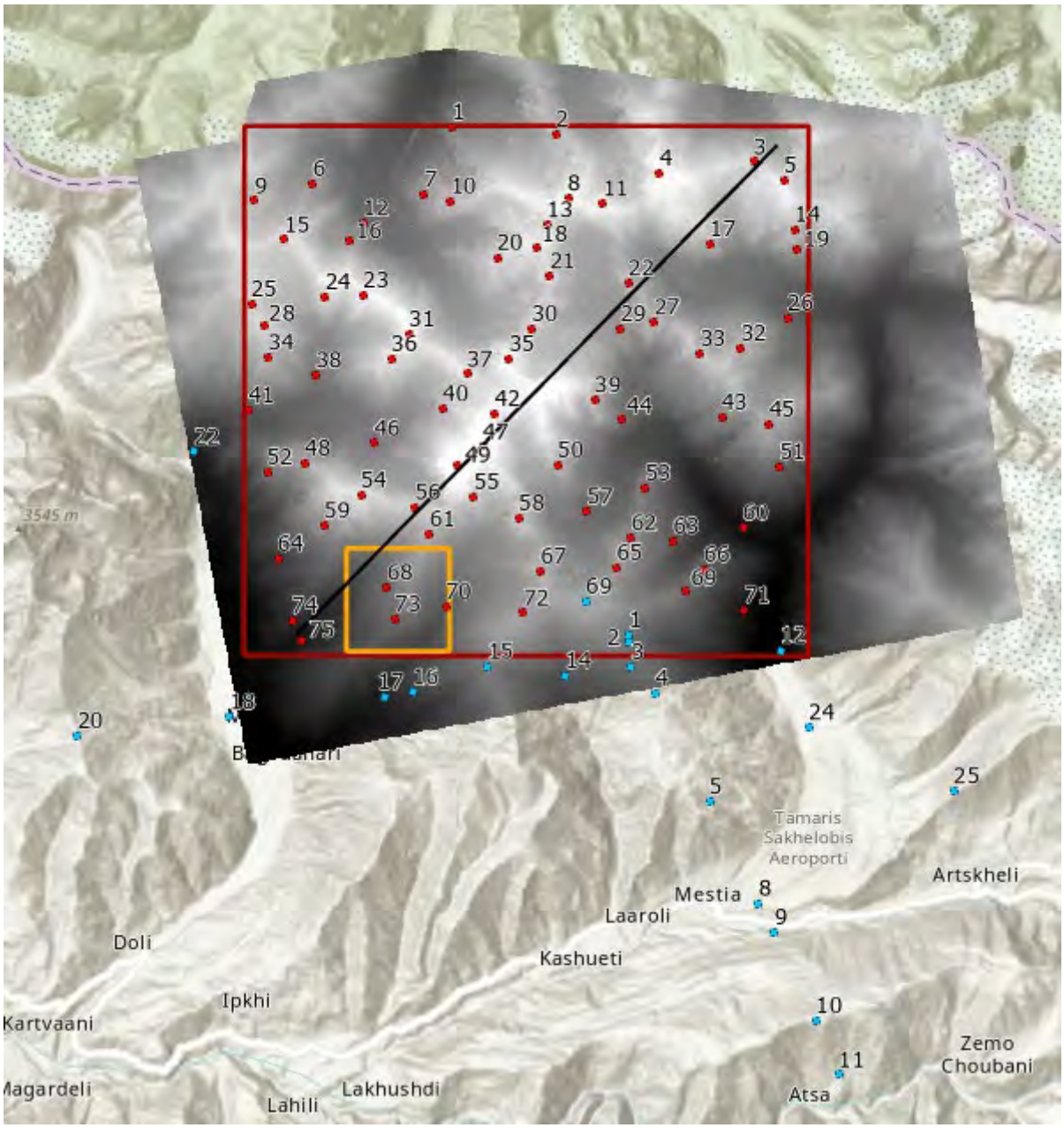

Figure 23 Profile line (black), field measurements (blue) and elevation points (red) from Geoland map. Field measurement 70 lies outside figure. Red rectangle is the research area and the orange rectangle is a selection with stable terrain.

The Geoland map sheets also contain points with their elevation. All points that lie in the research area (see red points within the red rectangle in Figure 23) are manually digitized in ArcGIS Pro. With the tool *Extract Multi Values to Points* the raster cell values from the PlanetScope DEM, SRTM DEM and the smoothened PlanetScope DEM are extracted for

the corresponding 75 points. The table with these values can be analyzed and the mean error and RMSE can be calculated.

4.4.3 Field measurements

During the mapping campaign in Georgia in the summer of 2021, elevation measurements were taken on several locations. Most of these points lie south of Mount Ushba, in the region that was accessible from Mestia. An overview of these points (blue) can be found in Figure 23.

The elevation measurements were taken with a Garmin GPSMAP 66sr. To measure the elevation, one would navigate to the location indicated on the map. After making sure the GPS device was linked with enough satellites, the GPS was placed a bit above the ground and left still for 20 to 30 minutes. The height above the ground was written down, so this could later be subtracted from the measured elevation.

The GPS devices provide multiple output files from the measurements. To retrieve the elevation the RINEX data is used. The Receiver Independent Exchange (RINEX) files contain the raw satellite navigation system data. With the use of the RINEX files the data can be processed more accurately. This because more data, unknown to the GPS device, can be added.

The first data that is added are the precise orbits for the satellites, for more accurate PPP (Precise Point Positioning) measurements. Also, the navigation data with an additional clock correction calculated from ground stations is added for each measurement. Both can be downloaded from the BKG GNSS Data Center (https://igs.bkg.bund.de/). Also, the most recent (GPS week 2163) antenna correction file in ANTEX format for satellite and receiver antennas is added.

To extract the elevation data from the RINEX files, the processing engine WaPPP is used. This software is developed by Pr. Lambert Wanninger (2020). “The Precise Point Positioning (PPP) processing engine WaPPP is designed for adding precise GNSS single station positioning capabilities to application software. WaPPP computes coordinates based on GNSS observations in RINEX-format.”

Running WaPPP is done in the command prompt from the folder with the program, antenna corrections, observations, satellite orbits and clock corrections. These files have to be in the right format for the program to be able to read them. The orbits file is converted from cod21673.eph_m to cod21673.sp3. The clock correction file is renamed from cod21673.clk_m to cod21673.clk. The antenna correction file (igs14_2163.atx) is already in the correct format, ANTEX. To only extract the elevation measurements for the points that were measured, the RINEX files are split. During the measurements it was exactly written down on which day and time the observations were made. With this

information, only the data during these observations is kept in the RINEX file for the observation.

The following command line is entered in the command prompt:

```
wappp punkt_01.21O +ASigs14_2163.atx -AR +L2 +FLpunkt_01.log
```

Punkt_01.21O is the RINEX file with the observation data. +AS tells the program which file contains the satellite antenna corrections. -AR indicates that there is no receiver antenna corrections file to be read. +L# determines the amount of information written in the log file, 2 is the command for the program to create an extended log file. +FL contains the output name of the log file.

In the logs first some general information is given, as below for point 25:

```
Scan punkt_25.21O     v3.04
  obs GPS     C1C C5X L1C L5X D1C D5X S1C S5X
  obs GLONASS C1C L1C D1C S1C
  obs Galileo C1Z C5X L1Z L5X D1Z D5X S1Z S5X
  receiver type and number:                        GPSMAP 66sr 3.30
  antenna type and number:
  marker coo. (RINEX) [m]: 3429858.7500  3168419.2500  4332484.5000
  vertical antenna height [m]:   0.0000
  start (date,time,week,sec): 2021-08-04 06:42:00  2169 283320
  end   (date,time,week,sec): 2021-08-04 07:12:00  2169 285120
  duration in [s], [min] or [h]:    1800.00 =    30.0 =   0.5
  interval [s]:                  1.00
  expected # of epochs:       1801
  actual   # of epochs:       1801
  missing  # of epochs:          0
```

For this point the GPS device was linked to GPS, GLONASS and Galileo satellites during the measurement. The vertical antenna height is not added here yet, this has to be subtracted later. The start and end time are the times in UTC±00:00. This means that the time of the measurement in Georgia is 4 hours later. It provides the duration of the observation and how many measurements were made in that time.

The processed input results into coordinate and elevation information for the observations.

```
  coordinates XYZ    3426285.9122  3171362.6357  4334408.1547
  coordinates UTM   38319832.5608  4770439.3431     2351.9139
  coo std dev UTM          0.0079        0.0048        0.0028
```

The coordinates that are given in UTM format are stored in an excel file for each location, together with the standard deviations (see appendix x). In the excel file the height of the device during the measurements is subtracted from the height value, to give the actual elevation. The UTM coordinates are reformatted to have the following syntax: 319832.5608,4770439.3431,38N. This way ArcGIS Pro can read the coordinate information, when importing the excel file. To get the points and their elevation into ArcGIS Pro, the tool *Coordinate Table to Point* is used. The excel file is set as input table. The input coordinate format to *Universal Transverse Mercator Zones* and the column with the adapted syntax is selected as source. A point feature class is generated that contains the location and elevation data for all 21 observations that were made.

In order to compare the observations with DEMs, the raster cell values have to be extracted at the same location as the points. With the tool *Extract Multi Values to Points* the raster cell values from the PlanetScope DEM, SRTM DEM and the smoothened PlanetScope DEM (more information on this DEM in chapter 4.5) are determined. To also compare the elevation of the observations and the Geoland map sheet, the elevation of the map sheet is read from the contour lines and manually added to the table. The contour lines and the elevation points on the map, are however likely based on a different vertical datum. The contour lines all have a lower elevation than the points that have a given elevation in the map and are likely based on the SRTM elevation data. To make a better comparison between the elevation values of the different sources, the manually entered height values for the map sheet are recalculated to represent the WGS84 ellipsoidal height.

4.5 Relief depiction

The generated PlanetScope DEM has a high resolution of 3.6 meters. This however also comes with a lot of (unnecessary) detail and noise. To generate a relief depiction that accurately represents the terrain but is at the same time also legible and pleasant to look at, the terrain needs to be smoothened. To achieve this without creating large elevation inaccuracies, multiple smoothing techniques have been tested.

When simply using an averaging or so called low-pass filter, most of the roughness, errors and unnecessary detail in the DEM gets removed. However, this filter also removes the peaks and the valleys in the terrain, resulting in a low height accuracy in these areas. It also negatively impacts the representation of drainage features and blurs sharp edges in the terrain.

Another option is to use a specific method created to denoise digital elevation models. A well known approach to denoise elevation data is Sun's denoising algorithm, which is freely available and can be run directly from within GRASS GIS, with the r.denoise tool.

Sun et al. (2007) developed this algorithm to smoothen the surface, while at the same time preserving the main features in the model. This algorithm was created to be used with point clouds datasets, but when applying it to raster datasets, it is highly inefficient. It was not created with the large data sets like DEMs in mind. The program will fit a triangular irregular network to each grid cell. This iterative TIN-based smoothing results in large computation times. Lindsay et al. (2019) therefore developed a feature-preserving DEM smoothing (FPDEMS) method that is based on the approach designed by Sun et al. to denoise 3D meshes. The FPDEMS method, however, is optimized to work with raster DEM data. With the settings that generated optimal smoothing results, as stated in the paper, the method was also applied to the PlanetScope DEM. Originally designed to smoothen and denoise DEMs generated with LiDAR data, the method was unfortunately not able to differentiate between the main features and the larger noise and unnecessary detail in the DEM generated with PlanetScope imagery. Most noise, errors and details are too large to get smoothened out and are therefore only more present after applying the algorithm, as can be seen in Figure 24.

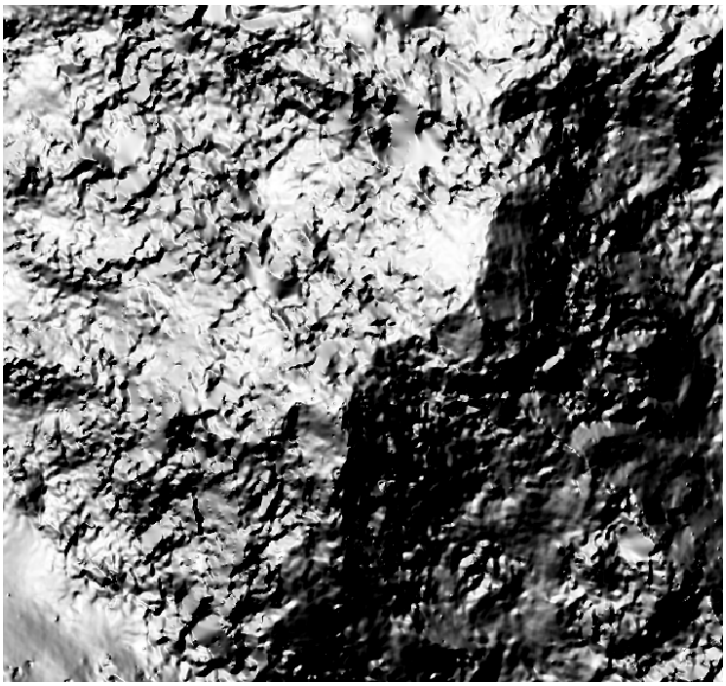

Figure 24 Hill shade of DEM smoothened with FPDEMS method

Because the above described commonly used methods did not result in the desired outcome, another approach was developed. To preserve the main features, while still smoothing and denoising the rest of the terrain, the ridges and drainage lines were detected. By separating these with the hydrology tools in ArcGIS Pro and only applying a low-pass filter to the rest of the terrain, before bringing them back together and connecting them with a spline interpolation, the main features and sharp edges are

preserved and keep their original height values. To achieve this, the following steps were followed:

1. The first step is to use the "*Fill*" tool. This tool fills all the sinks in the surface raster to remove small imperfections in the data. This is necessary to later determine the correct drainage lines in the terrain since the sinks contain the cells with an undefined drainage direction and would therefore result in errors when computing the flow direction.
2. The next step is to determine the *flow direction* for each cell. This is done with D8 as flow direction type. This method models the flow direction from each cell to its steepest downslope neighbor.

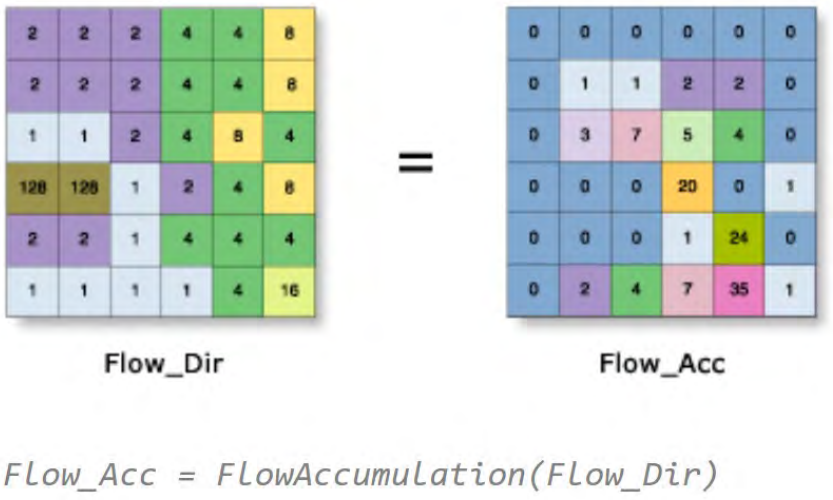

Figure 25 The flow accumulation can be calculated with the flow direction raster (Esri, n.d.-a)

3. Based on this the *flow accumulation* can be calculated for each cell. This tool creates a raster of accumulated flow into each cell and uses the flow direction type from the input (D8).

Based on the raster created in step 3 (see Figure 26) there are different steps to be taken to establish the ridgelines and the drainage lines.

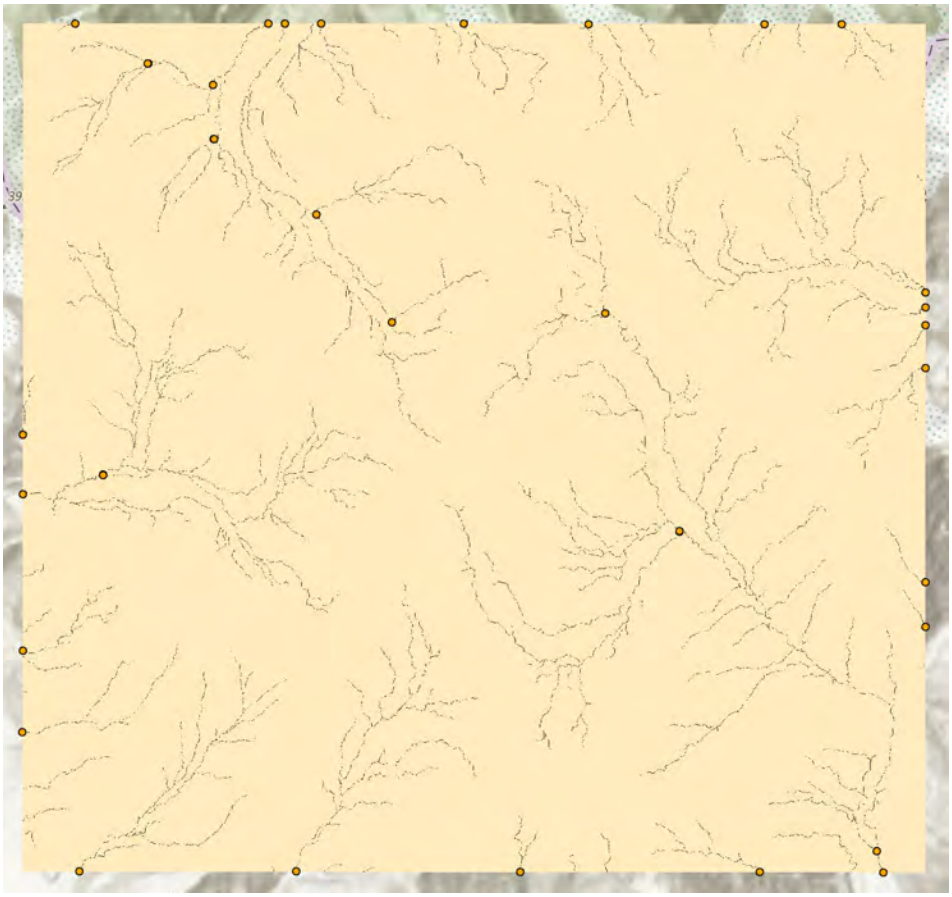

Figure 26 Drainage lines in research area, with cells that receive water from at least 10,000 cells displayed in black. The pour points are shown in orange.

4.5.1 Ridges

Cells with a flow accumulation of 0 are topographic highs and could be used to identify ridges. However, the terrain around mount Ushba is rather rough and has many local topographic highs, making it impossible to determine the ridgelines based only on the flow accumulation. The flow accumulation raster is therefore classified into 2 classes for the next steps. The cells in black are all cells that receive water from at least 10.000 other cells.

R1. With the flow accumulation information, it is possible to determine pour points in the area. These pour points are manually entered at the end of the drainage lines and at the locations where the main lines branch into different directions (see orange points in Figure 26).

R2. The next tool used is the *snap pour points* tool. This tool searches within a specified distance around the points created in the previous step for the cell with the highest accumulated flow and move the pour point to that location. Because the pour points were already placed in the exact cells at the end of the drainage lines are the branches, the snap distance is set to 0. In this case the tool thus only converts the points to a raster cell that corresponds with the DEM.

R3. Based on the pour points the *watersheds* can be determined. This tool takes the flow direction raster and the pour points to determine the contributing area to the selected cells.
R4. To extract the ridgeline from these watersheds the raster is converted to polygons based on the different watershed areas.
R5. Because only the outlines of the watersheds are needed, since these represent the ridgelines (highest points, where water flows in different directions), the polygons created in step 4 are converted into lines.

4.5.2 Valleys

To extract the drainage lines from the DEM, the flow accumulation raster is used once more.

V1. The flow accumulation raster holds the number of cells that flow into each cell. The threshold for the main drainage lines is set to 100.000. This means that water from at least 100.000 other cells will flow into the cell, before it is considered a main drainage line. To create a raster layer with only these cells the *raster calculator* is used:
`Int ( SetNull ( “FlowAccumulation” < 100000, “FlowAccumulation” ))`

4.5.3 Low-pass filter

To smoothen the PlanetScope DEM a multi-step mean filter is applied on the filled DEM from step 1. The mean filter is applied on a circle neighborhood with a radius of 3 cells with the *focal statistics* tool. This step is repeated 10 times.

4.5.4 Merge

In the next steps the previous sections will be brought together to create the final feature preserving smoothened DEM.

4. To extract the values of the DEM on the ridge and drainage lines, the lines from step R5 and V1 are merged. The original DEM is subsequently clipped with the merged lines.
5. To generate a smooth DEM without a jump between the smoothened section and the original values at the ridge and drainage lines, a buffer around these areas of 50 meters is generated.
6. This buffer area is converted back to raster with the *Polygon to Raster* tool. The cell size is set to match and snap to the original DEM.
7. To delete the buffer area from the smoothened DEM, the *raster calculator* is used:
`SetNull ( ~ ( IsNull ( “Buffer50m” )), “SmoothDEM” )`
8. The output of this calculation is then merged with the output of step 4. The result of this is shown in Figure 27.

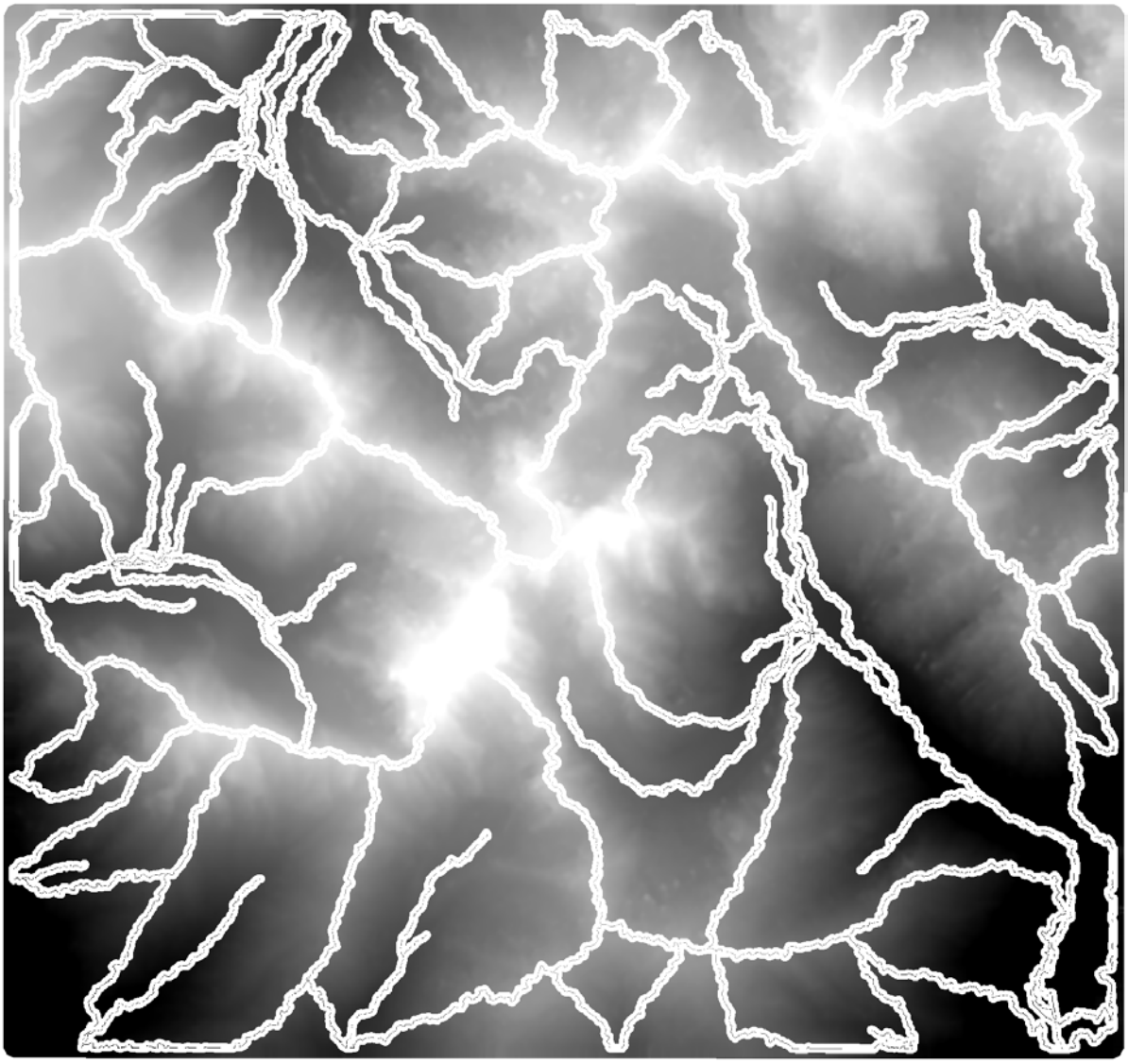

Figure 27 Smoothened DEM combined with the original values at the ridges and valleys

4.5.5 Spline interpolation

ArcGIS Pro does not offer the option to interpolate a raster with a spline. The raster is therefore exported as a tiff file and imported into QGIS. Here the r.fillnulls tool is used. This tool fills all the no data areas using a spline interpolation. This can be done with a regularized, cubic, or linear spline interpolation. In this case the cubic spline interpolation is used with the tension of the spline set to 40, the width of the edge of the no data area used for the interpolation at 3 cells and the smoothing is set to 0.5. All the other settings are left at default. The raster output of this step is imported back into ArcGIS pro and clipped with the original research area extent.

4.6 Contour lines

One of the methods to display the relief is with contour lines. The raster set that was previously generated contains the height values the contour lines will be based upon. For the intended scale of the map multiple distances between the contour lines were tested. Since the terrain has very different slope gradients, a certain equidistance might work well in one area, but work less in another. A balanced equidistance for the entire terrain is 20 meters, with an indexed contour in bold every 100 meters.

After generating to contour lines for the terrain, the labels have to be added to the height lines. Labels are only added to every 100-meter interval (based on the indexed contours), to keep the map legible. The color of the contour lines and label text are also adapted to match the background. At last, masks around the labels are created, masking out the contour line and busy background, to improve the legibility of the map.

4.7 Hill shading

To create the hill shading the same input is used as with the contour lines. This DEM shows a difference in detail in the smoothened parts of the DEM and the ridge and valley lines at the original detail level. The DEM is therefore slightly smoothened again, to create the same smoothness for the ridges and valleys as the rest of the area, without losing too much of the terrain features. This is done by applying the focal statistics tool once more with a circle with a radius 5 of cells as neighborhood. This step is repeated 5 times.

Blender will be used to create the hill shading. Blender is a 3D modeling program and uses the input object, a light source and camera to make 3D models. Hill shade options integrated in a GIS program produce rather noisy and harsh representation of the topography. This could be useful, if the topography is the main topic of the map, since these hill shading techniques often exaggerate the topological features. In case of a navigational map this is however not very useful nor realistic (Hoekstra, 2019). A more realistic hill shading technique is possible with the use of Blender. This is mainly because of its ability to scatter and bounce the light between topographical features. Blender is designed specifically to create realistic 3D models and therefore capable to recreate the way light scatters, reflects and bounces on the mountains and how its absence creates shadows. Because of its great and realistic lighting abilities, the hill shade also shows the main features in the terrain better.

To use the DEM in Blender the raster dataset is recalculated so that all cell values lie in the range of 0 to 65535, the maximum number of values in a 16-bit file. This way the hill

shade will show as much detail in the terrain as possible, since Blender only reads integer numbers. After exporting the DEM as a tiff file, it can be loaded into Blender.

The hill shade is then produced based on the ideas of Daniel Huffman (2020), more information on his workflow can be found on his website.

The first step is to set up the plane, the object the 3D model is created of. To develop the terrain model, the plane has to be shaped according to the heightmap that was generated previously. After adding a plane mesh to the project, the scale of the plane is adjusted to match the aspect ratio of the heightmap. An important aspect in order to create a realistic hill shade is to choose the best material for the plane. Different materials have different textures and colors and therefore reflect light in different ways. Blender simulates the lighting based on the properties of each of these materials. The surface is by default set to *Principled BSDF* (bidirectional scattering distribution function). This is also the selected surface for this project.

To shape the plane like the heightmap the *Shader Editor* is opened (see Figure 28). Here is a diagram that have all the settings for the different parts and contain how they are related and affect each other. The *Principled BSDF* box shows what was just set as material in the surface settings, together with its default settings. For the *Base Color* the grey value is increased a bit, to clearly show both the shadow areas and the high lighted lit-up areas of the terrain. The roughness is also increased to 1.0 and the *Specular* is reduced to 0.0. The *Principled BSDF* box in the diagram is linked to the *Material Output* box to the *Surface* node (according to the settings that were done before). It is also possible to link the *displacement* to this box, which is done with the heightmap. The *Image Texture* box is linked to the *displacement* node, where the DEM is loaded as texture. Blender reads the grey values of the image and applies it to the material. The first parameter of the box is changed to *Smart* and the last to *Linear*. This linearly converts each pixel in the heightmap to a displacement, so that each grey value will have an equal step in height. The parameter that says *Repeat* by default is changed to *Extend*. This means that Blender will not tile the image, making it a repeating pattern, but that it will stretch the image over the entire plane.

These settings do however not yet create a realistic representation of the terrain, since Blender is now only simulating the displacement, using a technique called bump mapping. It is only a quick simulation of depth but is does not actually apply the lighting to the terrain. The light does not get reflected by the mountains nor are any shadows cast by them. To change this ‘fake’ displacement into a real displacement of the plane based on the heightmap, the plane has to be transformed so it has many vertices that can be adjusted to take the shape of the terrain. For this a modifier is added, the Subdivision Surface modifier. This modifier increases the number of vertices of the plane, and it also smoothens and rounds them. This way complex shapes can be

generated based on simple meshes. The subdivision type is set to simple, and the *Adaptive* box is checked (this lets the program decide how much detail in which part if the terrain is needed).

To set the displacement of the heightmap to the plane, another box is added to the diagram, the *Displacement* box. The *displacement* node is connected to the node of the same name in the *Material Output* box and the *Height* node is connected to the *Color* node in the *Image Texture* box. This tells the program to turn the grey values into a displacement of the plane. The *Scale* number specifies how much the plane should be displaced and therefore influences the exaggeration of the terrain. To also make sure Blender actually applies the displacement, the displacement parameter in the *Settings* tab of the plane, is changed from *Bump Only* to *Displacement Only.*

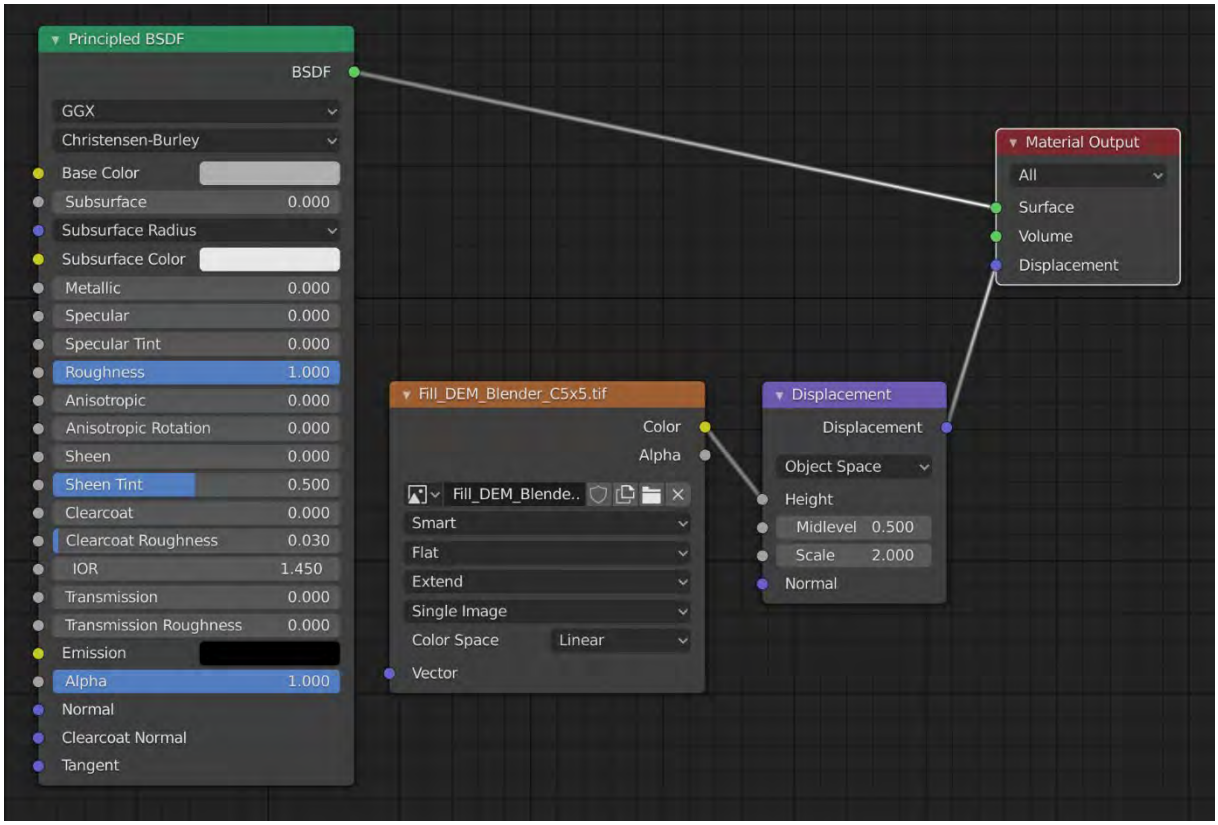

Figure 28 Shader Editor in Blender with settings applied for hill shade

After setting up the plane the camera and light source have to be set. The camera will be used to capture the relief (the plane) we just created form a certain angle and height. For a shaded relief the view will be from directly above the terrain. To capture exactly the area of the plane and from an orthogonal angle, a few settings were changed. The location of the camara is set to match the center of the plane by changing *Location X* en *Y*. The *Z* determines the distance between the plane and the camera and is set to 3 meters.

All three rotation parameters are also set to zero, so that the camera will look straight down on the plane. For the capture area of the camera to match exactly with the size of the plane, the resolution of the camera is changed. The *Resolution X* en *Y* should match the size of the heightmap in pixels. This way the camera view has the same aspect ratio as the terrain area for which the hill shade will be generated. For the size also to match, the view type first has to be changed from a perspective to an orthographic view. To make the camera view and the heightmap line up exactly, the *Orthographic Scale* is changed. By using two times the Y size of your plane, the view and plane exactly match.

The last step is to set up the light source. Since the output of the 3D modeling will be a realistic hill shade, the *Sun* is set as the light source. This way the light rays will reach the terrain almost parallel, while a point as light source has light rays going in all different directions and angles. The *Power* parameter specifies how bright the sun is. 1000 watts is too high for the shaded relief, so this is decreased to 5 watts. The *Angle* parameter contains the sun's angular diameter, which influences how soft or sharp the shadows are. For a realistic look of the shadows this parameter is set to 90 degrees.

The direction and the angle of where the sun is coming from can also be adjusted. A general rule is that the light source should come from the upper left, otherwise the relief will look inverted. To achieve this the rotation parameters for the light source are changed. The *X Rotation* is set to 0. The *Y Rotation* specifies the height of the Sun in the sky and influences the length of the shadows. 0 degrees means perpendicular to the ground, 90 degrees is parallel to the ground. For this shaded relief the *Y Rotation* is set to 60 degrees. The *Z Rotation* holds the direction the sun is coming from, where the light rays are coming from the east at 0 degrees. This angel is set to 135 degrees, which corresponds with the sun coming from the northwestern direction and corresponds with the angle used in the program for the rock depiction.

After completing all the settings for the plane, camera and light source, the 3D model can be rendered and exported as a PNG-file. The resulting shaded relief can be found in chapter 5.2.

4.8 Rock depiction

A slightly different way to depict the relief is by showing the terrain that is covered by rocks. Maximilian Schröder created rock masks based on the Sentinel-3 and Landsat 8 imagery from 2019 for his master's thesis.

This rock mask does however not differentiate between the different types of rock cover since this was not possible to detect with the NDSI and NDVI values used in his method. For the user of the hiking map, it is very useful to know if the terrain is made up by scree, debris or if it is solid bedrock that one can hike on. The bedrock was therefore traced manually, as agreed upon with the supervisor, based on the Georgian Topography maps by Geoland. These areas were traced and smoothed with the *Smooth Polygon* tool in ArcGIS pro. The rock mask generated by Schröder is used for the depiction of the other rock types.

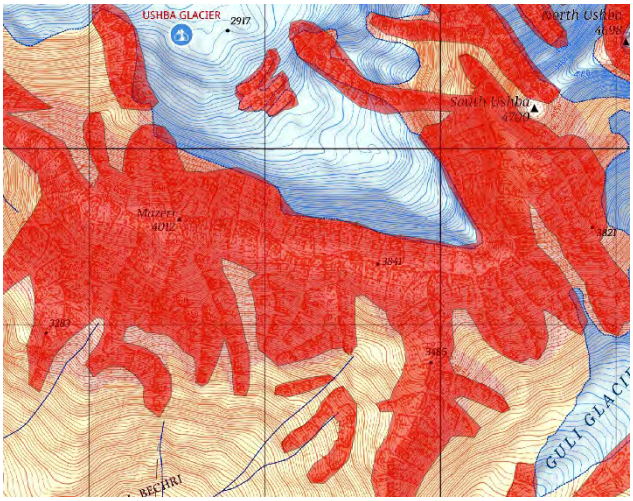

Figure 29 Rock mask drawn in ArcGIS based on the rock depiction in the Geoland maps

The rock depiction is created with the use of the PIOTR software (2019). This software has been developed by Roman Geisthövel (2017) and accompanies his PHD thesis on Automatic Swiss style rock depiction. The software can be downloaded for free (http://motlimot.net/software.html) and runs from the command prompt. As input the program needs a digital elevation model and a rock mask. The program then automatically generates a rock depiction based on the Swiss style.

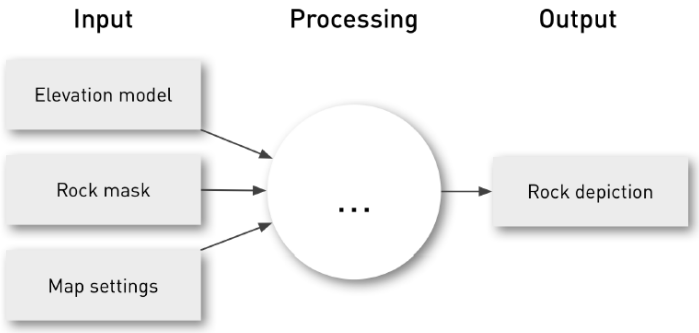

To create the rock hachures the program first generalizes the input elevation model and generates a shaded relief. For the generalization the program uses line integral convolution (LIC). This step can also be run separately using the QGIS 3 plugin KARIKA. The principle for the rock hachuring with the program is to cover the entire terrain specified as rock with the rock mask with equidistant horizontal hachures, terminating at the trenches. These horizontal hachures are subsequently filled with vertical hachures, indicating precipitous terrain, based on the slopes of the original DEM. The stroke width is also adapted, based on the shaded relief. The darker, shade sections of the relief have wider strokes, and the light sections have thinner strokes.

Figure 30 Example of rock depiction created by the Piotr program from Roman Geisthövel (Geisthövel, 2017)

To run the program the digital elevation model and rock mask need to be in the correct file format. The rock mask is dissolved so that all polygons have the same value and then converted to raster, with the same extent and snapped to the cells of the digital elevation model. Because the program only reads a binary raster dataset, the NODATA cells are reclassified to 0. Next, the DEM and rock mask are exported as ASCII-files, making sure they have exactly the same extent and number of pixels, for the program to process both.

Running PIOTR with these files is done by entering the following command into the command prompt.

```
piotr.exe -l 15 -d /tmp/piotr_out -m ~/mask.asc ~/test.asc
```

The directory has to be set to the folder where piotr.exe is stored. -l 15 is the generalization using LIC, with 15 being the customizable integration length. -d is the output directory for the generated files. -m is the path to the rock mask and the last parameter holds the path to the elevation model.

The program was first run with the DEM and rock mask at the original resolution (~3.6m). This did however not result in a suitable rock drawing as outcome (Figure 31). The hachure lines are too close together this way for the intended scale of the map (1:33,000).

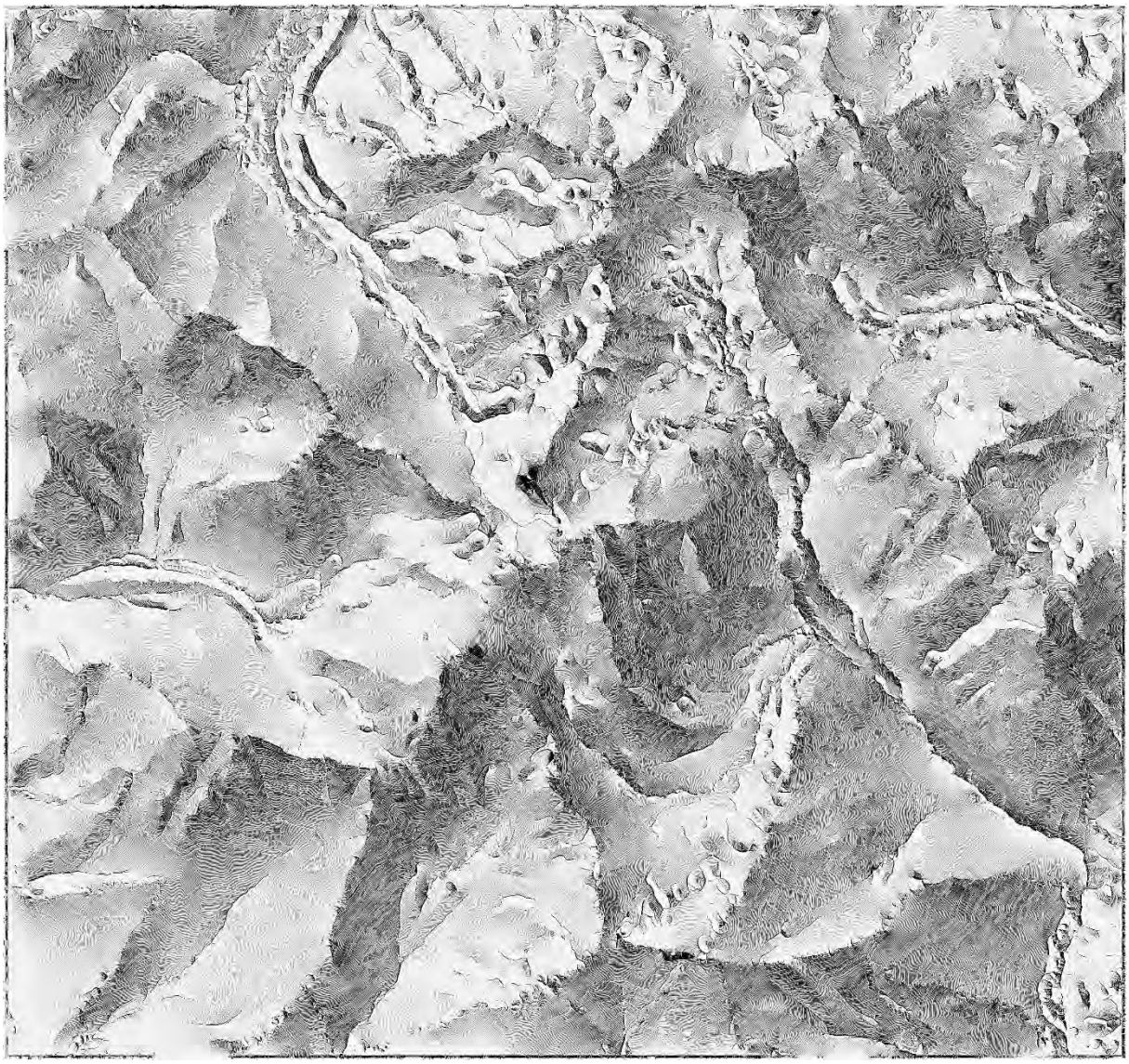

Figure 31 Rock depiction (without rock mask) created with Piotr with PlanetScope DEM at original resolution

To get some clearer hachure lines that would be legible at the intended scale, the DEM and rock mask were resampled to a 10-meter resolution, before running the program again. The results of this can be found in chapter 5.2.

5 Results

This chapter presents the results of the study. The generated PlanetScope DEM will be analyzed and an assessment of the accuracy of the DEM will be made. Also the different parts of the relief depiction and the final visualization are provided and reviewed.

5.1 Digital Elevation Model

With the use of the 11 selected satellite images made by the Dove-1 satellites of PlanetScope a digital elevation model could be created. After aligning the photos with tie points and building a dense point cloud, a DEM was generated in Agisoft Metashape. This DEM has a resolution of 3.64 m/pix and is 12307 by 6380 pixels. The elevation values are between 1530 and 4711 meter. When just looking at these numbers, the DEM seems to perform quit well. The height of Mount Ushba for example, the highest point in the study area, is exactly the same as the maximum elevation in the DEM.

When looking at the coverage of the DEM, some gaps are visible. In these areas Agisoft Metashape was unable to calculate the height. To fill these voids, Agisoft interpolates the surface using inverse distance weighting. This interpolation technique assumes that things closer to one another or more alike than the things further away. When predicting an unknown value, the measured values around the void will have more influence on the predicted value than those the lie further away.

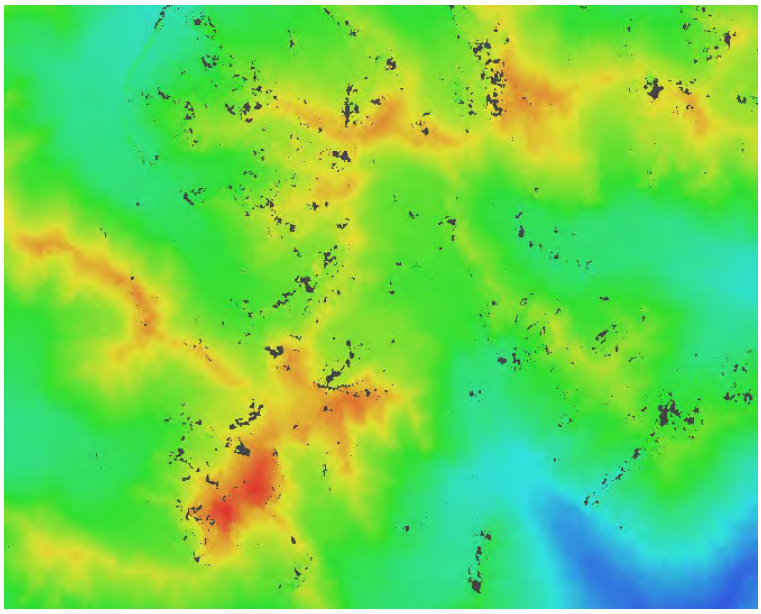

Figure 32 Section of the generated DEM with visible voids in the data

To be able to say more about the accuracy of the generated DEM, it has to be evaluated. This has been done by comparing the height values with a reference DEM, map sheets and field measurements.

5.1.1 Evaluation reference DEM

To simply detect the differences between the two DEMs, the raster datasets are subtracted from each other with the *Raster Calculator* (Figure 33). This does not provide a clear pattern. The difference is not always positive on the one side and negative on the other, which could indicate a shift in the raster data. The difference is also not approximately the same over the entire terrain, which could indicate a vertical offset. It is however visible that the glaciers have decreased over the years, according to the difference in these two DEMs. The largest deviations occur along the ridges (with the PlanetScope indicating higher elevations than the SRTM), and in certain sinks in the terrain. These negative deviations most likely occur due to errors and/or occlusions in the PlanetScope data since these gaps do not seem to actually be present in the terrain when comparing them to different satellite images. There are also some bumps present on the glaciers that seem to correspond with areas on the glacier with big crevasses. The more stable terrain on the south side of the study area, without glaciers, steep slopes, or occlusions due to the mountains, clearly shows smaller deviations.

With the deviations known for each cell in the raster data set, it is also possible to mathematically analyze these differences. The mean deviation is just under 10 meters between the two DEMs. With a 30-meter resolution of the SRTM and a 16-meter vertical accuracy, this difference lies within the variations of the reference DEM. The RMSE of the height difference is 46.9 meters. Both these numbers are calculated by using all cells in the raster within the research area. This is however a very rugged area, which often leads to a much lower accuracy in height values (see chapter 3.2). When looking at these numbers for only a small, selected area that is more stable, these numbers are also more stable. The mean error for the stable terrain is only -2.4m. This means that the PlanetScope lies a bit lower than the SRTM DEM for this area, but with the vertical accuracy for SRTM at 16 meters and a resolution of 30 meters, this difference is almost insignificant. The RMSE error is also way smaller for the stable terrain. With only 14 meters the deviations are a lot smaller than for the rugged terrain with steep slopes.

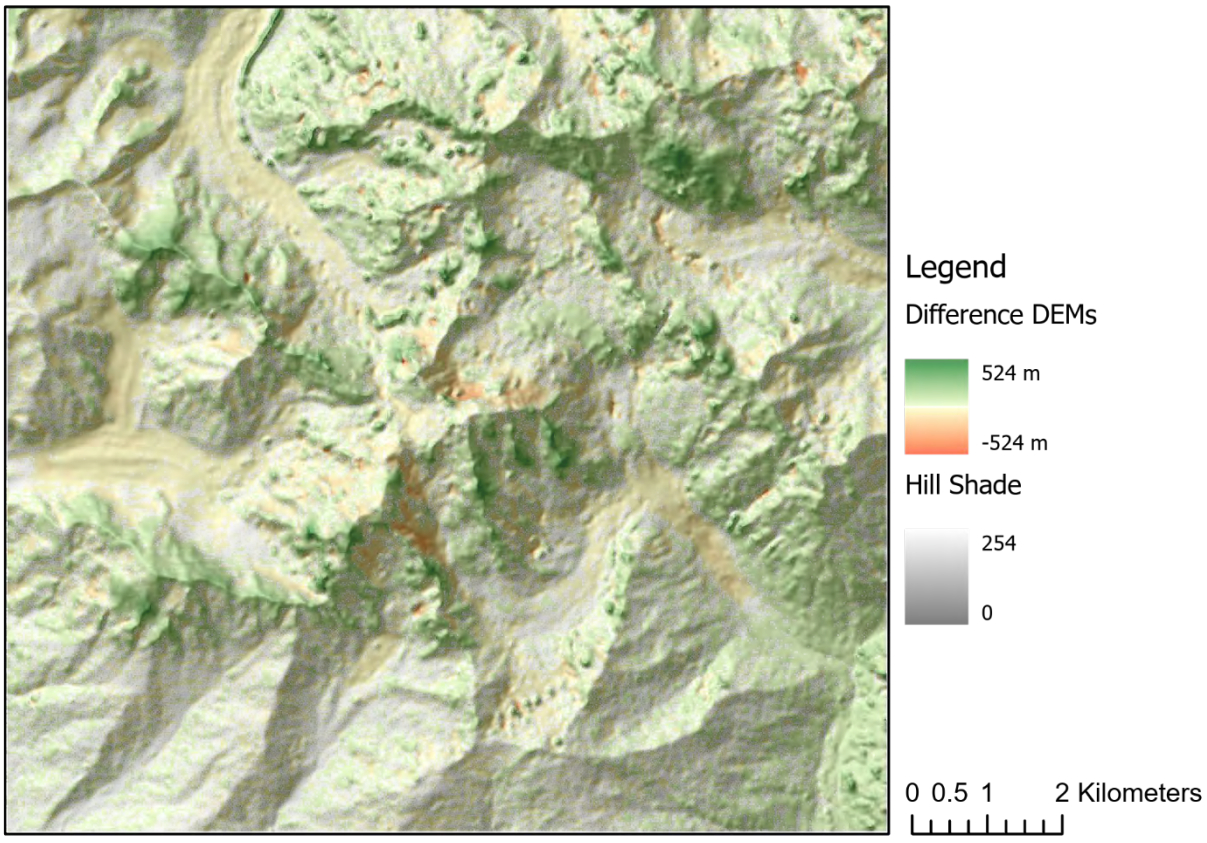

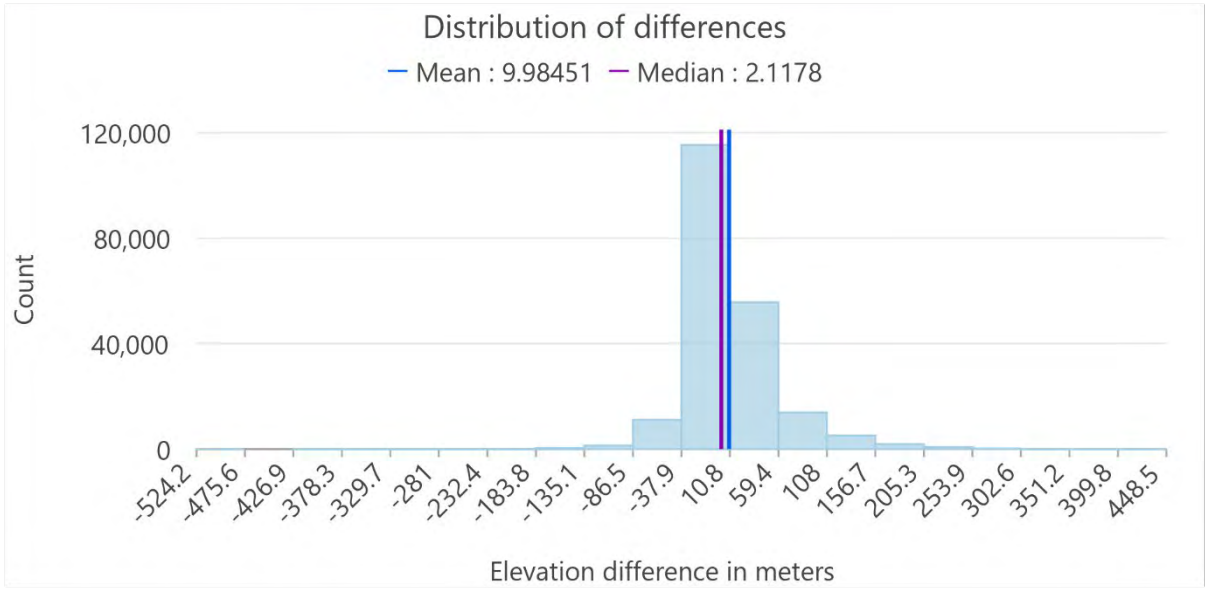

Figure 33 Elevation difference between SRTM and PlanetScope DEM

To get a better understanding of how well the DEM represents the topology of the terrain, a profile graph (Figure 34) was created for both DEMs. In orange (number 1) is the profile for the PlanetScope DEM and in grey (number 2) the SRTM elevation data on the same line.

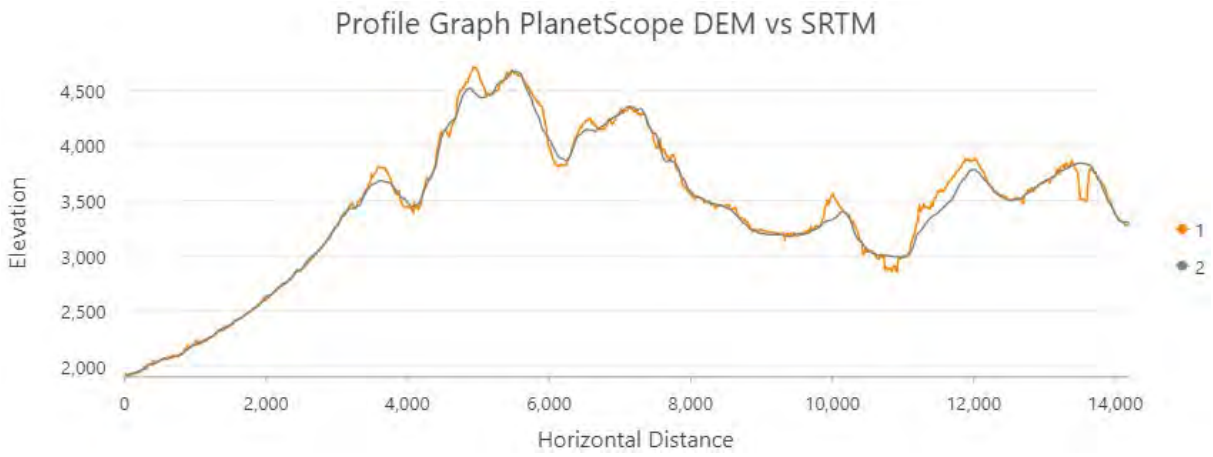

Figure 34 Elevation profile PlanetScope DEM (orange) and SRTM (grey)

The DEMs follow the same line for the most part, but there are also some differences visible. The peaks in the SRTM DEM are lower than in the PlanetScope DEM. It also seems like there are some small errors/noise in the PS DEM, and one major sink which is not visible in the terrain. The general shape of the terrain is similar, but there are also certainly areas that show significant differences.

5.1.2 Evaluation reference map sheets

One of the other reference sources to compare the PlanetScope DEM to, are the different map sheets. Two of these have been digitized and can been analyzed in comparison with the PS DEM. The EWP map is on a 1:50,000 scale and does not have as detailed contour lines as the Geoland map sheets. The green line in Figure 35 is therefore rather rough, but still shows a similar shape as the generated DEM. A better comparison could be made with the more detailed Geoland map. As suspected, the contour lines in this map follow the exact same heights as the SRTM DEM, which becomes visible when comparing the grey line 2 in Figure 34 and the blue line 3 in Figure 35. The deviations are therefore also the same as pointed out before.

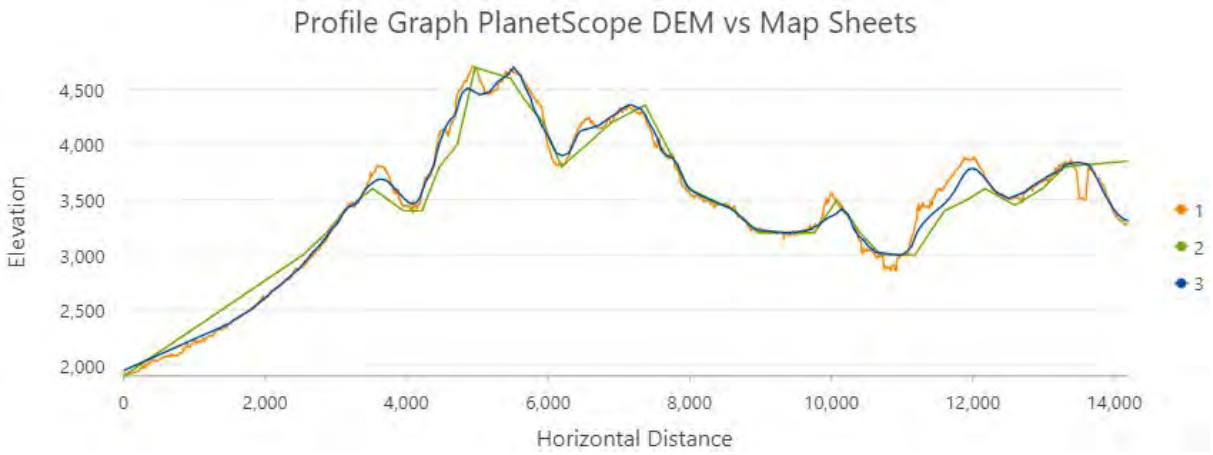

Figure 35 Elevation profile of PlanetScope DEM (orange) and the Geoland (blue) and EWP (green) map sheet

The second way to compare the generated PlanetScope DEM with the Geoland map sheet was by digitizing 75 elevation points from the map. The height data from the different DEMs are analyzed and compared with the measured elevation in the map. The complete table with all data and an extended graph can be found in the appendix, Table 5 and Figure 49, where the SRTM data clearly shows larger deviations than the PlanetScope DEM. When looking at the map points with ID 60 and higher, the elevation differences become lower. This is likely due to the fact that these IDs lie in the more stable part of the terrain. The results of the comparison are also displayed in Figure 36 and Table 3.

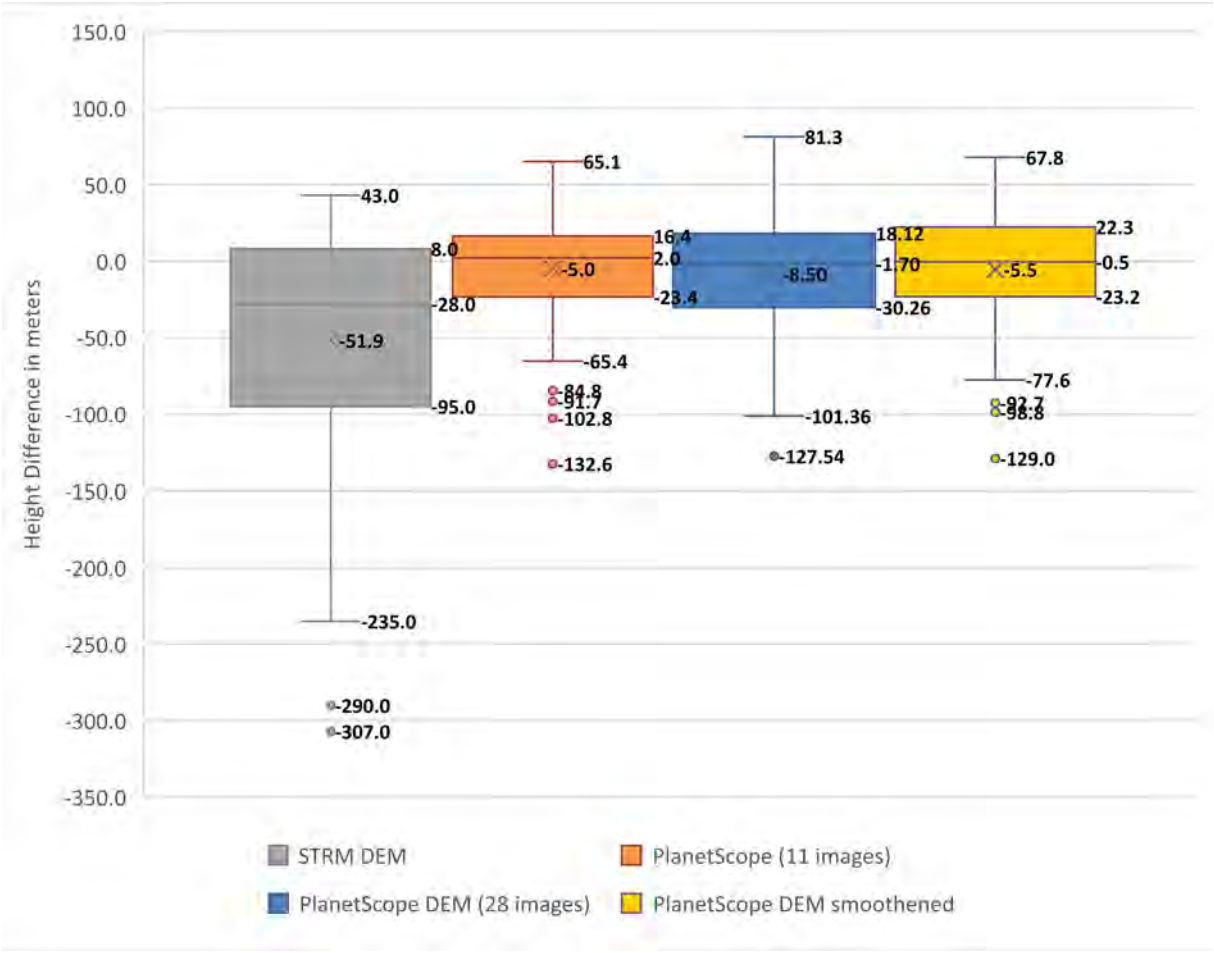

Figure 36 Box plots of height difference between Geoland map sheet and DEMs

	STRM DEM	PlanetScope (11 images)	PlanetScope DEM (28 images)	PlanetScope DEM smoothened
Mean Error	-51.9	-5.0	-8.5	-5.5
RMSE	94.1	36.8	39.9	39.0

Table 3 Mean error and RMSE of Geoland map sheet and DEMs

The box plots show the distribution of the data, in this case the distribution of the elevation differences relatively to the map sheet. The box section is the interquartile range (IQR) which shows the 25% to 75% of the dataset. The smaller this box and closer to 0, the closer the values are to the reference dataset. It also shows the average, median, maximum, minimum and outliers of the dataset.

When comparing the different DEMs, the PlanetScope DEMs perform much better than the SRTM DEM. The average of the differences for the PlanetScope DEM is only -5, while for the SRTM DEM it's more than five times as high at -51.9. This mostly says something

about the bias however, not much about the shape. The RMSE gives more information on the distribution, like the box plots. The PlanetScope DEM shows the smallest RMSE of 36.8 meters and the smallest box and whiskers, meaning the differences between the map sheet elevation and the PlanetScope DEM lie closer together than with the SRTM DEM. When looking at the other two PlanetScope DEMS, they also seem to be more accurate than the SRTM DEM. The RMSE of the smoothened and larger DEM (see chapter 6) are both around 39, a bit higher than the PS DEM, but still significantly better than the RSME of the SRTM DEM.

5.1.3 Field measurements

21 observations were made during the fieldtrip to the Caucasian mountains in Georgia. These measurements are compared with the generated PlanetScope DEM, the SRTM DEM, the smoothened DEM and the Geoland map sheet. To evaluate the performance of the DEMs, the raster cell value is subtracted from the measured elevation. This gives a graph with the difference in height for each of the points, shown in Figure 37.

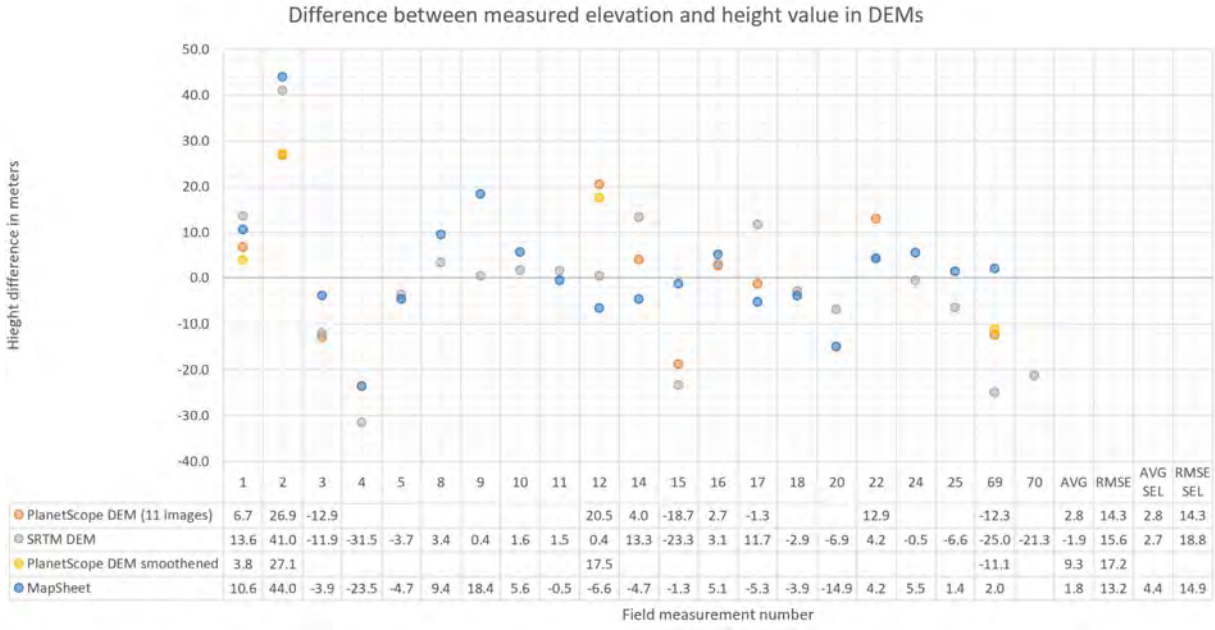

	1	2	3	4	5	8	9	10	11	12	14	15	16	17	18	20	22	24	25	69	70	AVG	RMSE	AVG SEL	RMSE SEL
PlanetScope DEM (11 images)	6.7	26.9	-12.9							20.5	4.0	-18.7	2.7	-1.3			12.9			-12.3		2.8	14.3	2.8	14.3
SRTM DEM	13.6	41.0	-11.9	-31.5	-3.7	3.4	0.4	1.6	1.5	0.4	13.3	-23.3	3.1	11.7	-2.9	-6.9	4.2	-0.5	-6.6	-25.0	-21.3	-1.9	15.6	2.7	18.8
PlanetScope DEM smoothened	3.8	27.1								17.5										-11.1		9.3	17.2		
MapSheet	10.6	44.0	-3.9	-23.5	-4.7	9.4	18.4	5.6	-0.5	-6.6	-4.7	-1.3	5.1	-5.3	-3.9	-14.9	4.2	5.5	1.4	2.0		1.8	13.2	4.4	14.9

Figure 37 Elevation difference field measurements and DEMs and Geoland map sheet

At the right end of the data table the average difference and the root mean square error of the elevation difference can be found. The first calculations are made with all available input for the different DEMs. The second calculations are based only on a selection (SEL) of the points that lie within the area of the generated PlanetScope DEM.

When comparing the different sources with the field observations it becomes clear that all of them show elevation deviations. The smoothened PlanetScope seems to perform the worst, with a 9.3-meter error on average and a 17.2-meter RMSE. These calculations are however only based on 4 measurements, and in all of those the smoothened DEM height values lay closer to the measurement than the PlanetScope DEM, and in three of them closer than the SRTM. The ME and RMSE for only these 4 points do thus not give very useful information on the accuracy.

To make a better comparison, the ME and RMSE are therefore calculated for only a selection of points that lie in all other three sources, so a fair comparison can be made. When looking at the mean error for those points, the PlanetScope DEM and SRTM DEM have almost the same value, respectively 2.8 and 2.7. The Geoland map sheet values that were manually entered from the contour lines have a ME of 4.4. The RMSE gives us a better understanding of the size of the deviations. Here the PlanetScope DEM (14.3m) and map sheet (14.9m) clearly perform better than the SRTM (18.8m).

5.2 Relief depiction

To convey the information from the height map to the user, a relief depiction is generated. This relief depiction consists of three main parts, the contour lines, a shaded relief, and a rock depiction. Additionally, the land cover and different type of ways (water and road) are added to the map.

To generate smooth contour lines that accurately represent the topology of the terrain, a low pass filter was applied to a part of the terrain. By keeping the original ridge and valley raster cells and using a spline interpolation to connect these to the smoothened DEM, a new raster data set is generated. Based on this DEM the contour lines were drawn. The difference between to contour lines based on the original DEM (red lines) and the contour lines of the smoothened DEM (brown lines) can be found in Figure 38. The legibility has greatly been improved.

To see how accurately this DEM still represents the topology and actual elevation, also after smoothing a part of it, this new DEM was also evaluated. By simply comparing the contour lines of the old and new DEM, beside being a lot smoother, the differences don’t seem to be too big. The different height lines do not show large displacements or shifts on the map.

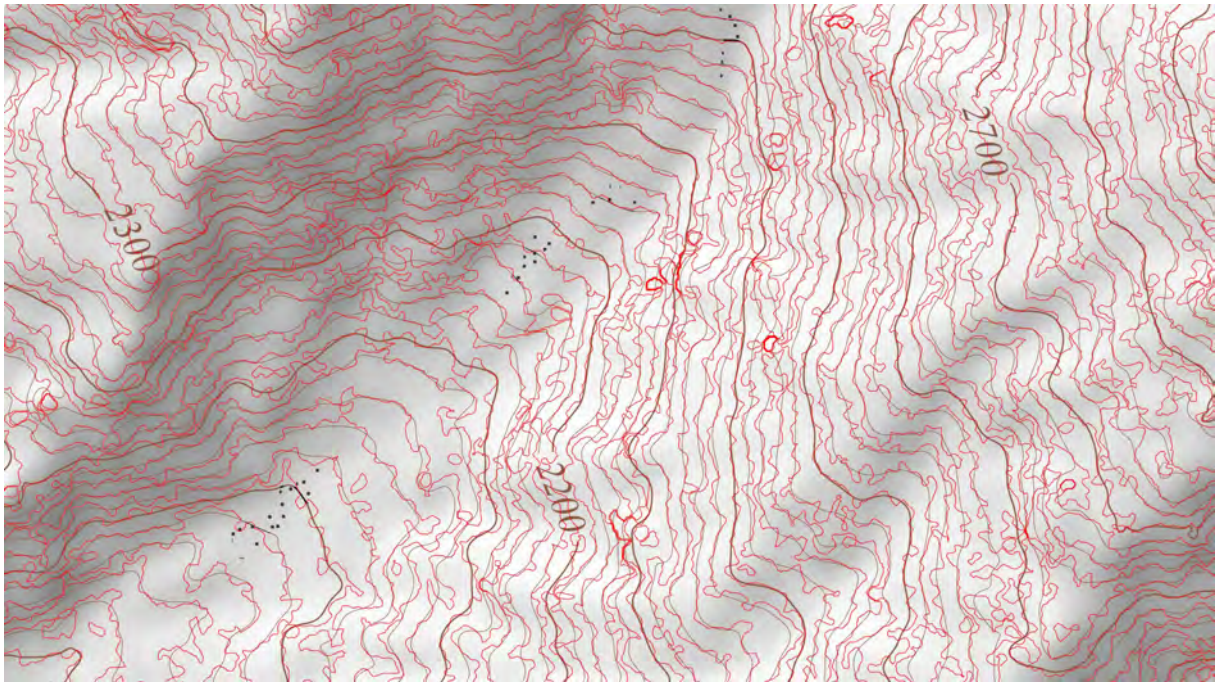

Figure 38 Contour lines based on original PlanetScope DEM in red and smoothened contour lines in brown

When comparing the smoothened DEM with the elevation points from the Geoland map sheet, it performs rather similarly to the original PlanetScope DEM. The smoothened DEM only has a slightly larger mean error (-5.0 versus -5.5) and RMSE (see Figure 36 and Table 3). The RMSE of the smoothened DEM is around 39, a bit higher than the PS DEM, but still significantly better than the RSME of the SRTM DEM. The median of the smoothened DEM of 0.5 comes even closer to 0 than the median of the original PS DEM with 2.0. Also the comparison with the field measurement values does not show any problems with the smoothing. Even though only 4 field observations lie within the area of the new DEM, all deviations were smaller than for the original PlanetScope DEM.

To evaluate how much the terrain has been changed by the smoothing, the DEMs are subtracted from eachother (Figure 39) and a profile graph of the original and smoothened DEM is created (see Figure 40). The subtraction is visualized with a standard deviation classification and shows that the stable areas are not influences much by the smoothing noir are the valleys or ridgeslines affected. Only the unessacary detail in the mountainous terrain is touched by the smoothing. This graph with the profile line also shows that the elevation values are not altered much by the smoothing, only the noise got smoothened out. Also the large error present along this profile line (around the 13500 meter marker) and some smaller sinks are now deleted, because the sinks were filled before the smoothing.

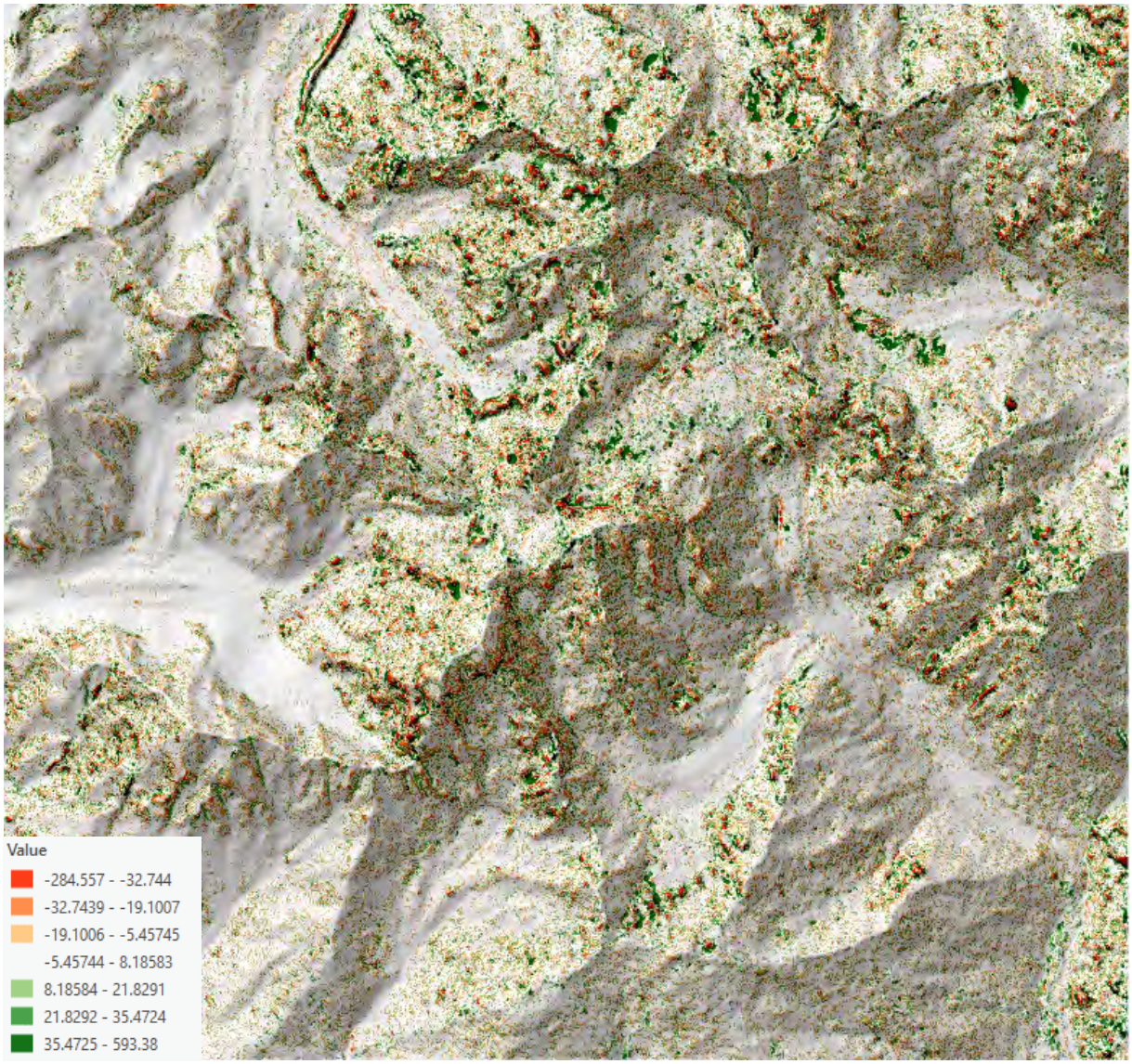

Figure 39 Comparison original and smoothened PlanetScope DEM

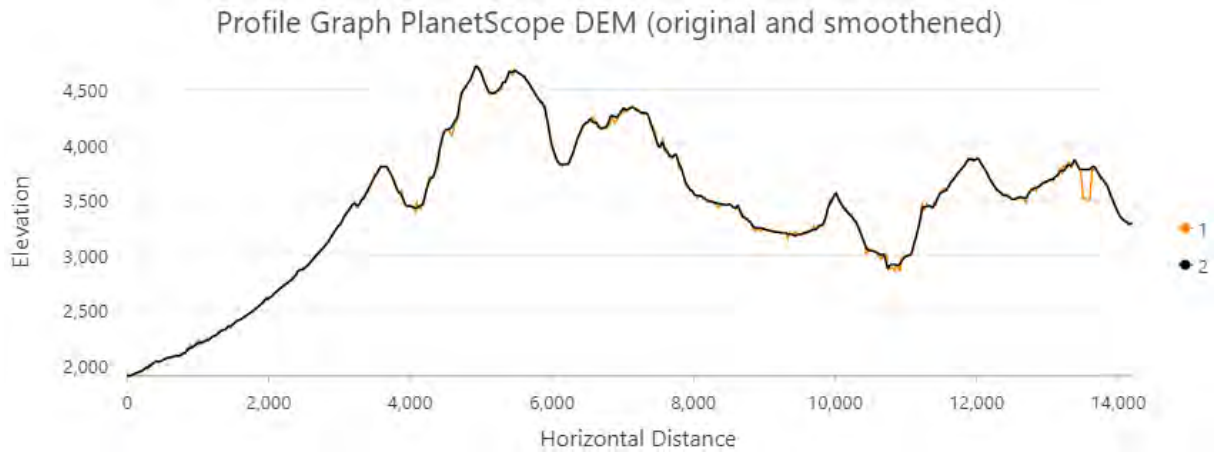

Figure 40 Elevation profile of original and smoothened PlanetScope DEM

Based on the generated PlanetScope DEM a relief depiction is created. The first step is the creation of contour lines based on the smoothened DEM. Based on common intervals for maps on this scale (see chapter 2.3), the equidistance is set to 20 meters with an index line every 100 meters. This equidistance works well for the hills and less steep mountains. The steeper sections do get a bit crammed. An equidistance of 25 meters with the index line still every 100 meters could also be considered, to create a bit more room between the contour lines. The best equidistance can be decided upon when creating the contour lines for the entire map extent, when all types of terrain and different slopes are present. The contour lines and labels are like most existing map sheets in the same color and based on the background color so the other items on the map will not be drowned out. The labels are placed in a gap in the contour line to keep them legible and placed west to east, so they can be read without turning the map. To avoid confusion on the aspect of the slope with this labeling approach the labels are placed in a ladder. Due to the restraints on the label placement, the maximum angle and a placement on a more or less straight part of the line, the ladder placement does not work very well for this part of the terrain. Most labels still end op a bit further apart, leaving only sporadic labeling in some parts. This way the aspect of the slope might be harder to interpretate, but this can be improved by using a shaded relief in combination with contour lines. Placing the contour labels manually in an editing program instead of doing the placement with GIS software, could also improve the labeling and interpretation of the terrain.

The final result of contour lines for the study area are shown in Figure 41, together with the additional data that was added in GIS. OpenStreetMap (OSM) data is used to display the roads and waterways. Also, the OSM landcover is used, except for the glaciers and rock areas. These are based on the layers that were created by Schröder (2020). These layers are exported together as a PNG-file for further processing.

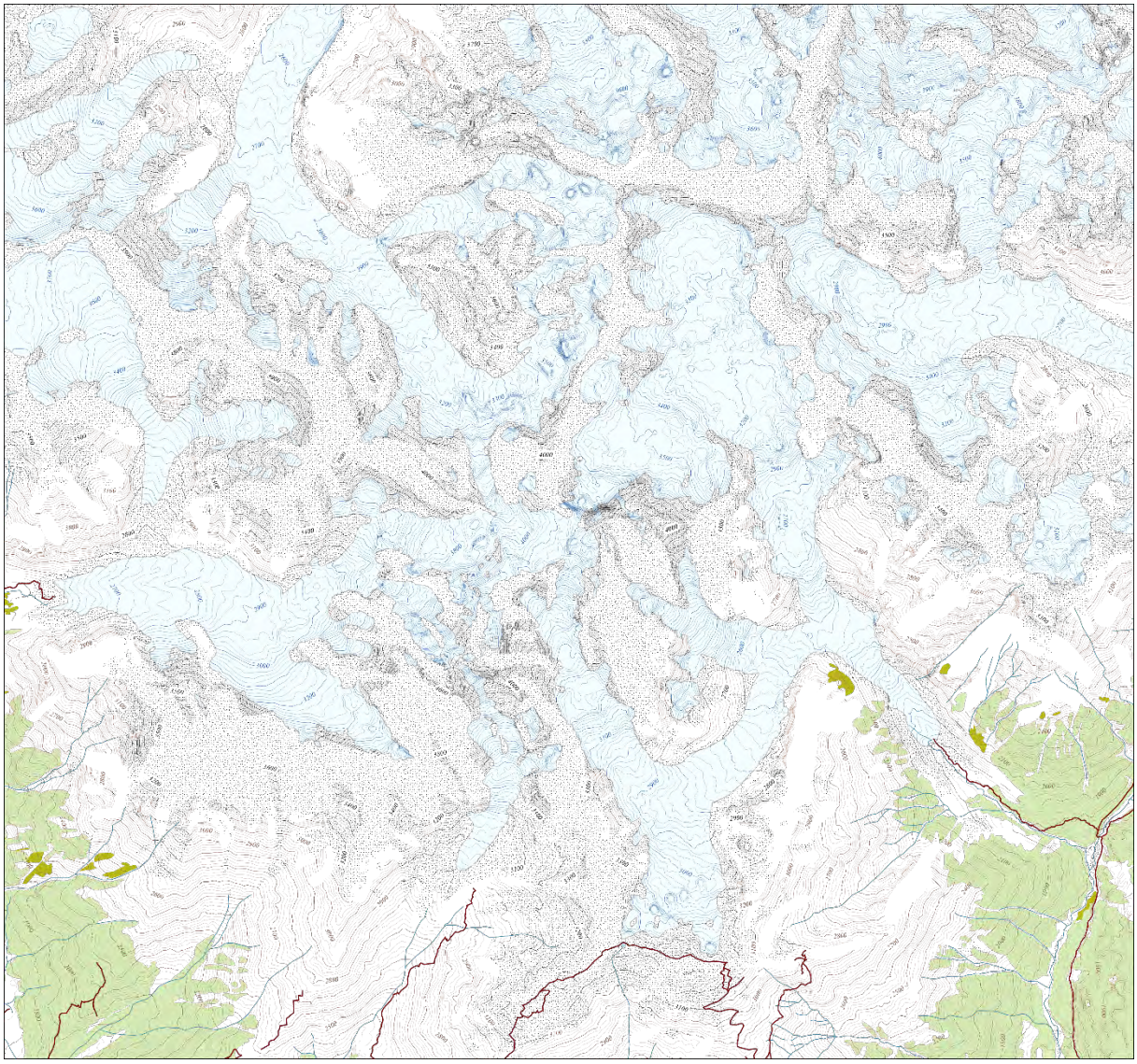

Figure 41 ArcGIS export with contour lines and OSM data

The shaded relief for the research area has been created in Blender. It is based on the smoothened PlanetScope DEM. There are still some bumps in the terrain, but it already looks a lot smoother when comparing it to a shaded relief of the original PlanetScope DEM, as can be seen in Figure 44 (a). The next figure (b) shows the smoothened DEM, but with the shaded relief created in ArcGIS. Here the material looks very shiny, and the light scattering does not look very realistic. The shaded relief created in Blender might look a bit grey, but this is helpful to only select the bright areas and shadow areas. By only adding those to the map, the other layers in the map will keep their vivid color and not be influenced by a grey middle tone of the hill shade.

When comparing the shaded relief to the five main principles by Becker (chapter 2.2.2), we find that these are mostly honored. There is a sharp tone difference at the ridges. The

illuminated side has the brightest tones, and the shadow side has the darkest tones. The strength of the shading also diminishes towards the valley. This is not only the shading from the shadow side of the mountain, but also a mild shadow cast by the mountain. This does however result in a more realistic shaded relief. For the legibility it could be decided to not cast shadows, but the current results do seem more intelligible. Terrain features are easier to read and interpret this way. An example of this difference becomes clear when looking at Figure 42. In the shaded relief on the left side, it is difficult to establish how wide the valley is that is running northeast-southwest. In the shaded relief created with Blender on the other hand, the feature is much clearer. Principle 3, to use a medium tone for the sections connecting the light and dark areas is also applied in the Blender hill shade. However, this will be left out when applying the shaded relief to the map. This way the grey does not influence the background colors. Only the areas that receive sunlight get lighter, and the shadow areas get darker. The last principle not discussed yet, number 4, has not been applied for this shaded relief.

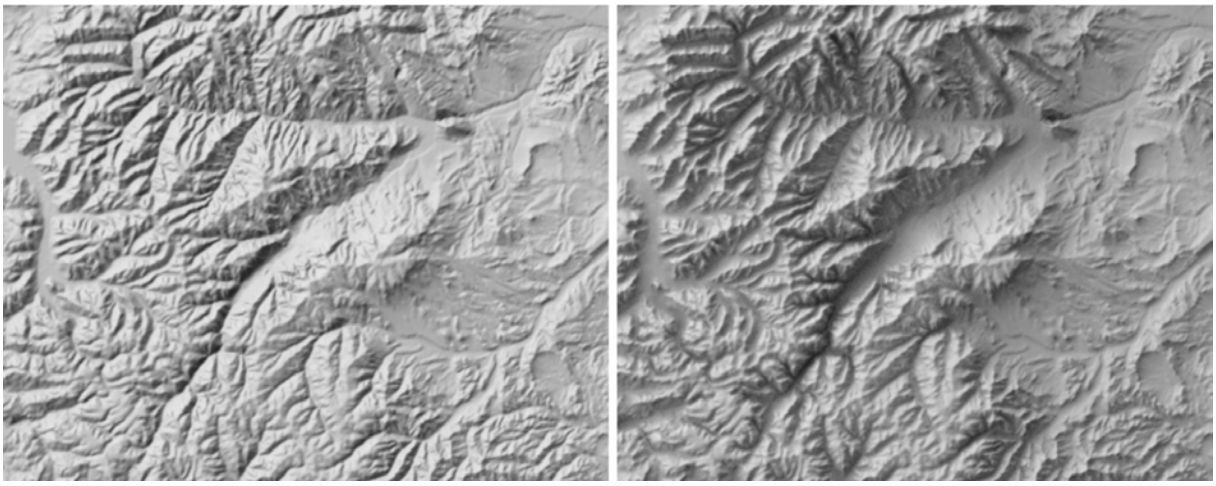

Figure 42 Difference in visibility of landforms in a standard hill shading (left) and a hill shading created with Blender (right) (Huffman, 2020)

In mountainous areas there is often a lot of unnecessary and undesirable detail in the shaded relief when these are generated analytically. A comparison of an analytical shaded relief and a manual shading in Figure 43 clearly shows this difference. The manual shading better shows the vertical transitions, focusing on the important features and landforms.

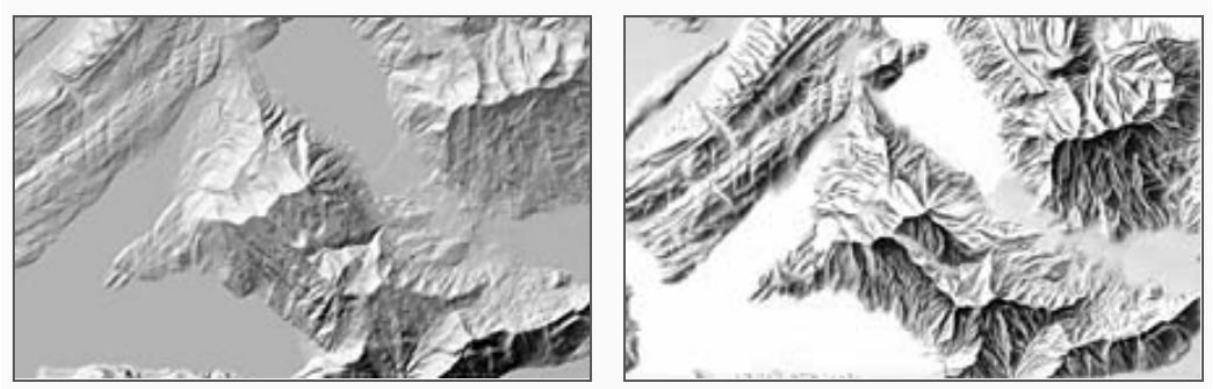

Figure 43 Analytical hill shading (left) and manual hill shading (right) (Jenny & Räber, 2015b)

Further improvements to the shaded relief created in Blender could be made in Adobe Photoshop. Unnecessary detail and artefacts can be removed from the shaded relief with the available image editing tools. This way the important landforms are easier to identify.

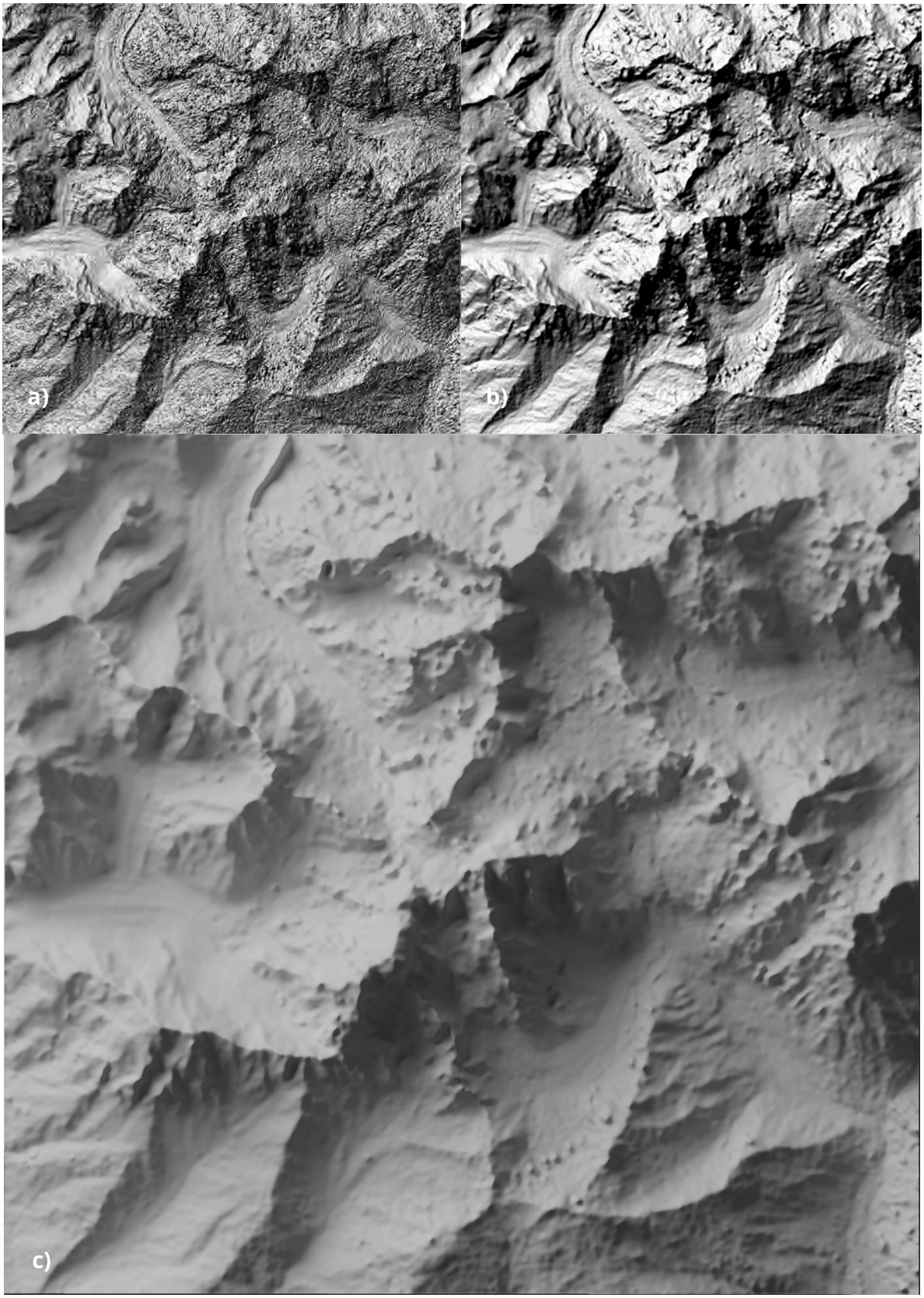

Figure 44 a) Hill shade based on original PlanetScope DEM, b) Hill shade created in ArcGIS based on smoothened DEM, c) Hill shade creatd in Blender based on smoothened DEM

The last part that is added to the relief depiction is the rock visualization. A rock drawing is created for the areas that were traced as bedrock from the map sheets. The generated and smoothed PlanetScope is resampled to 10 meters to generate a legible rock drawing. Together with the rock mask the DEM is entered into the Piotr software developed by Roman Geisthövel. This program automatically generates a rock depiction based on the Swiss rock depiction style and outputs it as a PNG-file (Figure 45). The shaded relief that the rock hachures are based on is also given (see appendix Figure 48) but will not be used for the final visualization. The hill shade is generated after the generalization using line integral convolution (LIC) and has many bulky vertices and no realistic lighting of the terrain. All in all, it does not provide a realistic shaded relief.

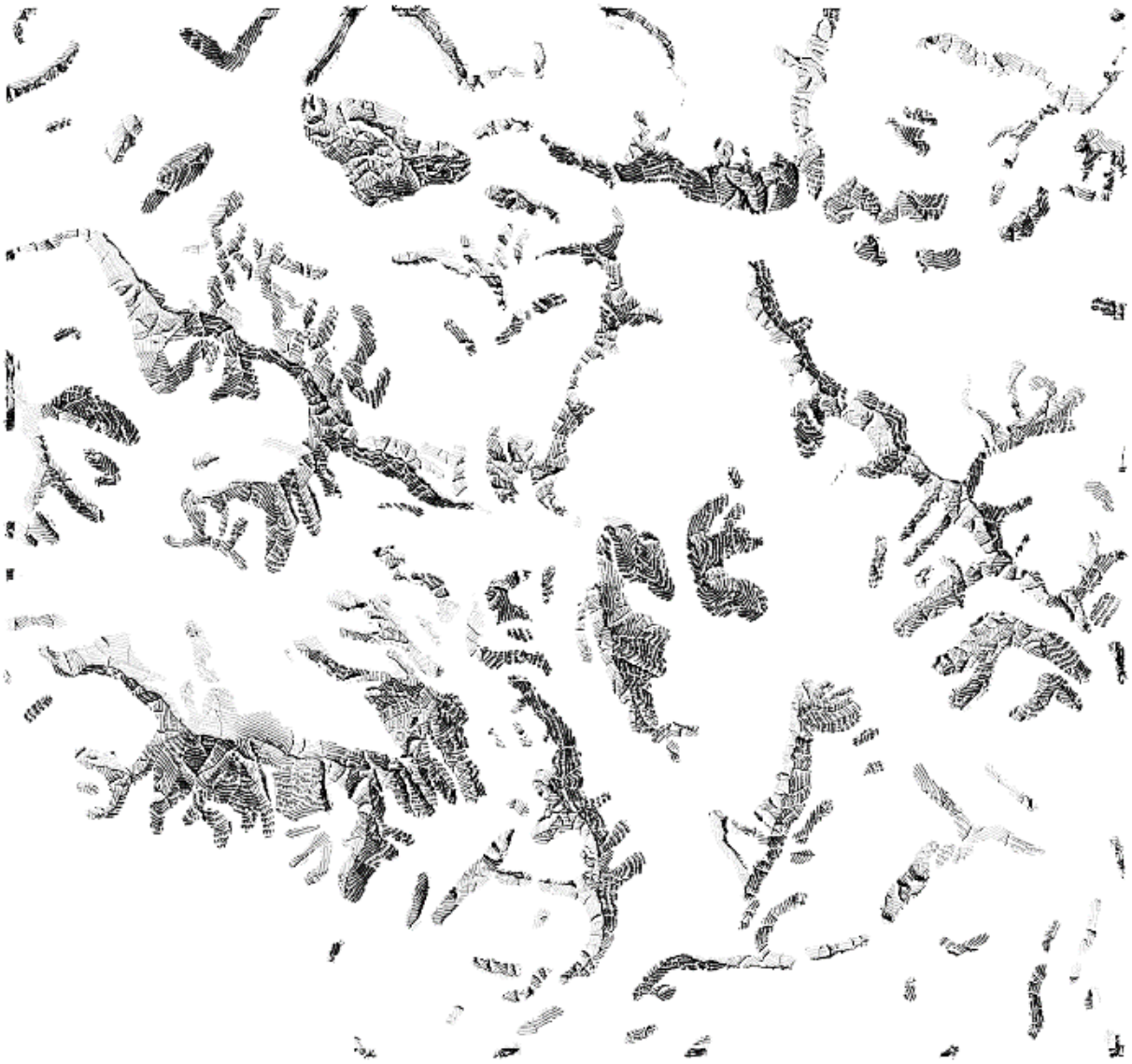

Figure 45 Rock depiction created with Piotr based on a smoothened 10-meter resolution PlanetScope DEM

Now all the different aspects of the relief depiction and all the information is available, the parts will be combined into a final map. All layers have been created at a scale of 1:33,000 as this is also the intended scale of the final map. To put together the map Adobe Photoshop is used. After creating a background layer, the base layer created in ArcGIS Pro is added. On top is this layer the rock depiction will be placed. But first the white background in the rock depiction is removed. After this, only the rock drawing remains and is placed on top of the base layer. The blending mode of the rock layer is set to *linear burn* and at 70% opacity to balance the items in the map. The last item to be added is the shaded relief. This is added on top of the other layers, so the shaded relief will be applied on all items of the map, except for the labels. The hill shade layer from Blender is added twice. From the first one only the darker colors are selected with a *levels adjustment* layer. This selection is then also applied to the map with a *linear burn* at an opacity of 40%, for the shadow not to be too dark or present and to keep everything legible. From the second hill shade layer only the light sections are selected. These will light up the areas in the mountainous terrain that receive light, either directly from the sun or from scatter. These are applied to the map with the blending mode set to *screen*. The result can be seen in Figure 46 on a smaller scale and in the appendix Figure 51 at the original 1:33:000 scale.

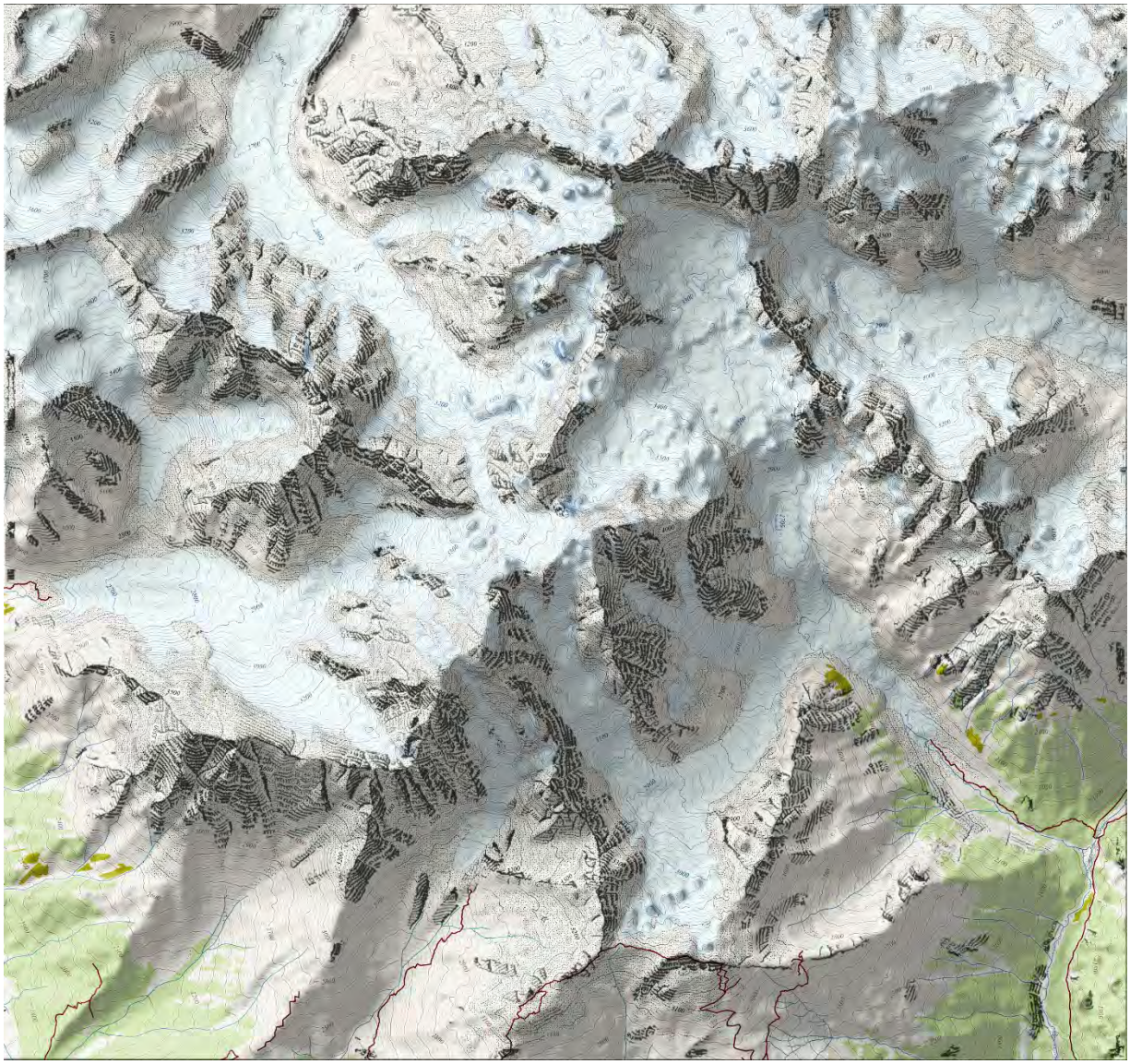

Figure 46 Final relief depiction based on generated PlanetScope DEM

6 Discussion

This chapter will provide a critical look at the used methodology and the results. What are the limitations of this study and/or recommendations for further research?

6.1 Digital elevation model

The digital elevation model that was created for this study only covers a small section of the entire map extent and is only based on 11 images, while Planet provided 34 photos from 2019 and another 14 from 2018. By using all imagery, a larger DEM can be generated. This can also be useful when evaluating the quality of the DEM, since many of the field measurement taken now lie outside the research area of this study (see Figure 23). Extending the DEM would also cover more stable terrain, which often provides better results in stereophotogrammetry.

A first attempt was already made to generate a DEM from 28 images that are available from 2019. Using the same workflow as with the DEM for the research area, this did however provide some issues. The digital elevation model has very different elevation values and lies approximately 170 meters lower. When equalizing the mean values of the digital elevation models (based on the extent of the research area) to compare if the shapes are at least similar and the problem would only be a vertical shift, the model still shows some differences. The two DEMs were subtracted from one another for the extent of the research area, which clearly shows a trend (see Figure 47). On the north-east side of the mountains all the elevation are lower in the new DEM, and on the south-west side they are the opposite. This could indicate a horizontal shift in the data. Where exactly this vertical and horizontal shift is coming from is however not easy to detect. Further research is needed to solve this issue.

The larger DEM that was equalized based on the mean elevation value, has already been included in the evaluation as well (see Figure 36 and Table 3) and compared to the elevation values in the Geoland map sheet. This shows that the larger DEM performs slightly worse than the PlanetScope DEM for the research area, but still shows better results than the SRTM DEM, with a RMSE of 39.9. The larger DEM was also evaluated with the use of the field measurements. These results can be found in the appendix (Table 7 and Figure 50). Here it becomes visible that the errors of the larger DEM are higher than those for the smaller DEM and SRTM, looking at the measurements they all share (see SEL statistics). The mean error is 6.3m instead of 2.8m and 2.7m for respectively the smaller PS DEM and SRTM. The RMSE is comparable to the SRTM DEM with 18.2m for the larger PlanetScope DEM and 18.8 for the SRTM DEM. The smaller PlanetScope DEM

clearly performs better here with an RMSE of 14.3 meters. One has to keep in mind that these statistics were only calculated after removing the vertical offset by adding 170 meters to the larger PlanetScope DEM, and the horizontal offset was not taken into account.

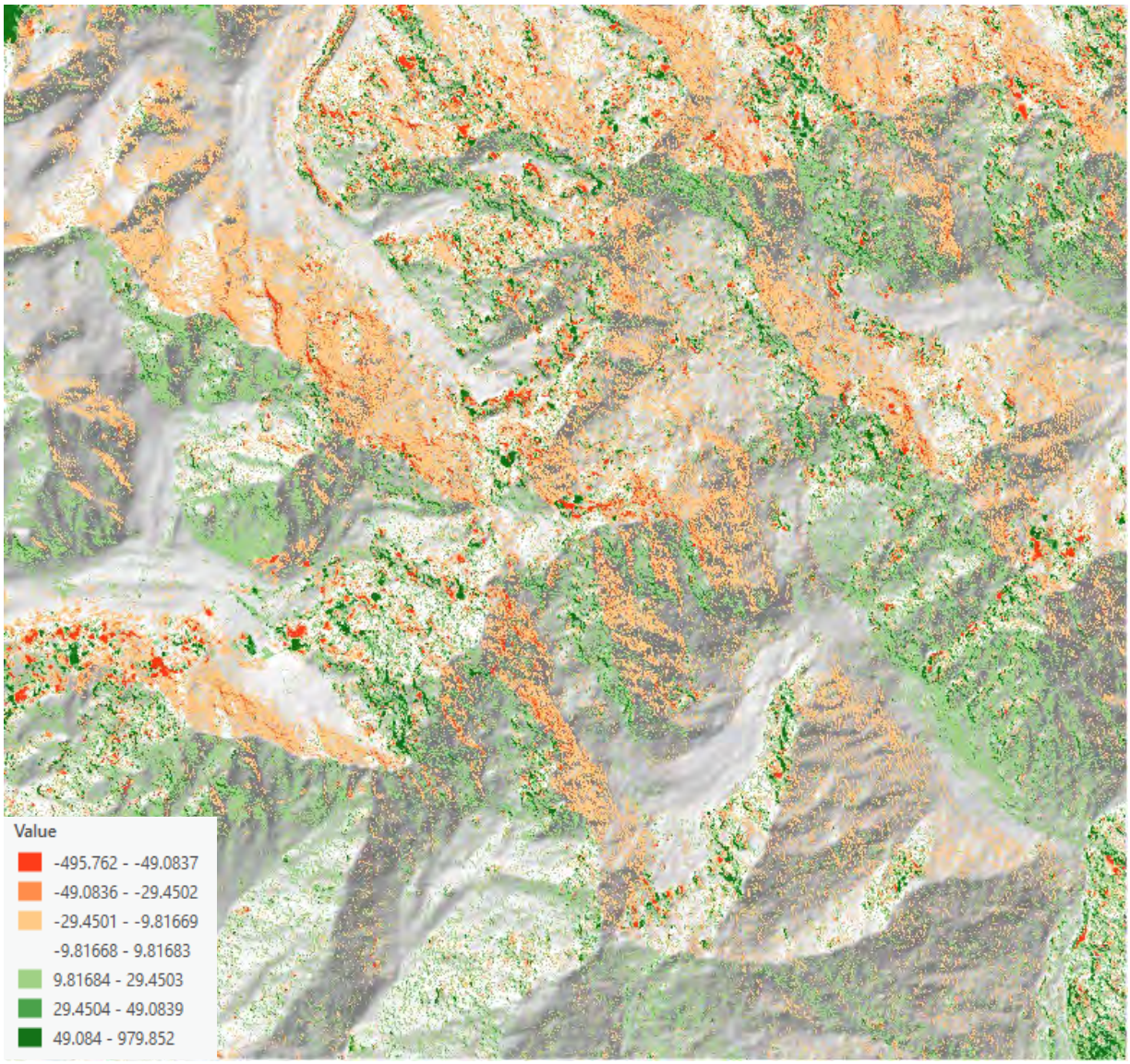

Figure 47 Comparison PlanetScope DEMs (equalized mean elevation)

To evaluate the generated DEMs better, it would also be good to make a comparison to another, higher resolution DEM. The SRTM data comes at a 30 meter resolution, while the PlanetScope data has a resolution of 3.6 meters. Free open-source digital elevation models often come at a low resolutions. When a DEM generated from for example LiDAR would be available of the terrain, a better and more accurate comparison could be made.

6.2 Relief depiction

Also for the relief depiction there are some aspects that could be improved or researched further.

In the Alpine Maps the direction of the light source often gets adapted locally, to emphasize and clarify topographic features (Hurni, 2008). This is a technique that is possible when creating the shaded relief manually. This has not been applied when creating the analytical hill shading in Blender for this study. Perhaps it is possible to add more light sources in the program, that can then be used locally to emphasize the important topographic features. This would need more research to see if this is possible and how to do this. It also needs to be studied if this provides an added value and actually improves the visualization.

Another technique applied to the creation of shaded reliefs is one of the principles by Becker (see chapter 2.2.2). This principle states that “the highest mountain peaks must be depicted with the strongest color contrast. Colors should be attenuated for lower areas to simulate the effect that aerial perspective has on colors. Color contrast must be reduced for the lowest terrain features (i.e., valley floors).” This is also something that has to be studied to see if it is possible to create this in Blender or other software, and if this impression of an aerial perspective would improve the interpretation of the map.

The shaded relief that was created in Blender is a lot smoother than the hill shade based on the original PlanetScope DEM. There is however still some noise and unnecessary detail present in the terrain. There are for example also some bumps present on the glaciers that seem to correspond with areas on the glacier with big crevasses. To improve the identification of important landforms and remove the unnecessary detail and artefacts, further improvements to the shaded relief could be made in Adobe Photoshop. This would require someone with a sound knowledge of the terrain and the representation of landforms, so only the unnecessary detail gets removed.

The rock depiction created with the software of Roman Geisthövel is based on the Swiss style. As mentioned in chapter 2.3 there are some differences between the Swiss style and the Alpine Club Map rock depiction. While there has been a lot of research from the ETH Zürich into the automation of rock depiction, there is not much research available on the rock depiction in Alpine Club Maps. There is therefore also no software available to create the rock depiction automatically. To mimic the current Alpine Club Map rock depiction style better, this would have to be created manually or more research into the automatic generation of the more realistic rock depiction style from the Alpine Club is needed.

7 Conclusion

The main research objective of this study was to develop a detailed high-quality cartographic depiction of the alpine and nival zone of Mount Ushba, Georgia. To reach this objective two subobjectives and their respective research questions were defined.

The first subobjective is the generation and evaluation of a Digital Elevation Model of the Mount Ushba region, Georgia, with the use of high-resolution PlanetScope Imagery.

1.1. How is it possible to photogrammetrically generate a DEM with PlanetScope Imagery and which spatial resolution and height accuracy can be reached?

1.2. How does the quality and accuracy of the generated DEM compare with existing elevation models and map sheets?

In the results it was shown that is it possible to generate a digital elevation model with the use of PlanetScope imagery, even with its small baseline to height ratio. The first method, with the use of the open-source program MicMac did not lead to satisfying results. The methodology presented in the study to generate a digital elevation model with the use of Agisoft Metashape did provide a good quality DEM. Because this DEM generation was performed with the highest quality settings, the generated DEM still has the original resolution of the imagery, approximately 3.6 meters.

To establish the accuracy of the DEM, it was compared to the SRTM DEM of the area, to existing map sheets of the region and to field measurements that were taken during the mapping campaign in Mestia, Georgia, in the summer of 2021. This comparison shows that the generated PlanetScope has a good quality and accuracy, but does show some errors that could be due to occlusions in the terrain. The ME of 10 meters and RMSE of 46.9 meters for the elevation difference between the SRTM DEM and PlanetScope DEM does indicate that there are some significant differences between the two DEMs.

The SRTM DEM itself does however also have elevation deviations, especially in mountainous terrain. Both DEMs were therefore compared with elevation points taken from the map sheets and measurements in the field. This shows that the PlanetScope performs better on the vertical accuracy than the SRTM DEM. The average of the differences with the map sheet for the PlanetScope DEM is only -5m, while for the SRTM DEM it’s more than five times as high at -51.9m. The RMSE gives more information on the distribution of the errors. The PlanetScope DEM shows the smallest RMSE of 36.8m, meaning that the differences between the map sheet elevation and the PlanetScope DEM lie closer together than those of the SRTM DEM that has an RMSE of 91.4m.

The same pattern is visible in the comparison of the elevation values with the field measurements. When looking at the mean error, the PlanetScope DEM and SRTM DEM

have almost the same value, respectively 2.8m and 2.7m. The RMSE however shows that the PlanetScope DEM (14.3m) clearly performs better than the SRTM (18.8m).

The second subobjective was the creation of a large-scale relief depiction based on the cartographic depiction of the Alpine Club, and has the following research questions:

1.3. Which relief depiction methods are currently used by the Alpine club?

1.4. How can the relief of Mount Ushba and the ice and rock surfaces be visualized?

Common methods to depict the relief in Alpine Club maps are the use of contour lines, shaded relief and a rock depiction. These depictions are commonly drawn manually. This requires someone that is able to read and interpret the terrain but also has the skill artistically to draw these relief depictions. Nowadays, with the availability of digital elevation models for most of the Earth's surface, these depictions can also be generated with the use of software. This software does however not have an understanding of the terrain, nor is it able to distinguish between unnecessary detail and important landforms that need to be emphasized for the map user.

The creation of contour lines is something that can be done automatically based on the generated PlanetScope DEM. Before this, the DEM first had to be smoothened. This smoothing was necessary the remove all unnecessary detail and noise from the DEM and create smooth legible contour lines. The smoothened DEM was also evaluated to make sure it still represents the correct elevation data. The smoothened DEM only shows a slightly larger ME (-5.5m) and RMSE (39m) than the original DEM when comparing the elevations to the Geoland map sheet, but does provide much better and legible contour lines.

The shaded relief has been produced with Blender. This program created realistic 3D models, where the light source does not only directly influences the terrain, but the light also gets scattered by the objects. This provides a much more realistic hill shade, than the analytical hill shading available in GIS software. There is however still some improvement possible by locally adapting the light direction to clearly depict certain landforms better that would otherwise lie in the same direction as the light source.

The last step of the relief depiction was the creation of a rock depiction. To distinguish between the bedrock and loose rock and scree, the bedrock was traced from existing map sheets. This mask was used to create a rock depiction with Piotr, based on the Swiss style rock depiction. This program gives good results, although the Swiss rock depiction does deviate slightly from the Alpine Club Map rock depiction.

All these visualizations were combined with OpenStreetMap data into a final map using Adobe Photoshop and provide an exemplary section for a hiking map of the Ushba region.

References

Agisoft Metashape Professional (1.6.5). (2021). [Software]. Agisoft LLC. https://www.agisoft.com/

Arnberger, E. (1970). *DIE KARTOGRAPHIE IM ALPENVEREIN*. Wissenschaftliche Alpenvereinshefte.

Automatic Swiss style rock depiction. (2003). [Software]. http://motlimot.net/software.html

Beyer, R. A., Alexandrov, O., & McMichael, S. (2018). The Ames Stereo Pipeline: NASA's Open Source Software for Deriving and Processing Terrain Data. *Earth and Space Science*, *5*(9), 537–548. https://doi.org/10.1029/2018ea000409

Blender (2.82a). (2020). [Software]. The Blender Foundation. https://www.blender.org/

Brandstätter, L. (1983). *Gebirgskartographie*. Deuticke.

Brunner, K. (2001). Die Kartographie im Deutschen Alpenverein. *KN - Journal of Cartography and Geographic Information*, *51*(1), 17–22. https://doi.org/10.1007/bf03544773

Brunner, K., & Welsch, W. (2002). High-mountain cartography of the German and the Austrian Alpine Clubs. *ISPRS Journal of Photogrammetry and Remote Sensing*, *57*(1–2), 126–133. https://doi.org/10.1016/s0924-2716(02)00108-9

Bürgmann, R., Rosen, P. A., & Fielding, E. J. (2000). Synthetic Aperture Radar Interferometry to Measure Earth's Surface Topography and Its Deformation. *Annual Review of Earth and Planetary Sciences*, *28*(1), 169–209. https://doi.org/10.1146/annurev.earth.28.1.169

Collier, H. (1972). A Short History of Ordnance Survey Contouring with particular reference to Scotland. *The Cartographic Journal*, *9*(1), 55–58. https://doi.org/10.1179/caj.1972.9.1.55

Collier, P., Forrest, D., & Pearson, A. (2003). The Representation of Topographic Information on Maps: The Depiction of Relief. *The Cartographic Journal*, *40*(1), 17–26. https://doi.org/10.1179/000870403235002033

Dahinden, T. (2002, October). *Existing rock representation in topographic maps and their suitability for digital generation*. The 2002 ICA Mountain Cartography Workshop, Mt. Hood, Oregon, USA. http://citeseerx.ist.psu.edu/viewdoc/download?doi=10.1.1.531.7616&rep=rep1&type=pdf

Dall'Asta, E., & Roncella, R. (2014). A comparison of semiglobal and local dense matching algorithms for surface reconstruction. *The International Archives of the Photogrammetry, Remote Sensing and Spatial Information Sciences, XL–5*, 187–194. https://doi.org/10.5194/isprsarchives-xl-5-187-2014

Dobrinić, D., Gašparović, M., & ŽUpan, R. (2018). HORIZONTAL ACCURACY ASSESSMENT OF PLANETSCOPE, RAPIDEYE AND WORLDVIEW-2 SATELLITE IMAGERY. *18th International Multidisciplinary Scientific GeoConference SGEM2018, Informatics, Geoinformatics and Remote Sensing*, 129–136. https://doi.org/10.5593/sgem2018/2.3/s10.017

Dukuzemariya, T. (2017). *DSM creation and image orthorectification from satellite and aerial very high resolution products: MICMAC application in hilly and urban area of Liège, Belgium.* http://hdl.handle.net/2268.2/3124

Esri. (n.d.-a). *Flow Accumulation (Spatial Analyst)—ArcGIS Pro | Documentation*. Retrieved 2021, from https://pro.arcgis.com/en/pro-app/latest/tool-reference/spatial-analyst/flow-accumulation.htm

Esri. (n.d.-b). *Geoid—ArcGIS Pro | Documentation*. Retrieved 2021, from https://pro.arcgis.com/en/pro-app/latest/help/mapping/properties/geoid.htm

Eynard, J. D., & Jenny, B. (2016). Illuminated and shadowed contour lines: improving algorithms and evaluating effectiveness. *International Journal of Geographical Information Science*, *30*(10), 1923–1943. https://doi.org/10.1080/13658816.2016.1144885

Farmakis-Serebryakova, M., & Hurni, L. (2020). Comparison of Relief Shading Techniques Applied to Landforms. *ISPRS International Journal of Geo-Information*, *9*(4), 253. https://doi.org/10.3390/ijgi9040253

Firdaus, M. I., & Rau, J. Y. (2017). Comparisons of the three-dimensional model reconstructed using MicMac, PIX4D mapper and Photoscan Pro. *38th Asian Conference on Remote Sensing-Space Applications: Touching Human Lives, ACRS.* https://www.researchgate.net/publication/325216490_COMPARISONS_OF_THE_THREE-DIMENSIONAL_MODEL_RECONSTRUCTED_USING_MICMAC_PIX4D_MAPPER_AND_PHOTOSCAN_PRO

Friedt, J. M. (2014, September 5). *Photogrammetric 3D structure reconstruction using Micmac* [Slides]. Jean-Michel Friedt. http://jmfriedt.free.fr/lm_sfm_eng.pdf

Geisthövel, R., & Hurni, L. (Eds.). (2015). *Automatic rock depiction via relief shading*. Proceedings of the 27th International Cartographic Conference.

Geisthövel, R., & Hurni, L. (2018). Automated Swiss-Style Relief Shading and Rock Hachuring. *The Cartographic Journal*, *55*(4), 341–361. https://doi.org/10.1080/00087041.2018.1551955

Geisthövel, R. M. (2017). *Automatic Swiss style rock depiction*. https://www.research-collection.ethz.ch/handle/20.500.11850/201368

Georgantas, A., Brédif, M., & Pierrot-Desseilligny, M. (2012). AN ACCURACY ASSESSMENT OF AUTOMATED PHOTOGRAMMETRIC TECHNIQUES FOR 3D MODELING OF COMPLEX INTERIORS. *ISPRS - International Archives of the Photogrammetry, Remote Sensing and Spatial Information Sciences*, *XXXIX-B3*, 23–28. https://doi.org/10.5194/isprsarchives-xxxix-b3-23-2012

Georgian National Tourism Administration. (0000). *Georgia Tourism Strategy*. http://www.economy.ge/uploads/ecopolitic/turizmi-/sakartvelos%20turizmis%20strategia%202025.pdf

Ghuffar, S. (2018). DEM Generation from Multi Satellite PlanetScope Imagery. *Remote Sensing*, *10*(9), 1462. https://doi.org/10.3390/rs10091462

Gómez, M. F., Lencinas, J. D., Siebert, A., & Díaz, G. M. (2012). Accuracy Assessment of ASTER and SRTM DEMs: A Case Study in Andean Patagonia. *GIScience & Remote Sensing*, *49*(1), 71–91. https://doi.org/10.2747/1548-1603.49.1.71

Gorokhovich, Y., & Voustianiouk, A. (2006). Accuracy assessment of the processed SRTM-based elevation data by CGIAR using field data from USA and Thailand and its relation to the terrain characteristics. *Remote Sensing of Environment*, *104*(4), 409–415. https://doi.org/10.1016/j.rse.2006.05.012

GRASS Development Team. (n.d.). *r.fillnulls - GRASS GIS manual*. GRASS GIS 8.0.Dev Reference Manual. Retrieved 2021, from https://grass.osgeo.org/grass80/manuals/r.fillnulls.html

Hallet, M. J. (2020, October). *Mapping the Vegetation of the Caucasian Ushba Region (Georgia Russian Federation) as a contribution to an Alpine Club Map* (Thesis). https://cartographymaster.eu/wp-content/theses/2020_Hallett_Thesis.pdf

Hasegawa, H., Matsuo, K., Koarai, M., Watanabe, N., Masaharu, H., & Fukushima, Y. (2000). DEM accuracy and the base to height (B/H) ratio of stereo images. *International Archives of Photogrammetry and Remote Sensing*, *33*(Part B4), 356–359. https://www.isprs.org/proceedings/XXXIII/congress/part4/356_XXXIII-part4.pdf

HASEGAWA, H., MATSUO, K., KOARAI, M., WATANABE, N., MASAHARU, H., & FUKUSHIMA, Y. (2000). DEM ACCURACY AND THE BASE TO HEIGHT (B/H) RATIO OF STEREO

IMAGES. *International Archives of Photogrammetry and Remote Sensing*, *XXXIII*(B4). https://www.isprs.org/proceedings/XXXIII/congress/part4/356_XXXIII-part4.pdf

Help Articles - ENVI & IDL | L3Harris Geospatial. (n.d.). L3Harris Geospatial. Retrieved November 2, 2021, from https://www.l3harrisgeospatial.com/Support/Self-Help-Tools/Help-Articles/Help-Articles-Detail/ArtMID/10220/ArticleID/18416/5012?gclid=Cj0KCQjww4OMBhCUARIsAILndv4ODFRSNZNcSU82vtN9n6_XUk2__AFlG5po-BiubZEsbn3hogZMmSAaAnnvEALw_wcB

Hirschmuller, H. (2008). Stereo Processing by Semiglobal Matching and Mutual Information. *IEEE Transactions on Pattern Analysis and Machine Intelligence*, *30*(2), 328–341. https://doi.org/10.1109/tpami.2007.1166

Hoekstra, B. (2019, February 22). *Photo-realistic shaded relief using Blender*. Bart Hoekstra. Retrieved 2021, from https://www.barthoekstra.com/blog/photo-realistic-shaded-relief-using-blender

Höhle, J., & Höhle, M. (2009). Accuracy assessment of digital elevation models by means of robust statistical methods. *ISPRS Journal of Photogrammetry and Remote Sensing*, *64*(4), 398–406. https://doi.org/10.1016/j.isprsjprs.2009.02.003

Huffman, D. (2020, November 22). *Creating Shaded Relief in Blender*. Somethingaboutmaps. Retrieved 2021, from https://somethingaboutmaps.wordpress.com/2017/11/16/creating-shaded-relief-in-blender/

Hurni, L. (2008, February). Cartographic Mountain Relief Presentation. *Mountain Mapping and Visualisation : Proceedings of the 6th ICA Mountain Cartography Workshop*, 85–91. http://www.mountaincartography.org/publications/papers/papers_lenk_08/hurni.pdf

HURNI, L., DAHINDEN, T., & HUTZLER, E. (2001). Digital Cliff Drawing for Topographic Maps: Traditional Representations by Means of New Technologies. *Cartographica: The International Journal for Geographic Information and Geovisualization*, *38*(1–2), 55–65. https://doi.org/10.3138/6r12-2gv6-x501-2306

Hurni, L., Jenny, B., Dahinden, T., & Hutzler, E. (2001). *Interactive Analytical Shading and Cliff Drawing: Advances in Digital Relief Presentation for Topographic Mountain Maps*. Proceedings of the 20th International Cartographic Conference, Beijing, China. http://www.mountaincartography.org/publications/papers/ica_cmc_sessions/2_Beijing_Session_Mountain_Carto/1_Beijing_Hurni.pdf

Imhof, E. (1965). *Kartographische Geländedarstellung (German Edition)* (1st ed.). De Gruyter.

Imhof, E. (2007). *Cartographic Relief Presentation*. Amsterdam University Press. https://books.google.nl/books/about/Cartographic_Relief_Presentation.html?id=cVy1Ms43fFYC&redir_esc=y

Introduction - CloudCompareWiki. (2016, November 17). CloudCompare Wiki. Retrieved April 20, 2021, from https://www.cloudcompare.org/doc/wiki/index.php?title=Introduction

Jacobsen, K. (2003). DEM generation from satellite data. *EARSeL*, *273276*(4). https://citeseerx.ist.psu.edu/viewdoc/download?doi=10.1.1.471.6412&rep=rep1&type=pdf

Jenny, B., Gilgen, J., Geisthövel, R., & Hurni, L. (2011, July). *Rock Drawing for Topographic Maps*. Proceedings of the 12th meeting of the ICA Commission on Mountain Cartography. http://www.mountaincartography.org/publications/papers/ica_cmc_sessions/7_Paris_Session_Mountain_Carto/paris_jenny_b.pdf

Jenny, B., Gilgen, J., Geisthövel, R., Marston, B. E., & Hurni, L. (2014). Design Principles for Swiss-style Rock Drawing. *The Cartographic Journal*, *51*(4), 360–371. https://doi.org/10.1179/1743277413y.0000000052

Jenny, B., & Räber, S. (2015a, January 21). *Analytical Relief Shading*. Relief Shading. Retrieved November 2, 2021, from http://www.reliefshading.com/analytical/

Jenny, B., & Räber, S. (2015b, January 21). *Shading Methods*. Relief Shading. Retrieved November 2, 2021, from http://www.reliefshading.com/analytical/shading-methods/

Kriz, K. (Ed.). (1999). *Perspectives and Design in High Mountain Cartography*. http://www.mountaincartography.org/publications/papers/ica_cmc_sessions/1_Ottawa_Session_Relief/04_Ottawa_Kriz.pdf

Letortu, P., Taouki, R., Jaud, M., Costa, S., Maquaire, O., & Delacourt, C. (2021). Three-dimensional (3D) reconstructions of the coastal cliff face in Normandy (France) based on oblique Pléiades imagery: assessment of Ames Stereo Pipeline® (ASP®) and MicMac® processing chains. *International Journal of Remote Sensing*, *42*(12), 4562–4582. https://doi.org/10.1080/01431161.2021.1892857

Lindsay, J. B., Francioni, A., & Cockburn, J. M. H. (2019). LiDAR DEM Smoothing and the Preservation of Drainage Features. *Remote Sensing*, *11*(16), 1926. https://doi.org/10.3390/rs11161926

Ludwig, R., & Schneider, P. (2006). Validation of digital elevation models from SRTM X-SAR for applications in hydrologic modeling. *ISPRS Journal of Photogrammetry and Remote Sensing*, *60*(5), 339–358. https://doi.org/10.1016/j.isprsjprs.2006.05.003

Masino, M. (2020). *Entwicklung eines Leitfadens zur Datenerfassung für eine Alpenvereinskarte der Region Ushba (Georgien) auf Basis von OpenStreetMap* (Thesis).

MeshLab. (n.d.). MeshLab. Retrieved April 20, 2021, from https://www.meshlab.net/

MicMac. (2018, February 19). MicMac Wiki. Retrieved March 12, 2021, from https://micmac.ensg.eu/index.php/Accueil

Niederheiser, R., Mokroš, M., Lange, J., Petschko, H., Prasicek, G., & Elberink, S. O. (2016). DERIVING 3D POINT CLOUDS FROM TERRESTRIAL PHOTOGRAPHS - COMPARISON OF DIFFERENT SENSORS AND SOFTWARE. *ISPRS - International Archives of the Photogrammetry, Remote Sensing and Spatial Information Sciences*, *XLI-B5*, 685–692. https://doi.org/10.5194/isprsarchives-xli-b5-685-2016

Pieczonka, T. (2017). *Untersuchung und Visualisierung von Gletschervolumenänderungen im Tarim-Einzugsgebiet, Zentralasien, unter Verwendung multi-temporaler digitaler Geländemodelle*. https://d-nb.info/1156851556/34

Pierrot-Deseilligny, M., & Paparoditis, N. (2006*). Multiresolution And Optimization-Based Image Matching Approach: An Application To Surface Reconstruction From Spot5-Hrs Stereo Imagery*. ISPRS Workshop On Topographic Mapping From Space (With Special Emphasis on Small Satellites), Ankara, Turkey.

Piotr. (2019). [Software]. Roman Geisthövel. http://motlimot.net/software.html

Planet. (n.d.). *Understanding PlanetScope Instruments*. Planet Developer Resource Center. Retrieved March 9, 2021, from https://developers.planet.com/docs/apis/data/sensors/

Planet. (2021, February). *Planet Imagery Product Specifications*. https://assets.planet.com/docs/Planet_Combined_Imagery_Product_Specs_letter_screen.pdf

Räber, S., Jenny, B., & Hurni, L. (2009, November). *Swiss Style Relief Shading Methodology: Knowledge base for further development and application in digital cartography*. ICC2009 the 24th International Cartographic Conference, Santiago de Chile, Chile. https://www.researchgate.net/profile/Bernhard-Jenny/publication/228913016_Swiss_Style_Relief_Shading_Methodology_Knowledge_base_for_further_development_and_application_in_digital_cartography/links/568082d608aebccc4e075878/Swiss-Style-Relief-Shading-Methodology-Knowledge-base-for-further-development-and-application-in-digital-cartography.pdf

Recommended Gradual Filter Settings. (2017). Agisoft Forum. Retrieved 2021, from https://www.agisoft.com/forum/index.php?topic=6888.0

Reuter, H. I., Nelson, A., & Jarvis, A. (2007). An evaluation of void-filling interpolation methods for SRTM data. *International Journal of Geographical Information Science*, *21*(9), 983–1008. https://doi.org/10.1080/13658810601169899

Rothermel, M., & Haala, N. (2012). POTENTIAL OF DENSE MATCHING FOR THE GENERATION OF HIGH QUALITY DIGITAL ELEVATION MODELS. *ISPRS - International Archives of the Photogrammetry, Remote Sensing and Spatial Information Sciences*, *XXXVIII-4/W19*, 271–276. https://doi.org/10.5194/isprsarchives-xxxviii-4-w19-271-2011

Rupnik, E., Daakir, M., & Pierrot Deseilligny, M. (2017). MicMac – a free, open-source solution for photogrammetry. *Open Geospatial Data, Software and Standards*, *2*(14), 1–9. https://doi.org/10.1186/s40965-017-0027-2

Rupnik, E., Pierrot-Deseilligny, M., & Delorme, A. (2018). 3D reconstruction from multi-view VHR-satellite images in MicMac. *ISPRS Journal of Photogrammetry and Remote Sensing*, *139*, 201–211. https://doi.org/10.1016/j.isprsjprs.2018.03.016

Schertenleib, U. (1997). Fridolin Becker (1854–1922) : Topograph, Kartograph, Innovator. *Cartographica Helvetica*, *15*. https://www.e-periodica.ch/digbib/view?pid=chl-001:1997:15::7#7

Schröder, M. (2020). *Erfassung und Kartierung von Fels- und Eisbedeckung in der Region Uschba (Georgien) mit multitemporalen optischen Fernerkundungsdaten*. Technische Universität Dresden.

Semyonov, D. (2011, May 3). *Algorithms used in Photoscan*. Agisoft Forum. Retrieved 2021, from https://www.agisoft.com/forum/index.php?topic=89.0

Singh, S. (2013, September 26). *DTM or DSM* [Image]. GIS Resources. http://gisresources.com/confused-dem-dtm-dsm/

Sun, G., Ranson, K., Kharuk, V., & Kovacs, K. (2003). Validation of surface height from shuttle radar topography mission using shuttle laser altimeter. *Remote Sensing of Environment*, *88*(4), 401–411. https://doi.org/10.1016/j.rse.2003.09.001

Sun, X., Rosin, P. L., Martin, R., & Langbein, F. (2007). Fast and Effective Feature-Preserving Mesh Denoising. *IEEE Transactions on Visualization and Computer Graphics*, *13*(5), 925–938. https://doi.org/10.1109/tvcg.2007.1065

Thevara, D. J., & Ch, V. K. (2018, September). Representation of stereo-photogrammetry technique demonstrating triangulation [Illustration]. In *Application of photogrammetry to automated finishing operations*.

Toschi, I., Capra, A., de Luca, L., Beraldin, J. A., & Cournoyer, L. (2014). On the evaluation of photogrammetric methods for dense 3D surface reconstruction in a metrological context. *ISPRS Annals of Photogrammetry, Remote Sensing and Spatial Information Sciences*, *II–5*, 371–378. https://doi.org/10.5194/isprsannals-ii-5-371-2014

USGS. (n.d.-a). *USGS EROS Archive - Digital Elevation - Shuttle Radar Topography Mission (SRTM) 1 Arc-Second Global*. U.S. Geological Survey. Retrieved November 2, 2021, from https://www.usgs.gov/centers/eros/science/usgs-eros-archive-digital-elevation-shuttle-radar-topography-mission-srtm-1-arc?qt-science_center_objects=0#qt-science_center_objects

USGS. (n.d.-b). *USGS EROS Archive - Digital Elevation - Shuttle Radar Topography Mission (SRTM) Void Filled*. U.S. Geological Survey. Retrieved November 2, 2021, from https://www.usgs.gov/centers/eros/science/usgs-eros-archive-digital-elevation-shuttle-radar-topography-mission-srtm-void?qt-science_center_objects=0#qt-science_center_objects

WaPPP (2.0). (2020). [Software]. Pr. Lambert Wanninger. http://wasoft.de/e/ppp/index.html

Wouda, B. (2014). *Mondt van de Maes* [Map]. Dieptelijnen uitgediept - Kartograaf Pierre Ancelin, uitvinder van het stelsel van dieptelijnen. CaertThresoor. https://caert-thresoor.nl/wp-content/uploads/sites/4/CT33-1.pdf

Appendix

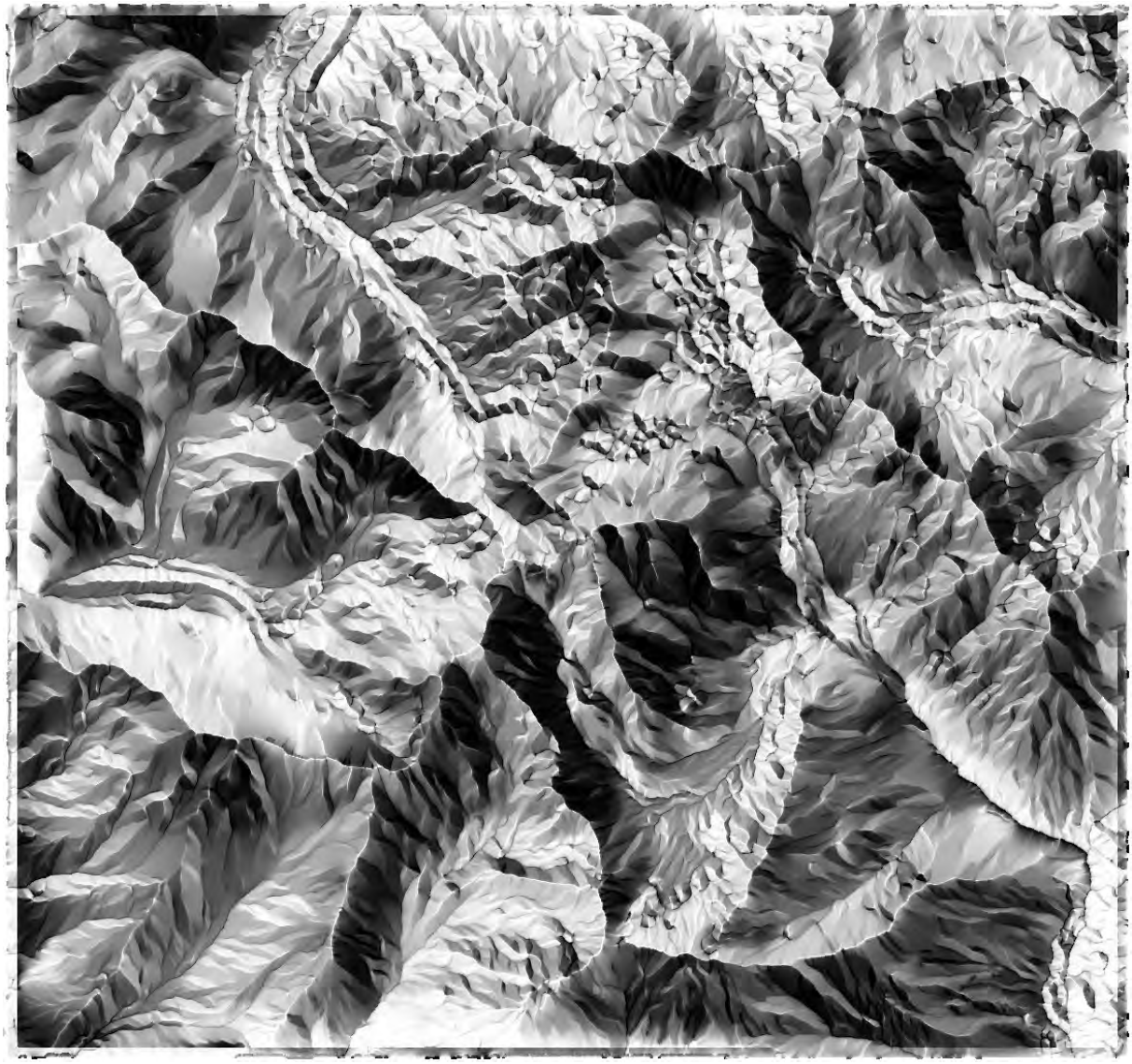

Figure 48 Hill shade based on LIC generalization, generated in Piotr

ID	POINT_X	POINT_Y	POINT_Z		PlanetScope DEM (28 images)	PlanetScope (11 images)	SRTM	PlanetScope DEM smoothened
1	309409.74	4784232.4	3025	3049	3044.780029	3031.118164	3002	3026.776123
2	311568.92	4784090.7	3657	3681	3670.911133	3690.862793	3620	3664.777602
3	315672.37	4783514.1	3822	3846	3759.143799	3782.874756	3825	3773.482666
4	313720.9	4783274.6	4302	4326	4232.295898	4268.43457	4177	4259.150655
5	316311.01	4783135.5	4162	4186	4060.641602	4029.417725	3872	4032.957551
6	306512.71	4783056.7	3358	3382	3297.229492	3273.19751	3208	3280.367629
7	308834.98	4782835.5	3227	3251	3257.639893	3243.390869	3223	3253.857068
8	311819.61	4782749.5	4280	4304	4249.743164	4257.598633	4229	4260.297698
9	305299.87	4782701.9	3611	3635	3603.196289	3615.166504	3611	3607.490967
10	309383.39	4782699.8	3578	3602	3601.928467	3592.394043	3546	3588.993102
11	312542.88	4782636.3	4163	4187	4104.242676	4097.577148	4011	4089.711914
12	307565.63	4782230.9	2800	2824	2839.390869	2829.138916	2814	2826.95752
13	311386.87	4782200	3871	3895	3884.205322	3883.570068	3881	3904.000103
14	316533.29	4782112.2	3691	3715	3674.656982	3681.407227	3620	3679.04886
15	305922.55	4781894.5	3957	3981	3870.633301	3915.489014	3864	3900.226503
16	307268.68	4781856.7	3281	3305	3253.741455	3253.721436	3254	3252.768129
17	314762.7	4781803.4	3510	3534	3550.54126	3521.905029	3382	3539.624268
18	311161.44	4781741.8	4055	4079	4058.751953	4064.144775	4046	4067.831522
19	316563.25	4781700.2	3243	3267	3300.523926	3308.118408	3213	3310.782645
20	310345.74	4781522.1	3843	3867	3806.059815	3857.64917	3756	3838.336664
21	311440.2	4781130.2	3927	3951	3923.214844	3934.859131	3756	3935.644022
22	313073.67	4780987.3	3572	3596	3584.89917	3559.658447	3374	3594.329142
23	307559.67	4780743	4159	4183	4096.836426	4116.399414	4020	4112.119044
24	306775.86	4780707.1	3891	3915	3889.02832	3894.1604	3784	3884.405273
25	305240.6	4780553.4	3825	3849	3781.036865	3787.934326	3815	3803.415385
26	316381.97	4780268.3	2662	2686	2695.988281	2710.011963	2666	2710.011963
27	313612.11	4780178.4	3522	3546	3488.65625	3508.894043	3468	3511.813341
28	305498.21	4780104.9	3867	3891	3849.492188	3856.902344	3854	3859.289365
29	312904.92	4780042.1	3131	3155	3176.062256	3172.985596	3142	3176.945801
30	311063.1	4780036.6	3871	3895	3841.912842	3853.133057	3763	3845.898057
31	308515.5	4779929.2	4368	4392	4240.460938	4329.320801	4182	4315.429147
32	315407.4	4779645.8	3532	3556	3543.978516	3540.783203	3531	3544.607339
33	314562.31	4779531.4	3751	3775	3671.068604	3686.547852	3516	3680.075066
34	305591.83	4779442.6	3574	3598	3540.447022	3550.558106	3536	3550.558105
35	310597.09	4779413.4	4277	4301	4256.715332	4238.602539	4189	4239.825728
36	308148.14	4779409	4032	4056	4037.797607	4034.002441	3991	4011.04814
37	309722.06	4779103.9	4052	4076	4025.321045	4028.554688	3933	4029.801496
38	306576.76	4779068.7	2896	2920	2843.740479	2855.472168	2917	2853.148095
39	312381.37	4778553.8	3738	3762	3699.929932	3684.830811	3431	3645.260986
40	309216.64	4778373.5	3548	3572	3529.598389	3553.162598	3569	3552.031738
41	305183.72	4778345.2	2575	2599	2556.57666	2566.737061	2562	2561.58374
42	310295.55	4778278.4	4234	4258	4201.327148	4203.439941	4218	4198.837891

ID	POINT_X	POINT_Y	POINT_Z		PlanetScope DEM (28 images)	PlanetScope (11 images)	SRTM	PlanetScope DEM smoothened
43	315014.47	4778200.7	3087	3111	3074.56543	3076.936279	3033	3087.399658
44	312922.85	4778176.9	2876	2900	2894.124023	2890.26294	2845	2894.222412
45	315999.25	4778065.4	3430	3454	3428.299316	3420.017822	3386	3424.387432
46	307789.18	4777668.5	2917	2941	2938.437744	2926.695557	2948	2933.842883
47	310056.01	4777592.8	4698	4722	4684.429688	4681.50293	4672	4684.264102
48	306348.02	4777253.4	3481	3505	3419.738281	3378.191406	3292	3383.589309
49	309534.31	4777216.4	4700	4724	4600.407715	4608.333008	4546	4601.22998
50	311604.56	4777212.8	3543	3567	3568.120117	3561.999756	3448	3562.125488
51	316215.6	4777176.7	2641	2665	2667.945557	2662.930664	2683	2670.685303
52	305571.37	4777063.9	2844	2868	2827.506836	2828.684815	2823	2820.778564
53	313426	4776741.2	2921	2945	2924.932617	2920.751953	2887	2920.500995
54	307515	4776593.8	4012	4036	4002.52124	3995.73169	3892	4003.404247
55	309864.66	4776549.5	3821	3845	3833.56543	3839.252441	3768	3832.053223
56	308641.85	4776341.7	3841	3865	3841.42334	3831.885254	3670	3829.375794
57	312216.84	4776238.3	2759	2783	2786.714844	2787.978027	2775	2787.824951
58	310798.21	4776103	3725	3749	3742.183594	3771.224365	3669	3769.266702
59	306753.04	4775948.9	3283	3307	3271.672607	3277.657959	3192	3279.628906
60	315451.67	4775909.6	1770	1794	1807.875122	1817.057983	1810	1815.721427
61	308946.48	4775782.7	3485	3509	3470.344238	3462.954102	3488	3470.809018
62	313132.73	4775693.2	3125	3149	3131.050781	3126.123047	3108	3133.147936
63	314003.58	4775636.4	2562	2586	2593.057373	2597.93457	2573	2584.638916
64	305793.89	4775271.7	2206	2230	2221.5979	2231.029053	2225	2229.509033
65	312824.17	4775086.3	3288	3312	3292.136475	3294.314453	3260	3301.093616
66	314643.7	4775039.7	2625	2649	2658.121094	2663.656982	2657	2663.656982
67	311245.27	4775014.8	3506	3530	3489.593262	3502.266846	3482	3501.105531
68	308064.23	4774664.3	2789	2813	2789.427979	2799.368897	2812	2798.298828
69	314257.58	4774601.9	2781	2805	2795.39209	2798.365723	2779	2797.581601
70	309278.57	4774278.7	2553	2577	2580.064697	2587.383545	2595	2584.660792
71	315484.6	4774196.2	1797	1821	1878.347046	1853.064941	1832	1853.046509
72	310893.59	4774143	3312	3336	3317.726563	3325.229248	3332	3323.082876
73	308223.96	4774018.2	2746	2770	2762.852295	2752.664795	2768	2760.035188
74	306082.86	4773978.2	2080	2104	2084.130127	2092.867188	2088	2114.734097
75	306291.67	4773577.7	1876	1900	1909.557007	1916.032837	1919	1918.702881

Table 4 Elevation at map points for the different DEMs

ID	On Glacier	STRM DEM	PlanetScope (11 images)	PlanetScope DEM (28 images)	PlanetScope DEM smoothened
1	N	-23.0	6.1	19.8	1.8
2	N	-37.0	33.9	13.9	7.8
3	N	3.0	-39.1	-62.9	-48.5
4	N	-125.0	-33.6	-69.7	-42.8
5	N	-290.0	-132.6	-101.4	-129.0
6	N	-150.0	-84.8	-60.8	-77.6
7	N	-4.0	16.4	30.6	26.9
8	N	-51.0	-22.4	-30.3	-19.7
9	N	0.0	4.2	-7.8	-3.5
10	N	-32.0	14.4	23.9	11.0
11	N	-152.0	-65.4	-58.8	-73.3
12	N	14.0	29.1	39.4	27.0
13	Y	10.0	12.6	13.2	33.0
14	N	-71.0	-9.6	-16.3	-12.0
15	N	-93.0	-41.5	-86.4	-56.8
16	Y	-27.0	-27.3	-27.3	-28.2
17	N	-128.0	11.9	40.5	29.6
18	N	-9.0	9.1	3.8	12.8
19	N	-30.0	65.1	57.5	67.8
20	N	-87.0	14.6	-36.9	-4.7
21	N	-171.0	7.9	-3.8	8.6
22	N	-198.0	-12.3	12.9	22.3
23	N	-139.0	-42.6	-62.2	-46.9
24	N	-107.0	3.2	-2.0	-6.6
25	N	-10.0	-37.1	-44.0	-21.6
26	N	4.0	48.0	34.0	48.0
27	N	-54.0	-13.1	-33.3	-10.2
28	Y	-13.0	-10.1	-17.5	-7.7
29	Y	11.0	42.0	45.1	45.9
30	N	-108.0	-17.9	-29.1	-25.1
31	N	-186.0	-38.7	-127.5	-52.6
32	N	-1.0	8.8	12.0	12.6
33	N	-235.0	-64.5	-79.9	-70.9
34	N	-38.0	-23.4	-33.6	-23.4
35	N	-88.0	-38.4	-20.3	-37.2
36	N	-41.0	2.0	5.8	-21.0
37	N	-119.0	-23.4	-26.7	-22.2
38	Y	21.0	-40.5	-52.3	-42.9
39	N	-307.0	-53.2	-38.1	-92.7
40	N	21.0	5.2	-18.4	4.0
41	N	-13.0	-8.3	-18.4	-13.4
42	Y	-16.0	-30.6	-32.7	-35.2
43	N	-54.0	-10.1	-12.4	0.4

ID	On Glacier	STRM DEM	PlanetScope (11 images)	PlanetScope DEM (28 images)	PlanetScope DEM smoothened
44	N	-31.0	14.3	18.1	18.2
45	Y	-44.0	-10.0	-1.7	-5.6
46	N	31.0	9.7	21.4	16.8
47	N	-26.0	-16.5	-13.6	-13.7
48	N	-189.0	-102.8	-61.3	-97.4
49	N	-154.0	-91.7	-99.6	-98.8
50	N	-95.0	19.0	25.1	19.1
51	N	42.0	21.9	26.9	29.7
52	N	-21.0	-15.3	-16.5	-23.2
53	N	-34.0	-0.2	3.9	-0.5
54	N	-120.0	-16.3	-9.5	-8.6
55	N	-53.0	18.3	12.6	11.1
56	N	-171.0	-9.1	0.4	-11.6
57	Y	16.0	29.0	27.7	28.8
58	N	-56.0	46.2	17.2	44.3
59	N	-91.0	-5.3	-11.3	-3.4
60	N	40.0	47.1	37.9	45.7
61	N	3.0	-22.0	-14.7	-14.2
62	N	-17.0	1.1	6.1	8.1
63	N	11.0	35.9	31.1	22.6
64	N	19.0	25.0	15.6	23.5
65	N	-28.0	6.3	4.1	13.1
66	N	32.0	38.7	33.1	38.7
67	N	-24.0	-3.7	-16.4	-4.9
68	N	23.0	10.4	0.4	9.3
69	N	-2.0	17.4	14.4	16.6
70	N	42.0	34.4	27.1	31.7
71	N	35.0	56.1	81.3	56.0
72	N	20.0	13.2	5.7	11.1
73	N	22.0	6.7	16.9	14.0
74	N	8.0	12.9	4.1	34.7
75	N	43.0	40.0	33.6	42.7
	Average	**-51.9**	**-5.0**	**-8.5**	**-5.5**
	RMSE	**94.1**	**36.8**	**39.9**	**39.0**
	Average excl. Glacier	**-57.5**	**-5.1**	**-8.8**	**-6.0**

Table 5 Elevation differences map points and DEMs

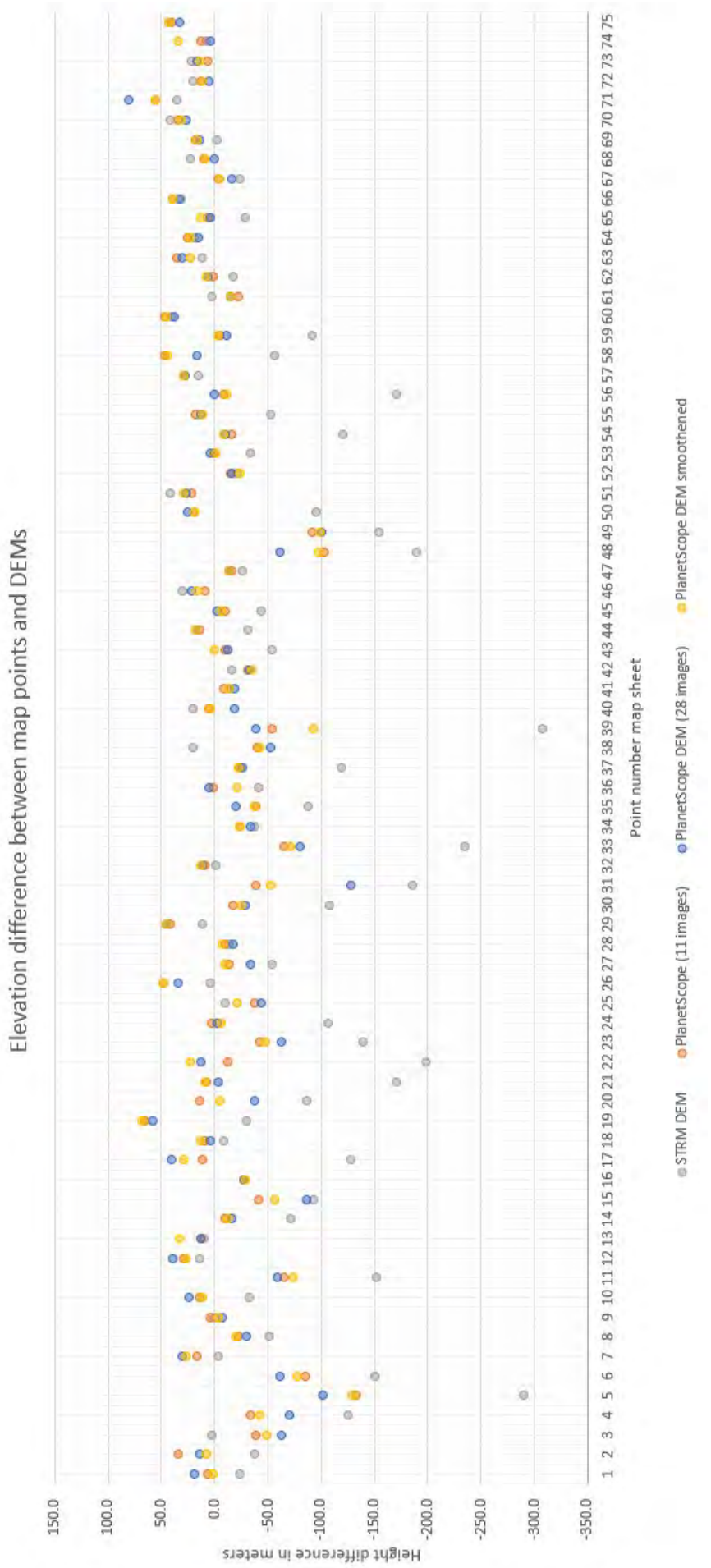

Figure 49 Graph with elevation differences between map points and different DEMs

Point	Easting	Northing	Zone	UTM	Elevation	AboveGround	RealElevation	StdDevE	StdDevN	StdDevEl	StartDate	EndDate	DDLat	DDLon
1	313083.5203	4773677.93	38N	313083.5203,4773677.9304,38N	2844.3644	0.95	2843.4144	0.4837	0.0472	0.0841	29/07/2021 09:00	29/07/2021 09:30	43.09277968	42.70336457
2	313064.5109	4773516.092	38N	313064.5109,4773516.0922,38N	2775.9601	0.95	2775.0101	1.1952	1.2114	1.5683	29/07/2021 08:15	29/07/2021 08:45	43.09131882	42.70318563
3	313128.9721	4773029.767	38N	313128.9721,4773029.7673,38N	2773.8836	0.95	2772.9336	0.5008	0.1366	0.0421	29/07/2021 06:50	29/07/2021 07:20	43.0869589	42.70414055
4	313638.9727	4772480.685	38N	313638.9727,4772480.6851,38N	2663.1397	0.6	2662.5397	0.1877	0.0506	0.0666	29/07/2021 08:40	29/07/2021 09:10	43.0821439	42.71058549
5	314754.7226	4770215.725	38N	314754.7226,4770215.7245,38N	2137.1045	0.4	2136.7045	0.0104	0.0045	0.0049	25/07/2021 06:25	25/07/2021 06:55	43.06203742	42.72503598
8	315779.9901	4768111.26	38N	315779.9901,4768111.2603,38N	1480.2779	0.7	1479.5779	0.0057	0.0024	0.0045	22/07/2021 11:00	22/07/2021 11:30	43.04335104	42.73831376
9	316107.2202	4767509.04	38N	316107.2202,4767509.0402,38N	1606.1032	0.5	1605.6032	0.0059	0.0071	0.0132	22/07/2021 09:00	22/07/2021 09:30	43.03801155	42.74252692
10	316975.7987	4765671.122	38N	316975.7987,4765671.1215,38N	2377.7492	0.35	2377.3992	0.0146	0.0059	0.0119	21/07/2021 11:31	21/07/2021 11:46	43.02168353	42.75378502
11	317443.8672	4764546.702	38N	317443.8672,4764546.7016,38N	1769.6795	1.15	1768.5295	0.0084	0.0068	0.0091	24/07/2021 08:45	24/07/2021 09:15	43.01167838	42.7598932
12	316232.6347	4773365.526	38N	316232.6347,4773365.5256,38N	1576.1346	0.5	1575.6346	0.2062	0.0307	0.0405	24/07/2021 13:28	24/07/2021 13:45	43.0907385	42.74213127
14	311765.5752	4772837.768	38N	311765.5752,4772837.7683,38N	2514.3204	0.6	2513.7204	0.0322	0.0083	0.0196	29/07/2021 10:35	29/07/2021 11:05	43.08489418	42.68746846
15	310151.3241	4773035.338	38N	310151.3241,4773035.3383,38N	2981.8945	2.55	2979.3445	0.0203	0.0075	0.0133	30/07/2021 12:03	30/07/2021 12:25	43.08626944	42.66758531
16	308596.0294	4772493.63	38N	308596.0294,4772493.6299,38N	2234.4447	0.5	2233.9447	0.0454	0.0124	0.0112	30/07/2021 13:38	30/07/2021 13:54	43.08100455	42.6486797
17	308004.1458	4772392.81	38N	308004.1458,4772392.81,38N	2004.7884	0.5	2004.2884	0.0168	0.0094	0.0132	30/07/2021 14:11	30/07/2021 14:26	43.07994785	42.64144948
18	304789.0144	4771977.703	38N	304789.0144,4771977.7027,38N	1633.8365	0.95	1632.8865	0.0127	0.0046	0.0052	28/07/2021 14:06	28/07/2021 14:26	43.07539251	42.60213288
20	301626.4979	4771591.181	38N	301626.4979,4771591.1808,38N	2454.8401	0.95	2453.8901	0.0037	0.0031	0.0049	30/07/2021 09:05	30/07/2021 09:35	43.07109473	42.56345818
22	304047.3774	4777486.293	38N	304047.3774,4777486.293,38N	1965.7627	0.95	1964.8127	0.2882	0.3656	0.4599	28/07/2021 08:30	28/07/2021 09:00	43.12476192	42.59108759
24	316822.06	4771757.725	38N	316822.06,4771757.7253,38N	1523.9949	0.45	1523.5449	0.2669	0.0372	0.0311	24/07/2021 13:53	24/07/2021 14:10	43.07641414	42.74989758
25	319832.5608	4770439.343	38N	319832.5608,4770439.3431,38N	2351.9139	0.35	2351.5639	0.0079	0.0048	0.0028	04/08/2021 06:42	04/08/2021 07:12	43.06527198	42.78727745
69	312197.8942	4774373.714	38N	312197.8942,4774373.7141,38N	3427.0049	0	3427.0049	0.0042	0.0053	0.0062	30/07/2021 08:53	30/07/2021 09:23	43.09882123	42.69225634
70	307180.686	4758580.063	38N	307180.686,4758580.0627,38N	2650.5941	0.3	2650.2941	0.0061	0.0016	0.008	26/07/2021 12:30	26/07/2021 13:00	42.95546058	42.63611695

Table 6 Field measurements

Point	PlanetScopeDEM	SRTM	MapSheet	MapSheet Corrected	PlanetScope DEM smoothened	PS DEM (28 images)	PlanetScope DEM (11 images)	SRTM DEM	PlanetScope DEM smoothened	MapSheet	PlanetScope DEM (28 images)	PSDEM (11) SEL	SRTM SEL	MapSheet SEL	PSDEM (28) SEL
1	2850.1	2857	2830	2854	2847.3	2839.3	6.7	13.6	3.8	10.6	4.1	6.7	13.6	10.6	4.1
2	2802.0	2816	2795	2819	2802.1	2796.2	26.9	41.0	27.1	44.0	-21.1	26.9	41.0	44.0	-21.1
3	2760.1	2761	2745	2769		2747.0	-12.9	-11.9		-3.9	25.9	-12.9	-11.9	-3.9	25.9
4		2631	2615	2639		2625.3		-31.5		-23.5	37.2				
5		2133	2108	2132		2123.9		-3.7		-4.7	12.8				
8		1483	1465	1489		1459.6		3.4		9.4	20.0				
9		1606	1600	1624		1616.8		0.4		18.4	-11.2				
10		2379	2360	2383		2367.5		1.6		5.6	9.9				
11		1770	1745	1768		1740.7		1.5		-0.5	27.8				
12	1596.1	1576	1545	1569	1593.1	1573.6	20.5	0.4	17.5	-6.6	2.0	20.5	0.4	-6.6	2.0
14	2517.7	2527	2485	2509		2506.0	4.0	13.3		-4.7	7.8	4.0	13.3	-4.7	7.8
15	2960.6	2956	2954	2978		2953.4	-18.7	-23.3		-1.3	25.9	-18.7	-23.3	-1.3	25.9
16	2236.6	2237	2215	2239		2222.1	2.7	3.1		5.1	11.8	2.7	3.1	5.1	11.8
17	2003.0	2016	1975	1999		1992.4	-1.3	11.7		-5.3	11.9	-1.3	11.7	-5.3	11.9
18		1630	1605	1629				-2.9		-3.9					
20		2447	2415	2439				-6.9		-14.9					
22	1977.7	1969	1945	1969		1991.3	12.9	4.2		4.2	-26.5	12.9	4.2	4.2	-26.5
24		1523	1505	1529		1513.0		-0.5		5.5	10.5				
25		2345	2330	2353		2353.5		-6.6		1.4	-1.1				
69	3414.7	3402	3405	3429	3415.9	3405.6	-12.3	-25.0	-11.1	2.0	21.4	-12.3	-25.0	2.0	21.4
70		2629						-21.3							
						Average	**2.8**	**-1.9**	**9.3**	**1.8**	**9.4**				
						RMSE	**14.3**	**15.6**	**17.2**	**13.2**	**18.8**				
						Average SEL	**2.8**	**2.7**		**4.4**	**6.3**				
						RMSE SEL	**14.3**	**18.8**		**14.9**	**18.2**				

Table 7 Elevation and elevation differences in DEMs for field measurement locations

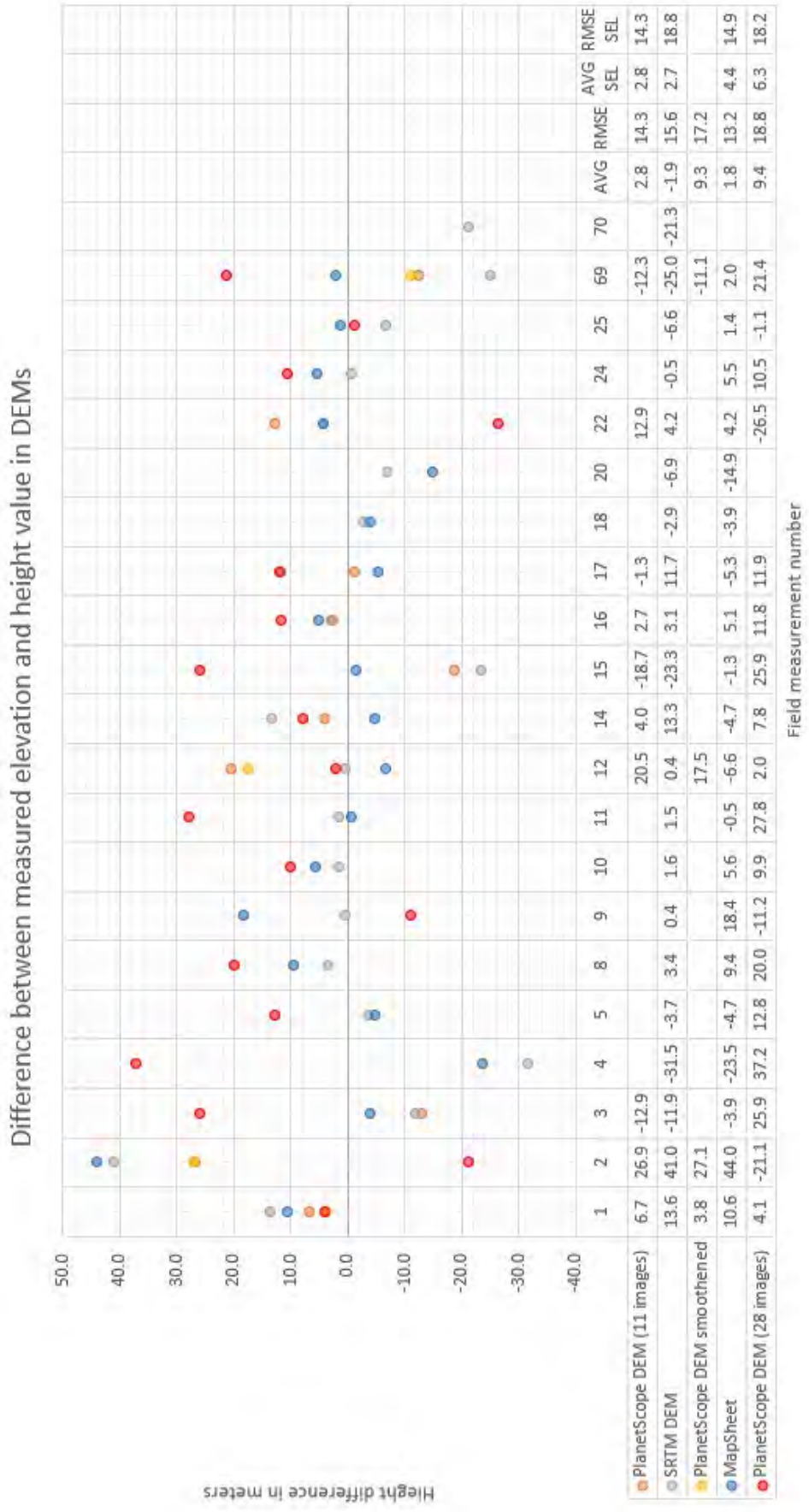

Figure 50 Elevation difference between measured elevation and height value in DEMs (incl. larger PlanetScope DEM)

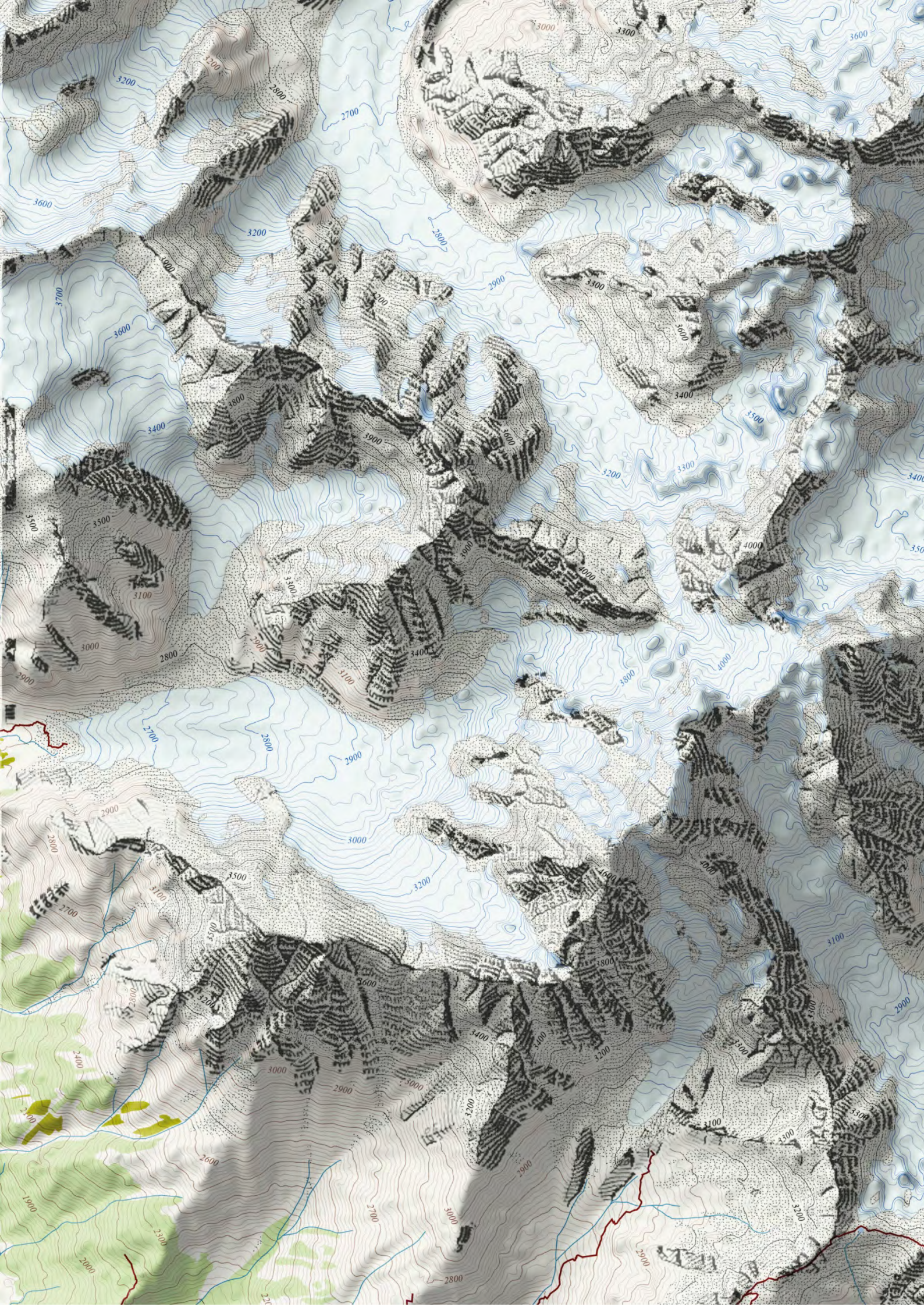

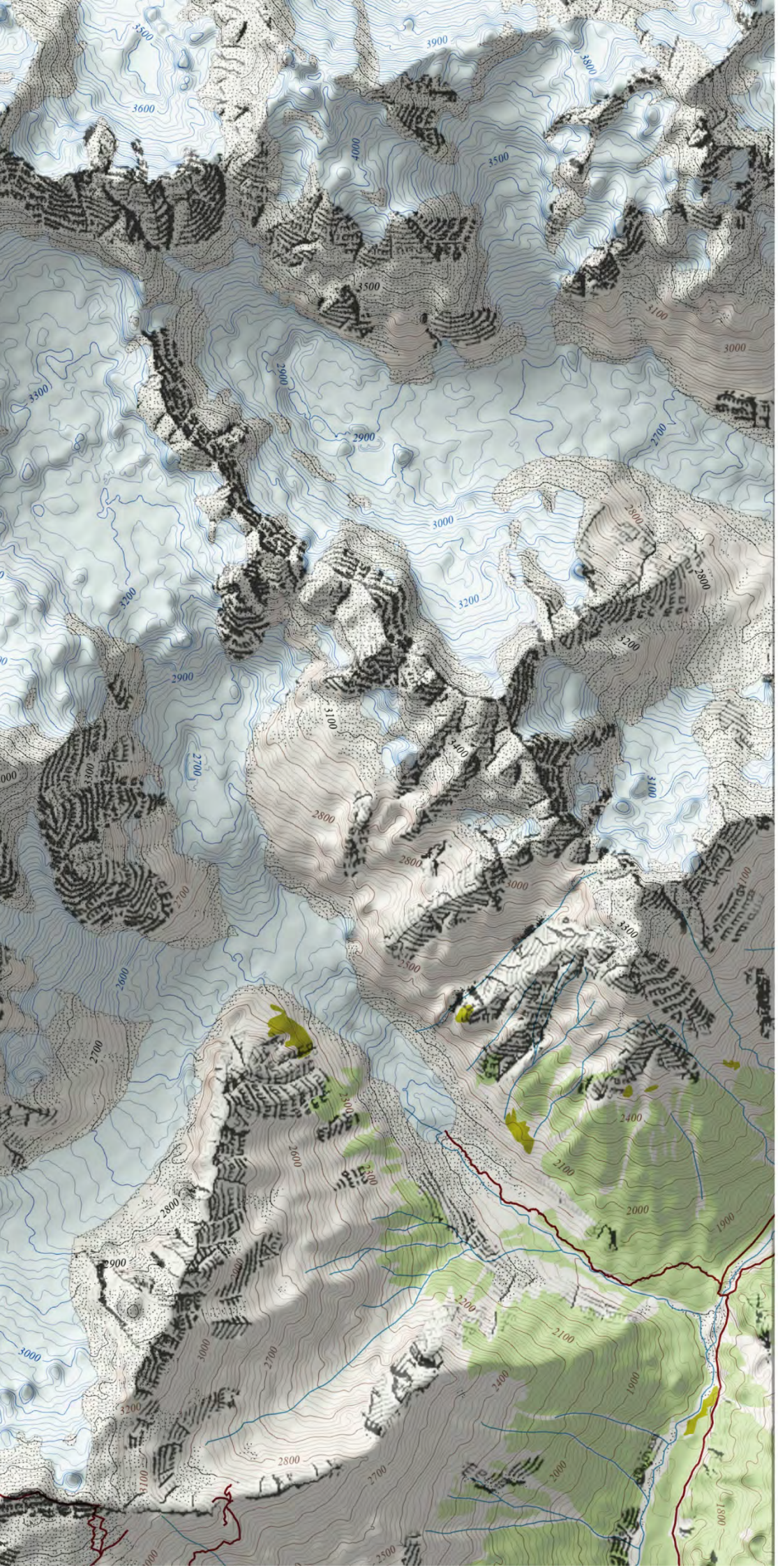
Path
Glacier
forest
scrub
Waterways
Rock
0 0.25 0.5 1 Kilometers
Anouska Jaspersen, 2021